Synthesis and Structure-Activity Relationships of Iminopyridazine Competitive Antagonists in Insect GABA Receptors

(昆虫 GABA 受容体におけるイミノピリダジン競合アンタゴニストの合成および構造活性相関)

Mohammad Mostafizur Rahman

2014

Synthesis and Structure-Activity Relationships of Iminopyridazine Competitive Antagonists in Insect GABA Receptors

A dissertation submitted to the United Graduate School of Agricultural Sciences Tottori University for the degree of Doctor of Philosophy

Mohammad Mostafizur Rahman

Tottori University

Japan

Supervisor

Prof. Yoshihisa Ozoe

2014

Contents

List of Figures

Chapter 3. Synthesis of 1,3-di- and 1,3,4-trisubstituted IPs as competitive antagonists of insect GABARs

Abbreviations

AC	American cockroach
CC	Common cutworm
DMF	*N, N*-Dimethylformamide
DMSO	Dimethyl sulfoxide
EC_{50}	Half maximal effective concentration
FLIPR	Fluorometric imaging plate reader
FMP	FLIPR membrane potential
GABA	γ-Aminobutyric acid
GABAR	GABA receptor
GluCl	Glutamate-gated chloride channel
HF	Housefly
5-HT	5-Hydroxytryptamine (Serotonin)
IC_{50}	Half maximal inhibitory concentration
IP	1,6-Dihydro-6-iminopyridazine
M1-M4	The first to fourth transmembrane domains
nACh	Nicotinic acetylcholine
n_H	Hill coefficient
Rdl	An insect GABA receptor subunit gene
Rdl	An insect GABA receptor protein
SBP	Small brown planthopper
TEVC	Two-electrode voltage clamp

CHAPTER 1

Introduction

1.1. Neurotransmitter and neurotransmission

Neurotransmitters are endogenously synthesized chemicals that convey signals across a synapse from one neuron to another. When a neurotransmitter is released from presynaptic neuron binds to a receptor in the postsynaptic neuron. As a result of binding, the receptor rapidly undergoes a conformational change to open an integral ion channel, which allows ions to cross the postsynaptic membrane and set up an electrical signal conduction along an axon through the neuron. The conduction of this signal along the axon is known as an action potential. The neurotransmitters are categorized into two types: the excitatory and inhibitory neurotransmitters. Acetylcholine and glutamic acid are excitatory type neurotransmitters. On the other hand, γ-aminobutyric acid (GABA) and glycine are inhibitory type neurotransmitters. By binding of an excitatory or inhibitory neurotransmitter to its receptors, the ligand-gated ion channels (LGICs) can contribute to either excitatory postsynaptic potentials (EPSPs), resulting in depolarization or inhibitory postsynaptic potentials (IPSPs), resulting in hyperpolarization. If the integration of the depolarizing and hyperpolarizing postsynaptic potentials is adequate enough to promote the membrane potential above a threshold, the postsynaptic neuron produces action potentials in the axon. In contrast, if the inhibition becomes effective, then the postsynaptic neuron is unable to produce action potentials. The procedure from neurotransmitter release to the postsynaptic response takes place in less than a millisecond.

1.2. LGICs

LGICs are a group of structurally related receptors that consist of an extracellular ligand binding domain, and a transmembrane domain containing the ion pore. In response to the binding of neurotransmitter molecules, the LGICs open and mediate fast synaptic neurotransmission. The LGICs are classified into three major classes: Cys-loop receptors, ionotropic glutamate receptors (*N*-methyl-D-aspartate, α-amino-3-hydroxy-5-methyl-4-isoxazolepropionic acid, and kainite receptors), and ATP-gated ion channels (P2XRs).[1] Nicotinic acid adenine dinucleotide phosphate (NAADP), ryanodine, and inositol 1,4,5-trisphosphate (IP_3) receptors are intracellular second messenger-activated receptors, which are also included in ligand-gated ion channels. These receptors are involved in the release of intracellular calcium stores.[2]

1.3. Cys-loop receptor family

The pentameric Cys-loop receptor family includes the nicotinic acetylcholine receptor (nAChRs), the serotonin type 3 receptor (5-HT_3R), the γ-aminobutyric acid (GABA) receptor type A ($GABA_AR$) and C ($GABA_CR$), and the glycine receptor (GlyR).[3-7] Zinc-activated channels (ZACs) were also reported as a member of Cys-loop receptor family.[8] They are known as 'Cys-loop receptors' due to the presence of a pair of disulfide-bonded cysteine in all family subunits. The disulfide-bonded cysteines are separated by 13 residues, which form a closed loop situated at the interface between extracellular and transmembrane channel domain.[9,10]

Cys-loop receptors can be further divided by their sensitivity to agonist and their intrinsic ionic selectivity. The nAChRs and 5-HT_3Rs have cation-selective channels, which generally results in EPSPs supporting the generation of action potentials in the postsynaptic neuron. The nAChR is widely distributed throughout the animal kingdom.[11] This receptor is expressed in

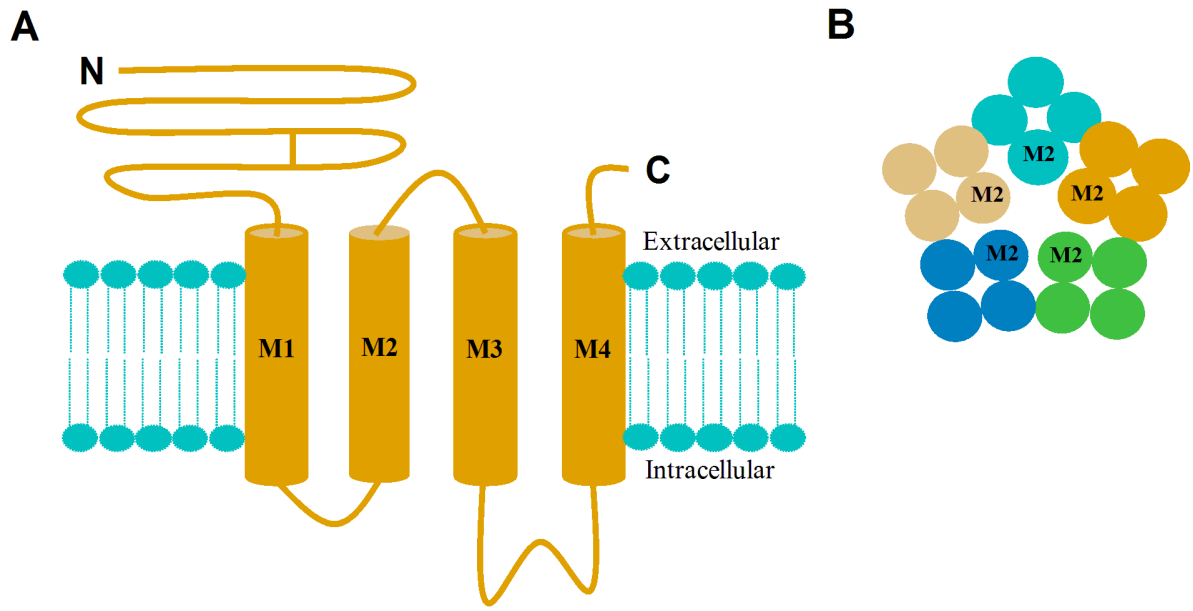

Figure 1.1 Schematic presentation of a Cys-loop receptor. (A) Side view. (B) Top view. Four transmembrane domains are labeled M1, M2, M3, and M4. An extended intracellular loop is shown between M3 and M4.

many regions of the central and peripheral nervous systems and plays important function in the neuromuscular transmission. The 5-HT_3Rs are also distributed in the central and peripheral nervous system and involved in sensory processing, nociception, emesis, cardiovascular regulation, and gut function.[12] In contrast, the $GABA_{A/C}$R and GlyR contain anion-selective channels, which usually mediate postsynaptic inhibition of neurotransmission by generating IPSPs in the postsynaptic neuron. $GABA_A$Rs and GlyRs are mostly involved in inhibition in the central nervous system. The $GABA_A$Rs are distributed throughout the central nervous system and the GlyRs are mainly found in the brainstem and spinal cord. The selectivity of the channels for cations or anions regulates the sign to the current. In most cases, the inhibitory responses are from anionic channels because they hyperpolarize the cell, and the excitatory responses are from cationic channels because they depolarize the cell. The activation of $GABA_A$Rs results in a

hyperpolarization of the postsynaptic neuron, which inhibits the opening of voltage-gated ion channels and generation of action potentials. Cys-loop receptors have also been found in insect species. The Cys-loop receptors have been identified in the fruit fly (*Drosophila melanogaster*), the honey bee (*Apis mellifera*), and the red flour beetle (*Tribolium castaneum*), etc.[13-15] These include nAChRs,[16] GABA-, glutamate-, and histamine-gated anion channels.[17-19] A wide range of Cys-loop receptors are present in the nematode *Caenorhabditis elegans*, in which a total of 90 LGIC genes were identified.[20,21]

1.4. GABA

GABA is the primary inhibitory neurotransmitter in the nervous system of animals. It was known to function as microbial and plant metabolism.[22] GABA was identified as a free amino acid in the brain in 1950s.[23,24] GABA is synthesized by decarboxylation of glutamate, a reaction that is catalyzed by the enzyme L-glutamic acid decarboxylase (GAD) (Fig. 1.2). The inhibitory action of GABA is mediated by GABA-gated chloride channels, i.e., $GABA_ARs$.[25] The activation of $GABA_ARs$ in vertebrates generally allows the chloride ion flux into the cell, causes the membrane hyperpolarization, and supresses the excitability of the cell.

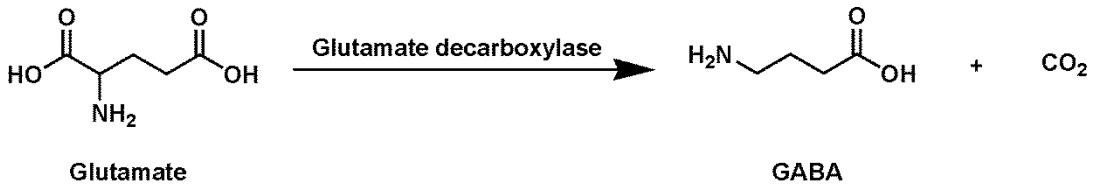

Figure 1.2 Biosynthesis pathway of GABA.

1.5. GABARs

GABARs are transmembrane proteins on postsynaptic membranes that respond to GABA molecules. In vertebrates, GABA mediates inhibitory neurotransmission through two types of receptors: the ionotropic and metabotropic receptors.[26-29] Ionotropic GABARs are classified into two types: heteropentameric $GABA_A$Rs that can be assembled with various stoichiometries, and homopentameric $GABA_C$Rs. In mammals, 19 distinct GABAR subunits (α1-6, β1-3, γ1-3, δ, ε, θ, π, and ρ1-3) have been identified by cDNA cloning and complete genome sequence.[30,31] Receptors containing ρ subunits are referred to as $GABA_C$Rs,[31] although this type of receptors are considered as a sub-class of $GABA_A$ receptors.[32] $GABA_C$Rs containing ρ subunits are localized in the retinal bipolar cells, with a very low density in the brain.[33] A subtype of $GABA_A$Rs containing two α subunits, two β subunits, and one γ subunit are the most abundant in the adult brain.[30,34] $GABA_A$Rs are antagonized by the competitive antagonist bicuculline and the noncompetitive antagonist picrotoxinin. However, $GABA_C$ receptors are antagonized by picrotoxinin, but not by bicuculline.[35] Each subunit consists of a large extracellular GABA-binding domain, a transmembrane domain containing four membrane spanning α-helices (M1-M4), and a large intracellular loop. The second transmembrane domain (M2) of five subunits are thought to line the channel pore.[36] When GABA binds to the orthosteric GABA-binding site in the extracellular interface between α and β subunits of $GABA_A$Rs, the integral channel rapidly opens to enhance the chloride permeability through the neuronal membrane, thereby suppressing the generation of action potentials. The orthosteric binding site is composed of six discontinuous loops, A–F and is located at the extracellular interface of adjacent subunits; loops A–C from the principal face and loops D–F from the complementary face.[36] Competitive antagonists share a common orthosteric binding site with the agonist GABA.

1.6. Insect GABARs

Insect GABARs are major targets of insecticides and paraciticides.[37] Both ionotropic and metabotropic GABARs have been found in insects.[17,38] The ionotropic GABARs are the major targets of insecticides. Insect GABARs are localized not only in the central nervous system but also in the peripheral tissues.[39,40] Insect ionotropic GABARs are distinct from mammalian GABARs in three ways: (1) Structurally, mammalian ionotropic GABARs are composed of α, β, γ, δ, ε, θ, π, and ρ subunits, whereas three different types of ionotropic GABAR subunits have been cloned from several insect species: Rdl (a subunit encoded by the gene *Rdl* (resistant to dieldrin)), GRD (the $GABA_A$ and glycine receptor-like subunit of *Drosophila*), and LCCH3 (ligand-gated chloride channel 3).[17,35,38] (2) Functionally, mammalian ionotropic GABARs can mediate fast synaptic transmission in the central nervous system, but in insects, they exist in both central and peripheral nervous system.[41] (3) Pharmacologically, insect and mammalian ionotropic GABARs showed different pharmacological sensitivities to a variety of chemicals. For example, bicuculline is a competitive antagonist for mammalian $GABA_A$Rs, whereas it shows no effects on most insect GABARs.[38,42] Benzodiazepines, such as diazepam and flunitrazepam, showed higher affinity for mammalian $GABA_A$Rs but not for insect GABARs.[38]

A GABAR subunit was identified from the fruit fly *Drosophila melanogaster* showing resistance to the cyclodiene insecticide dieldrin targeting insect GABA-gated chloride channels and named 'Rdl'.[43,44] GABARs containing Rdl subunits are the best studied GABA-activated receptors in insects. Dieldrin blocks the channel of Rdl GABARs and a mutation at residue 301 (Ala301→Ser) in the pore-lining M2 region is responsible for resistance to dieldrin. cDNAs (Ala301→Ser) in the pore-lining M2 region is responsible for resistance to dieldrin.

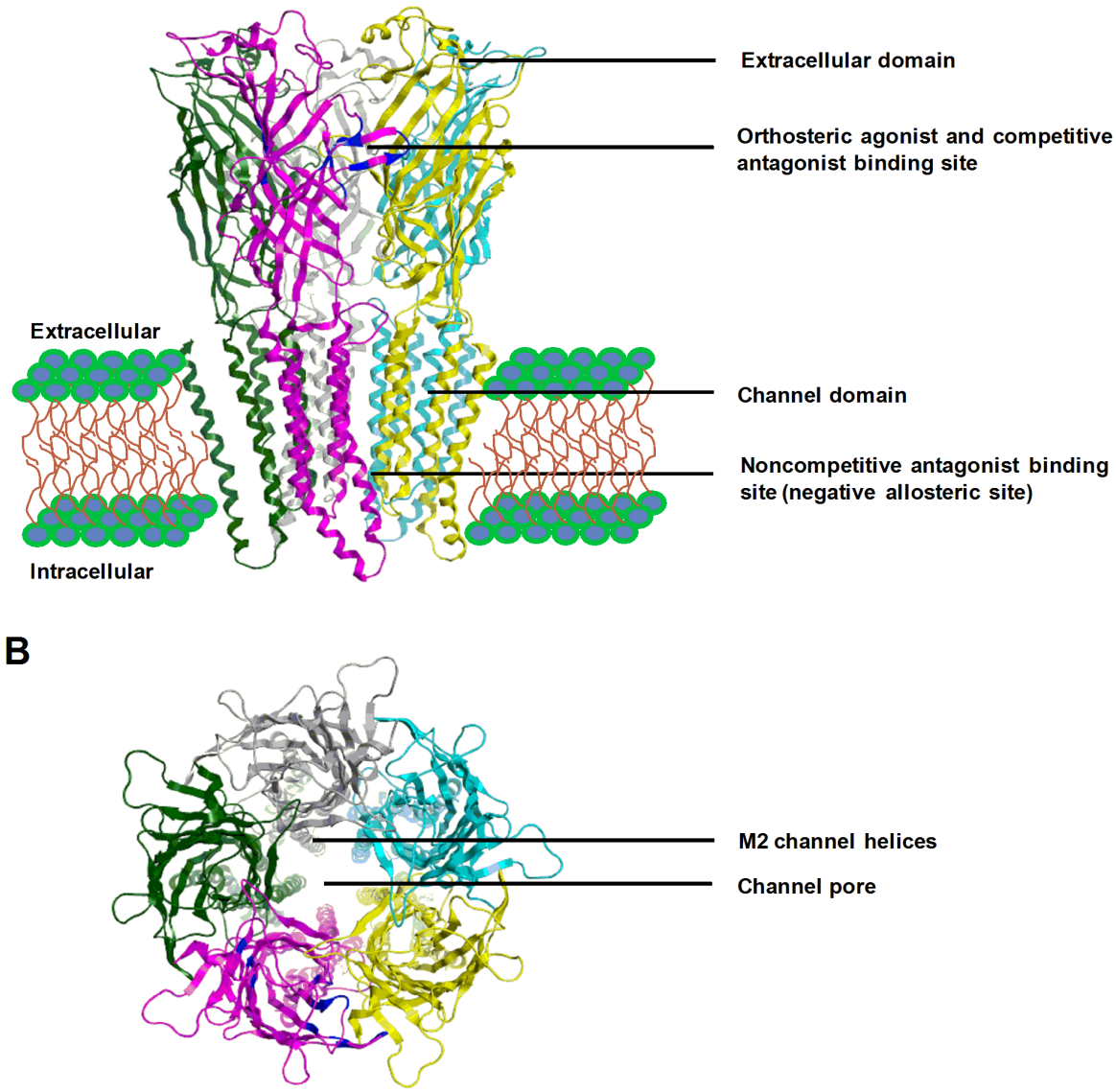

Figure 1.3 Structure of housefly Rdl GABAR. The model was built based on X-ray crystal structure of *C. elegans* GluCl (PDB ID: 3RIF). (A) Side view. The large extracellular domains are β-sandwiches and the transmembrane domains are α-helical. (B) Top view. The five subunits form a water-filled channel pore and are labeled in cyan, grey, green, magenta, and yellow for distinction. The orthosteric agonist and competitive antagonist binding site is shown in blue. An intracellular loop between M3 and M4 is omitted.

The cloning of full-length cDNAs encoding Rdl subunits have been identified in several other insect species.[45-47] Rdl subunits exist all through the adult and embryonic *Drosophila melangaster* central nervous system.[48]

1.7. GABAR ligands

A variety of compounds act on GABARs and disturb or enhance the receptor function. The agonists act to activate GABARs. The antagonists are ligands that can block agonist-induced responses in receptor. There are two types of antagonists for the Cys-loop receptors: competitive and noncompetitive antagonists. Competitive antagonists block the GABA-activated responses and stabilize the closed conformation of the channel by sharing a common binding site with the agonist GABA. Noncompetitive antagonists bind to allosteric binding sites distant from the agonist binding site and block GABA-induced responses.[49,50]

1.7.1. Noncompetitive GABAR antagonists

Ionotropic insect GABARs are the important target sites for a variety of insecticidally active compounds and antagonized by a wide range of structurally diverse noncompetitive antagonists.[51-53] Noncompetive antagonists are also termed as negative allosteric modulators because their actions are directed to the GABA-mediated chloride channel rather than the GABA recognition site of GABARs.[49] The structures of representative noncompetitive $GABA_A$ receptors antagonists are shown in Fig. 1.4. Picrotoxin is a natural product isolated from the fruit of the climbing plant *Anamirta cocculus*. It contains an equimolar mixture of the relatively potent $GABA_AR$ antagonist pictotoxinin (PTX) and less potent picrotin. PTX inhibits GABA-gated chloride channels by acting as a noncompetitive antagonist. The PTX binding site was identified with [^{3}H]dihydropicrotoxin and used as an early molecular probe of insect GABAR

research, which was replaced later by [^{35}S]*tert*-butylbicyclophosphorothionate ([^{35}S]TBPS). The inhibitory blocking potency of PTX in American cockroaches (ACs, *Periplaneta americana*) and the convulsion behavior of picrotoxin analogs in houseflies (HFs, *Musca domestica*) were reported.[54] The chlorinated hydrocarbon dieldrin is a highly active insecticide and used extensively during last few decades. It is now banned in most of the world because of its threats

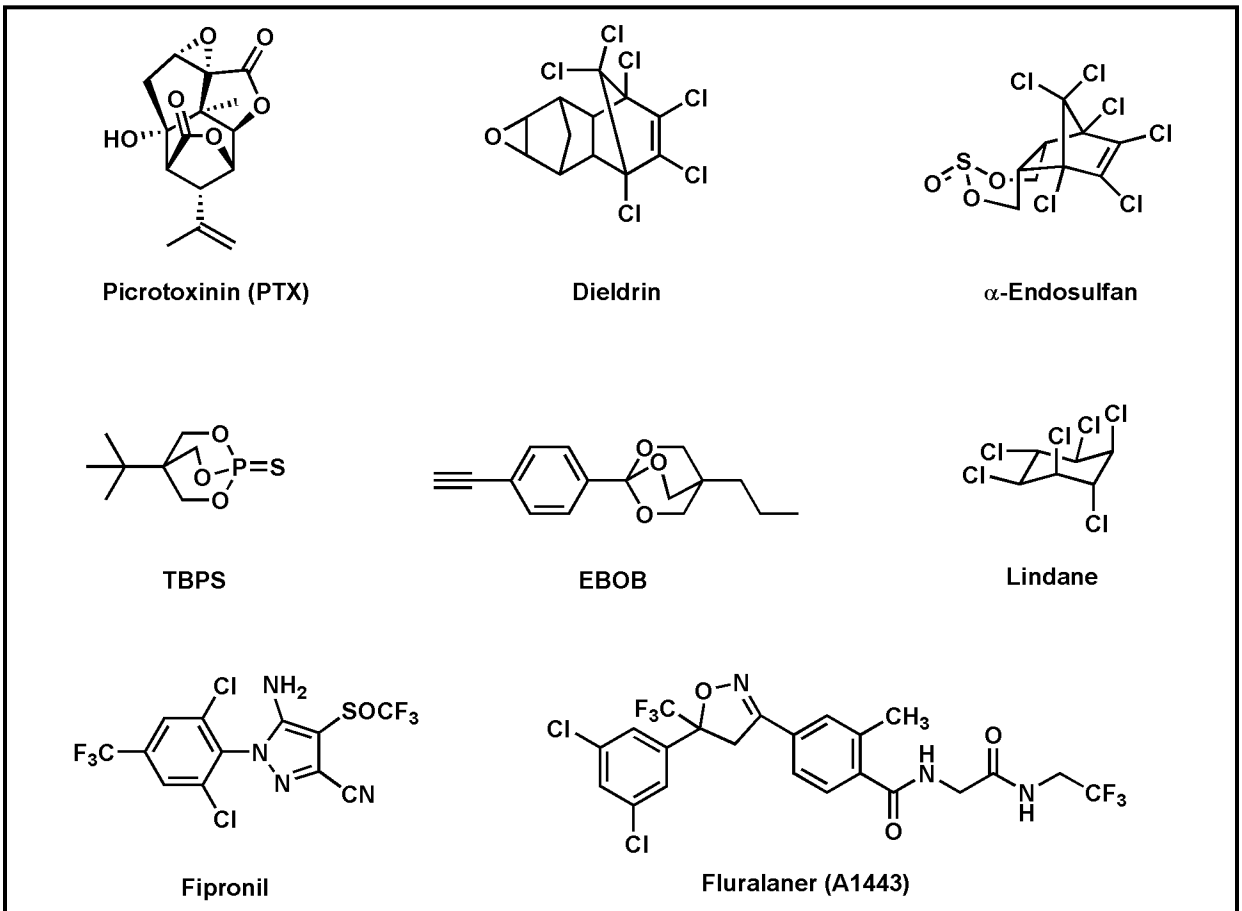

Figure 1.4 Chemical structures of representative noncompetitive GABAR antagonists.

to human health and its extreme persistent properties in the environment. α-Endosulfan was widely used as insecticides. Recently, it has been banned in many countries, with a limited uses for a few years. However, it is still used extensively in several countries. Bicyclophosphorothonates such as TBPS showed low affinity to HF GABARs compared to rat brain GABARs.[55] Synthetic efforts continue to increase the selectivity for insect and reduce the mammalian toxicity. An analog with an isopropyl group at the 3-position and a five-carbon alkyl group at the 4-position of bicyclophosphorothionates showed greater potency and selectivity in HF GABARs compared with rat GABARs.[56] [^{3}H]4′-Ethynyl-4-*n*-propylbicycloorthobenzoate ([^{3}H]EBOB) is an extensively used radioligand for labeling the noncompetitive antagonist blocker sites of insect and mammalian GABARs.[57-59] 5-Amino-1-(2,6-dichloro-4-trifluoromethylpheny)-4-trifluorometanaesulfinyl-1*H*-pyrazole-3-carbonitrile (fipronil) is the first successful commercially used phenylpyrazole insecticide that acts as a GABA-gated chloride channel inhibitor with high potency and selectivity for insect pests.[60] It has low mammalian toxicity and less persistence property in the environment. The GABA-activated responses in the *Drosophila* Rdl GABARs expressed in S2 cell line and in the GABARs of native AC neurons were inhibited by fipronil with IC_{50} values of 240 nM and 28 nM, respectively.[61,62] Recently, fluralaner (A1443), a novel class of isoxazoline ectoparasiticide was reported to have low mammalian toxicity.[40,63,64-66] The [^{3}H]EBOB site of HF head membranes was highly sensitive to fluralaner with an IC_{50} value of 0.455 nM, whereas the IC_{50} value was >10 μM in [^{3}H]EBOB binding to rat brain membranes.[63] In HF GABARs, fluralaner might bind to a site that is different from the EBOB binding site.[63] A recent report showed that fluralaner displayed high miticidal activity against two-spotted spider mite (*Tetranychus urticae*) compared with fipronil.[64]

1.7.2. GABAR agonists and competitive antagonists

The inhibitory nature of the neurotransmitter GABA accelerated the development of structurally diverse types of GABAR agonists. Conformational restriction of the different parts of GABA led to specific $GABA_A$ agonists. Some of these agonists played important roles in the development of $GABA_AR$ pharmacology. Structures of some representative GABAR agonists are shown in Fig. 1.5. Muscimol (5-aminomethyl-3-isoxazolol), a cyclic analog of GABA is a potent $GABA_AR$ agonist isolated from the mushroom *Amanita muscaria*.[67] It was used as a lead compound for the design of different classes of GABA analogs without significant loss of $GABA_AR$ agonism. THIP (4,5,6,7-tetrahydroisoxazolo[5,4-c]pyridin-3-ol) is a conformationally restricted bicyclic analog of muscimol. Its agonist behavior at $GABA_AR$ depends on subunit composition. THIP displayed a low agonist efficacy at α4β3γ2 GABARs, whereas it was a super agonist at α4β3δ GABARs.[68] 4-PIOL (5-(4-piperidyl)-3-isoxazolol), a nonfused analog of THIP, is a $GABA_AR$ partial agonist.[69]

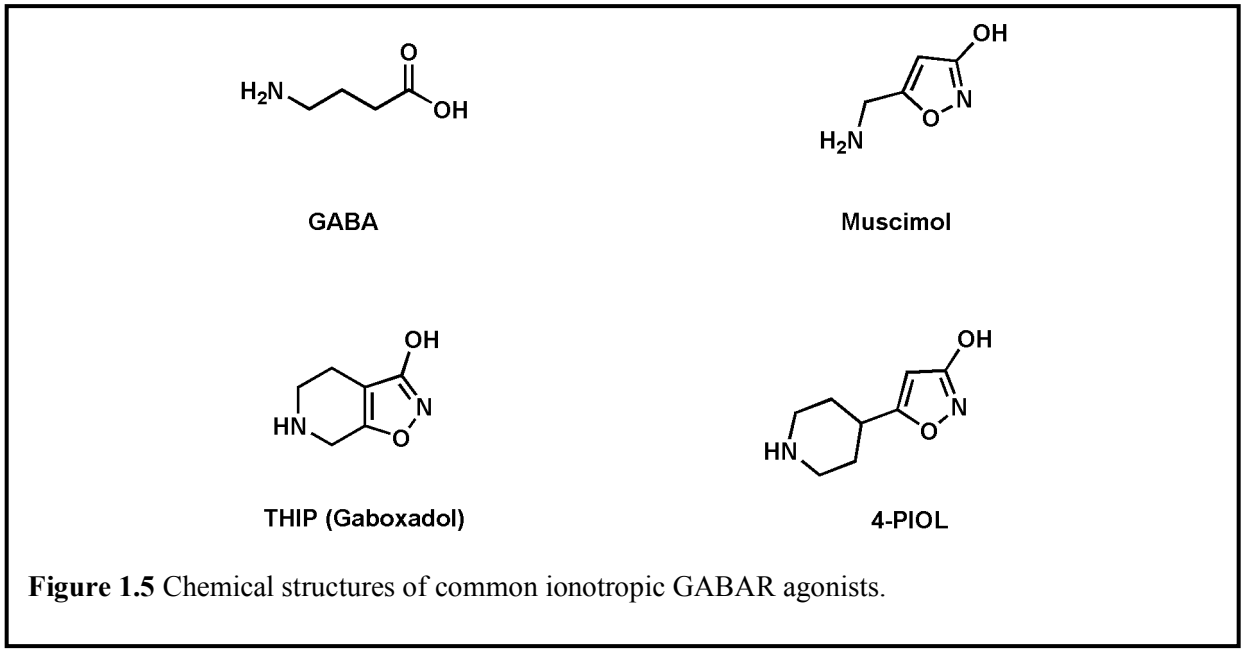

Figure 1.5 Chemical structures of common ionotropic GABAR agonists.

GABARs are antagonized by competitive antagonists. Bicuculline and gabazine (SR 95531) are two representative $GABA_AR$ antagonists for mammals (Fig. 1.6). TPMPA [(1,2,5,6-tetrahydropyridin-4-yl)methylphosphinic acid] is the most selective antagonist at $GABA_CR$.

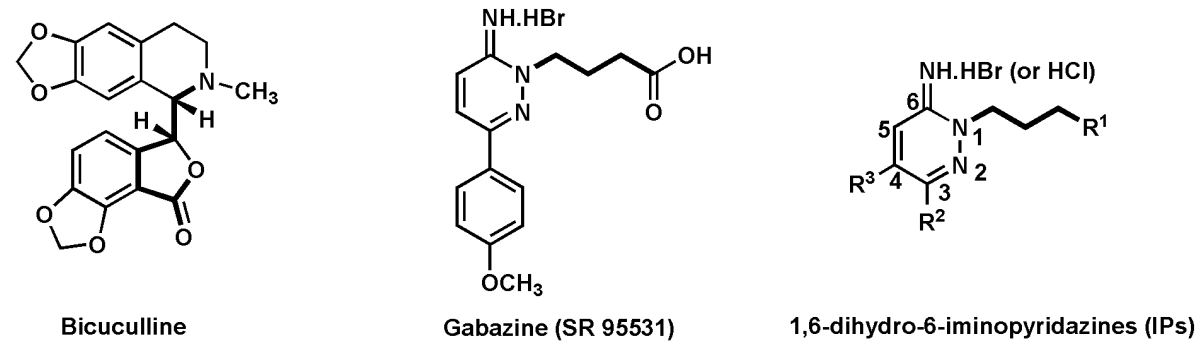

Figure 1.6 Chemical structures of competitive GABAR antagonists bicuculline, gabazine (SR 95531), and 1,6-dihydro-6-iminopyridazines (IPs). Bold lines indicate the GABA structural scaffold. The numbers of the carbon atoms of IPs are indicated at their sides.

1.8. Objective of the study

Insect GABARs represent important target sites for insecticides and paraciticides.[17,39,40] Phenylpyrazoles such as fipronil are used as insecticide and exert insecticidal effects by acting as a noncompetitive GABAR antagonist at a site within the channel.[70] However, the development of fipronil resistance in several insect species such whitebacked planthoppers (*Sogatella furcifera*) and small brown planthoppers (SBPs, *Laodelphax striatellus*) were reported.[46,47,71] Although two novel classes of insecticidal GABAR targeting compounds – isoxazolines and 3-benzamido-*N*-phenylbenzamides – have recently been reported,[40,63,72,73] efforts continues to develop novel GABAR insecticides. Bicuculline and gabazine (SR 95531) are typical

competitive antagonists for mammalian $GABA_AR$.[74,75] In contrast, no potent competitive antagonist has been developed as an insecticide. Whereas bicuculline is inactive against most insect GABARs, gabazine displays weak or moderate antagonistic activity against insect GABARs.[45,76,77] In the present study, I synthesized 1,6-dihydro-6-iminopyridazine (IP) analogs by modifying the substituents on the pyridazine ring of gabazine to examine whether this modification can increase the antagonistic activity of gabazine against insect GABARs.

1.8.1. Synthesis

The arylpyridazine moiety of the IP analogs plays important role in exerting their GABAR antagonistic activity. The additional change of the GABA scaffold may provide an extra benefit (Fig. 1.6). However, the existence of a positive charge on the GABA scaffold is required for $GABA_AR$ site recognition.[74] Wermuth and coworkers first described a seven-step synthetic method, including the synthesis of an pyridazinone intermediate to synthesize IP analogs.[74] The major drawbacks of this procedure are the use of toxic chemicals, the limited availability of appropriate substrates, and inconvenient operations. The important initial step for the synthesis of gabazine and its analogs involved the synthesis of 3-amino-(substituted aryl/heteroaryl)pyridazines. A protocol using a Michael-type addition reaction was reported for the synthesis of pyridazines starting with 4-chloro-1,2-diaza-1,3-butadienes and an active methylene cyano compounds.[78] Initially, to synthesize gabazine analogs with structurally diverse functional groups in pyridazine ring, I designed an eight-step synthesis strategy starting with acetophenone and semicarbazide with a Dean-stark attachment. Unfortunately, the product formed in this reaction was not stable enough to perform further reaction. A palladium-catalyzed Suzuki-Miyaura or Stille cross coupling reactions starting with 3-amino-6-chloropyridazine and aryl/heteroarylboronic acids was reported for the synthesis of 3-amino-6-

(aryl/heteroaryl)pyridazines.[79] Recently, Gavande and coworkers reported a four-step synthesis procedure for gabazine under microwave irradiation conditions starting with 3,6-dichoropyridazine.[80] Iqbal and coworkers reported several gabazine-based IPs as $GABA_AR$ antagonists.[81] In this study, I synthesized the first series of twelve IP analogs by changing the 3-substituent on the pyridazine ring of gabazine. I demonstrated an efficient three-step synthesis of eleven IPs, in which the substituent at the 3-position of the pyridazine ring was modified starting with 3-amino-6-chloropyridazine and a two-step synthesis of a 3-unsubstituted IP from 3-aminopyridazine. The detail synthesis of these twelve IP analogs is described in Chapter 2.

Some of the synthesized 3-substituted IPs displayed enhanced antagonistic activity than that of gabazine against insect GABARs. Therefore, further attempts were made to increase the activity of IP analogs. The antagonism of *Ascaris suum* GABARs by gabazine was enhanced by introducing different arylalkyl groups into the 5-position of the pyridazine ring of gabazine.[82,83] The alkyl group located between the aryl and the pyridazine ring might increase the probability of interacting with binding site residues because of their flexible structure. In the next strategy, I synthesized a total of thirteen 1,3-di- and 1,3,4-trisubstituted IPs in three categories. In this synthesis, I examined the effects of the 4-substituent and the carboxylate bioisosteres at the 1-position on the antagonist potency of IP derivatives in insect GABARs. The detailed synthesis of these IPs is described in Chapter 3.

1.8.2. Biological activity and homology modeling

The antagonism of insect GABARs by the first series of twelve synthesized IPs were examined using GABARs cloned from two insect species, small brown planthoppers (SBPs, *Laodelphax striatella*) and common cutworms (CCs, *Spodoptera litura*) by flurometric imaging

plate reader (FLIPR) membrane potential (FMP) assays. The antagonism of native AC GABARs was examined using whole-cell patch clamp technique. Homology modeling and ligand docking studies were performed using a homology model of HF GABARs. The details are described in Chapter 2.

The antagonism of insect GABARs by the second series of thirteen synthesized IPs was examined using GABARs cloned from SBPs and CCs using FMP assays. The antagonism of HF GABARs expressed in *Xenopus* oocytes was also examined using a two-electrode voltage clamp technique. Homology modeling and ligand docking studies were performed using a homology model of HF GABARs. The details are described in Chapter 3.

References

1. Hogg, R. C.; Buisson, B.; Bertrand, D. Allosteric modulation of ligand-gated ion channels. *Biochem. Pharmacol*. **2005**, *70*, 1267−1276.
2. Taylor, C. W.; Laude, A. J. IP_3 receptors and their regulation by calmodulin and cytosolic Ca^{2+}. *Cell Calcium* **2002**, *32*, 321−334.
3. Grenningloh, G.; Gundelfinger, E.; Schmitt, B.; Betz, H. Glycine vs GABA receptors. *Nature* **1987**, *330*, 25−26.
4. Olsen, R. W.; Tobin, A. J. Molecular biology of $GABA_A$ receptors. *FASEB J*. **1990**, *4*, 1469−1480.
5. Barnard, E. A. Receptor classes and the transmitter-gated ion channels. *Trends Biochem. Sci.* **1992**, *17*, 368−374.
6. Lester, H. A.; Dibas, M. I.; Dahan, D. S.; Leite, J. F.; Dougherty, D. A. Cys-loop receptors: new twist and turns. *Trends Neurosci.* **2004**, *27*, 329−336.

7. Bartos, M.; Corradi, J.; Bouzat, C. Structural basis of activation of Cys-loop receptors: the extracellular-transmembrane interface as a coupling region. *Mol. Neurobiol.* **2009**, *40*, 236−252.

8. Davies, P. A.; Wang, W.; Hales, T. G.; Kirkness, E. F. A novel class of ligand-gated ion channel is activated by Zn^{2+}. *J. Biol. Chem.* **2003**, *278*, 712−717.

9. Sine, S. M.; Engel, A. G. Recent advances in Cys-loop receptor structure and function. *Nature* **2006**, *440*, 488−455.

10. Bouzat, C. New insights into the structural bases of activation of Cys-loop receptors. *J. Physiol.* **2012**, *106*, 23−33.

11. Novère, N. L.; Changeux, J.-P. Molecular evolution of the nicotinic acetylcholine receptor: an example of multigene family in excitable cells. *J. Mol. Evol.* **1995**, *40*, 155−172.

12. Thompson, A. J.; Lummis, S. C. R. The 5-HT_3 receptor as a therapeutic target. *Expert Opin. Ther. Targets* **2007**, *11*, 527−540.

13. Littleton, J. T.; Ganetzky, B. Ion channels and synaptic organization: analysis of the *Drosophila* genome. *Neuron* **2000**, *26*, 35−43.

14. Jones, A. K.; Sattelle, D. B. The Cys-loop ligand-gated ion channel superfamily of the honeybee, *Apis mellifera*. *Invert. Neurosci.* **2006**, *6*, 123−132.

15. Jones, A. K.; Sattelle, D. B. The Cys-loop ligand-gated ion channel gene superfamily of the red flour beetle, *Tribolium castaneum*. *BMC Genomics* **2007**, *8*, 327.

16. Sattelle, D. B.; Jones, A. K.; Sattelle, B. M.; Matsuda, K.; Reenan, R.; Biggin. P. C. Edit, cut and paste in the nicotinic acetylcholine receptor gene family of *Drosophila melanogaster*. *BioEssays* **2005**, *27*, 366−376.

17. Buckingham, S. D.; Biggin, P. C.; Sattelle, B. M.; Brown, L. A.; Sattelle, D. B. Insect GABA receptors: splicing, editing, and targeting by antiparasitics and insecticides. *Mol. Pharmacol.* **2005**, *68*, 942−951.

18. Vassilatis, D. K.; Elliston, K. O.; Paress, P. S.; Hamelin, M.; Arena, J. P.; Schaeffer, J. M.; Van der Ploeg, L. H. T.; Cully, D. F. Evalutionary relationship of the ligand-gated ion channels and the avermectin-sensitive, glutamate-gated chloride channels. *J. Mol. Evol.* **1997**, *44*, 501−508.

19. Gisselmann, G.; Pusch, H.; Hovemann, B. T.; Hatt, H. Two cDNAs coding for histamine-gated ion channels in *D. melanogaster*. *Nat. Neurosci.* **2002**, *5*, 11−12.

20. Bargmann, C. I. Neurobiology of the *Caenorhabditis elegans* genome. *Science* **1998**, *282*, 2028−2033.

21. Jones, A. K.; Sattelle, D. B. The cys-loop ligand-gated ion channel gene superfamily of the nematode, *Caenorhabditis elegans*. *Invert. Neurosci.* **2008**, *8*, 41−47.

22. Cooper, J. R.; Bloom. F. E.; Roth, R. H. The biochemical basis of neuropharmacology. Oxford University Press. **2003**; pp. 106.

23. Awapara, J.; Landua, A. J.; Fuerst, R.; Seale, B. Free γ-aminobutyric acid in brain. *J. Biol. Chem.* **1950**, *187*, 35−39.

24. Roberts, E.; Frankel, S. γ-Aminobutyric acid in brain: its formation from glutamic acid. *J. Biol. Chem.* **1950**, *187*, 55−63.

25. Schofield, P. R.; Darlison, M. G.; Fujita, N.; Burt, D. R.; Stephenson, F. A.; Rodriguez, H.; Rhee, L. M.; Ramachandran, J.; Reale, V.; Glencorse, T. A.; Seeburg, P. H.; Barnard, E. A. Sequence and functional expression of the $GABA_A$ receptor shows a ligand-gated receptor superfamily. *Nature* **1987**, *328*, 221−227.

26. Chebib, M.; Johnston, G. A. R. GABA-activated ligand-gated ion channels: medicinal chemistry and molecular biology. *J. Med. Chem.* **2000**, *43*, 1427−1447.

27. Bowery, N. G.; Enna, S. J. γ-Aminobutyric $acid_B$ receptors: first of the functional metabotropic heterodimers. *J. Pharmacol. Exp. Ther.* **2000**, *292*, 2−7.

28. Bettler, B.; Kaupmann, K.; Mosbacher, J.; Gassmann, M. Molecular structure and physiological functions of $GABA_B$ receptors. *Physiol. Rev.* **2004**, *84*, 835−867.

29. Olsen, R. W.; Sieghart, W. $GABA_A$ receptors: subtypes provide diversity of function and pharmacology. *Neuropharmacology* **2009**, *56*, 141−148.

30. Whiting, P. J.; Bonnert, T. P.; McKernan, R. M.; Farrar, S.; Le Bourdellès, B.; Heavens, R. P.; Smith, D. W.; Hewson, L.; Rigby, M. R.; Sirinathsinghji, D. J.; Thompson, S. A.; Wafford, K. A. Molecular and functional diversity of the expanding GABA-A receptor gene family. *Ann. N. Y. Acad. Sci.* **1999**, *868*, 645−653.

31. Zhang, D.; Pan, Z.-H.; Awobuluyi, M.; Lipton, S. A. Structure and function of $GABA_C$ receptors: a comparison of native versus recombinant receptors. *Trends Pharmacol. Sci.* **2001**, *22*, 121−132.

32. Barnard, E. A.; Skolnick, P.; Olsen, R. W.; Mohler, H.; Sieghart, W.; Biggio, G.; Braestrup, C.; Bateson, A. N.; Langer, S. Z. International Union of Pharmacology. XV. Subtypes of γ-aminobutyric $acid_A$ receptors: classification on the basis of subunit structure and receptor function. *Pharmacol. Rev.* **1998**, *50*, 291−313.

33. Enz, R.; Cutting, G. R. $GABA_C$ receptor ρ subunits are heterogeneously expressed in the human CNS and form homo- and heterooligomers with distinct physical properties. *Eur. J. Neurosci.* **1999**, *11*, 41−50.

34. Mckernan, R. M.; Whiting, P. J. Which GABA-A receptor subtypes really occur in the brain. *Trends Neurosci.* **1996**, *19*, 139−143.

35. Hoise, A. M.; Aronstein, K.; Sattelle, D. B.; ffrench-Constant, R. H. Molecular biology of insect neuronal GABA receptors. *Trends Neurosci.* **1997**, *20*, 578−583.

36. Miller, P. S.; Smart, T. G. Binding, activation and modulation of Cys-loop receptors. *Trends Pharmacol. Sci.* **2010**, *31*, 161−174.

37. Raymond-Delpech, V.; Matsuda, K.; Sattelle, B. M.; Rauh, J. J.; Sattelle, D. B. Ion channels: molecular targets of neuroactive insecticides. *Invert. Neurosci.* **2005**, *5*, 119−133.

38. Sattelle, D. B.; Lummis, S. C. R.; Wong, J. F. H.; Rauh, J. J. Pharmacology of insect GABA receptors. *Neurochem. Res.* **1991**, *16*, 363−374.

39. Buckingham, S. D.; Sattelle, D. B. In Gilbert, L. I., Gill, S. S., Eds.; Insect Pharmacology: Channels, Receptors, Toxins and Enzymes; Elsevier: Amsterdam, 2010; pp. 29−64.

40. Ozoe, Y. γ-Aminobutyrate- and glutamate-gated chloride channels as targets of insecticides. *Adv. Insect Physiol.* **2013**, *44*, 211−286.

41. Bloomquist, J. R. Chloride channels as tools for developing selective insecticides. *Arch. Insect. Biochem. Physiol.* **2003**, *54*, 145−156.

42. Sattelle, D. B.; Bai, D.; Chen, H. H.; Skeer, J. M.; Buckingham, S. D.; Rauh, J. J. Bicuculline-insensitive GABA-gated Cl^- channels in the larval nervous system of the moth *Manduca sexta*. *Invert. Neurosci.* **2003**, *5*, 37−43.

43. ffrench-Constant, R. H.; Mortlock, D. P.; Shaffer, C. D.; MacIntyre, R. J.; Roush, R. T. Molecular cloning and transformation of cyclodiene resistance in *Drosophila*: an invertebrate γ-aminobutyric acid subtype A receptor locus. *Proc. Natl. Acad. Sci. USA* **1991**, *88*, 7209−7213.

44. ffrench-Constant, R. H.; Steichen, J. C.; Rocheleau, T. A.; Aronstein, K.; Roush, R. T. A single-amino acid substitution in a γ-aminobutyric acid subtype A receptor locus is associated with cyclodiene insecticide resistance in *Drosophila* populations. *Proc. Natl. Acad. Sci. USA* **1993**, *90*, 1957−1961.

45. Narusuye, K.; Nakao, T.; Abe, R.; Nagatomi, Y.; Hirase, K.; Ozoe, Y. Molecular cloning of a GABA receptor subunit from *Laodelphax striatella* (Fallén) and patch clamp analysis of the homo-oligomeric receptors expressed in a *Drosophila* cell line. *Insect Mol. Biol.* **2007**, *16*, 723−733.

46. Nakao, T.; Naoi, A.; Kawahara, N.; Hirase, K. Mutation of the GABA receptor associated with fipronil resistance in the whitebacked planthopper, *Sogatella furcifera*. *Pestic. Biochem. Physiol.* **2010**, *97*, 262−266.

47. Nakao, T.; Hama, M.; Kawahara, N.; Hirase, K. Fipronil resistance in *Sogatella furcifera*: molecular cloning and functional expression of wild-type and mutant RDL GABA receptor subunits. *J. Pestic. Sci.* **2012**, *37*, 37−44.

48. Aronstein, K.; Auld, V.; ffrench-Constant, R. Distribution of two GABA receptor-like subunits in the *Drosophila* CNS. *Invert. Neurosci.* **1996**, *2*, 115−120.

49. Johnston, G. A. R. $GABA_A$ receptor pharmacology. *Pharmacol. Ther.* **1996**, *69*, 173−198.

50. Krishek, B. J.; Moss, S. J.; Smart, T. G. A functional comparison of the antagonists bicuculline and picrotoxin at recombinant $GABA_A$ receptors. *Neuropharmacology* **1996**, *35*, 1289−1298.

51. Deng, Y.; Palmer, C. J.; Casida, J. E. Housefly brain γ-aminobutyric acid-gated chloride channel: target for multiple classes of insecticide. *Pestic. Biochem. Physiol.* **1991**, *41*, 60−65.

52. Rauh, J. J.; Benner, E.; Schnee, M. E.; Cordova, D.; Holyoke, C. W.; Howard, M. H.; Bai, D.; Buckingham, S. D.; Hutton, M. L.; Hamon, A.; Roush, R. T.; Sattelle, D. B. Effects of [^{3}H]-BIDN, a novel bicyclic dinitrile radioligand for GABA-gated chloride channels of insect and vertebrates. *Br. J. Pharmacol.* **1997a**, *121*, 1496−1505.

53. Rauh, J. J.; Holyoke, C. W.; Kleier, D. A.; Presnail, J. K.; Benner, E. A.; Cordova, D.; Howard, M. H.; Hosie, A. M.; Buckingham, S. D.; Baylis, H. A.; Sattelle, D. B. Polycyclic dinitriles: a novel class of potent GABAerginc insecticides provides a new radioligand, [^{3}H]BIDN. *Invert. Neurosci.* **1997b**, *3*, 261−268.

54. Miller, T. A.; Maynard, M.; Kennedy, J. M. Structure and insecticidal activity of picrotoxinin analogs. *Pestic. Biochem. Physiol.* **1979**, *10*, 128−136.

55. Ju, X.-L.; Ozoe, Y. Bicyclophosphorothionate antagonists exhibiting selectivity for housefly GABA receptors. *Pestic. Sci.* **1999**, *55*, 971−982.

56. Ju, X.-L.; Fusazaki, S.; Hishinuma, H.; Qiao, X.; Ikeda, I.; Ozoe, Y. Synthesis and structure-activity relationship analysis of bicyclophosphorothionate blockers with selectivity for housefly γ-aminobutyric acid receptor channels. *Pest Manag. Sci.* **2010**, *66*, 1002−1010.

57. Cole, L. M.; Casida, J. E. GABA-gated chloride channel: binding site for 4´-ethylnyl-4-*n*-[2,3-$^3H_2$]propylbicycloorthobezoate ([^{3}H]EBOB) in vertebrate brain and insect head. *Pestic. Biochem. Physiol.* **1992**, *44*, 1−8.

58. Deng, Y.; Palmer, C. J.; Casida, J. E. Housefly head GABA-gated chloride channel: four putative insecticide binding sites differentiated by [^{3}H]EBOB and [^{35}S]TBPS. *Pestic. Biochem. Physiol.* **1993**, *47*, 98−112.

59. Cole, L. M.; Roush, R. T.; Casida, J. E. *Drosophila* GABA-gated chloride channel: modified [^{3}H]EBOB binding site associated with Ala → Ser or Gly mutants of *Rdl* subunit. *Life Sci.* **1995**, *56*, 757−765.

60. Zhao, X.; Yeh, J. Z.; Salgado, V. L.; Narahashi, T. Fipronil is a potent open channel blocker of glutamate-activated chloride channels in cockroach neurons. *J. Pharmacol. Exp. Ther.* **2004**, *310*, 192−201.

61. Grolleau, F.; Sattelle, D. B. Single channel analysis of the blocking actions of BIDN and fipronil on a *Drosophila melanogaster* GABA receptor (RDL) stably expressed in a *Drosophila* cell line. *Br. J. Pharmacol.* **2000**, *130*, 1833−1842.

62. Zhao, X.; Salgado, V. L.; Yeh, J. Z.; Narahashi, T. Differential actions of fipronil and dieldrin insecticides on GABA-gated chloride channels in cockroach neurons. *J. Pharmacol. Exp. Ther.* **2003**, *306*, 914−924.

63. Ozoe, Y.; Asahi, M.; Ozoe, F.; Nakahira, K.; Mita, T. The antiparasitic isoxazoline A1443 is a potent blocker of insect ligand-gated chloride channels. *Biochem. Biophys. Res. Commun.* **2010**, *391*, 744−749.

64. Asahi, M.; Kobayashi, M.; Matsui, H.; Nakahira, K. Differential mechanisms of action of the novel γ-aminobutyric acid receptor antagonist ectoparasiticides fluralaner (A1443) and fipronil. *Pest Manag. Sci.* **2014**, DOI 10.1002/ps.3768.

65. Gassel, M.; Wolf, C.; Noack, S.; Williams, H.; Ilg, T. The novel isoxazoline ectoparasiticide fluralaner: selective inhibition of arthropod γ-aminobutyric acid- and L-glutamate-gated chloride channels and insecticidal/acaricidal activity. *Insect Biochem. Mol. Biol.* **2014**, *45*, 111−124.

66. Zhao, C.; Casida, J. E. Insect γ-aminobutyric acid receptors and isoxazoline insecticides: toxicological profiles relative to the binding sites of [^{3}H]fluralaner, [^{3}H]-4′-ethynyl-4-*n*-propylbicycloorthobenzoate, and [^{3}H]avermectin. *J. Agric. Food Chem.* **2014**, *62*, 1019−1024.

67. Krogsgaard-Larsen, P.; Frølund, B.; Jørgensen, F. S.; Schousboe, A. $GABA_A$ receptor agonists, partial agonists, and antagonists. Design and therapeutic prospects. *J. Med. Chem.* **1994**, *37*, 2489−2505.

68. Brown, N.; Kerby, J.; Bonnert, T. P.; Whiting, P. J.; Wafford, K. A. Pharmacological characterization of a novel cell line expressing human $\alpha_4\beta_3\delta$ $GABA_A$ receptors. *Br. J. Pharmacol.* **2002**, *136*, 965−974.

69. Kristianse, U.; Lambert, J. D. C.; Falch, E.; Krogsgaard-Larsen, P. Electrophysiological studies of the $GABA_A$ receptor ligand, 4-PIOL, on cultured hippocampal neurons. *Br. J. Pharmacol.* **1991**, *104*, 85−90.

70. Perret, P.; Sarda, X.; Wolff, M.; Wu, T.-T.; Bushey, D.; Goeldner, M. Interaction of non-competitive blockers within the γ-aminobutyric acid type A chloride channel using chemically reactive probes as chemical sensors for cysteine mutants. *J. Biol. Chem.* **1999**, *274*, 25350−25354.

71. Nakao, T.; Kawase, A.; Kinoshita, A.; Abe, R.; Hama, M.; Kawahara, N.; Hirase, K. The A2'N mutation of the RDL gamma-aminobutyric acid receptor conferring fipronil resistance in *Laodelphax striatellus* (Hemiptera: Delphacidae). *J. Econ. Entomol.* **2011**, *104*, 646−652.

72. Lahm, G. P.; Cordova, D.; Barry, J. D.; Pahutski, T. F.; Smith, B. K.; Long, J. K.; Benner, E. A.; Holyoke, C. W.; Joraski, K.; Xu, M.; Schroeder, M. E.; Wagerle, T.; Mahaffey, M. J.;

Smith, R. M.; Tong, M.-H. 4-Azolylphenyl isoxazoline insecticides acting at the GABA gated chloride channel. *Bioorg. Med. Chem. Lett.* **2013**, *23*, 3001−3006.

73. Nakao, T.; Banba, S.; Nomura, M.; Hirase, K. Meta-diamide insecticides acting on distinct sites of RDL GABA receptor from those for conventional noncompetitive antagonists. *Insect Biochem. Mol. Biol.* **2013**, *43*, 366−375.

74. Wermuth, C.-G.; Bourguignon, J.-J.; Schlewer, G.; Gies, J.-P.; Schoenfelder, A.; Melikian, A.; Bouchet, M.-J.; Chantreux, D.; Molimard, J.-C.; Heaulme, M.; Chambon, J.-P.; Biziere, K. Synthesis and structure-activity relationships of a series of aminopyridazine derivatives of γ-aminobutyric acid acting as selective GABA-A antagonists. *J. Med. Chem.* **1987**, *30*, 239−249.

75. Ueno, S.; Bracamontes, J.; Zorumski, C.; Weiss, D. S.; Steinbach, J. H. Bicuculline and gabazine are allosteric inhibitors of channel opening of the $GABA_A$ receptor. *J. Neurosci.* **1997**, *17*, 625−634.

76. Hosie, A. M.; Sattelle, D. B. Agonist pharmacology of two *Drosophila* GABA receptor splice variants. *Br. J. Pharmacol.* **1996**, *119*, 1577−1585.

77. Satoh, H.; Daido, H.; Nakamura, T. Preliminary analysis of the GABA-induced current in cultured CNS neurons of the cutworm moth, *Spodoptera litura*. *Neurosci. Lett.* **2005**, *381*, 125−130.

78. Attanasi, O. A.; Favi, G.; Filippone, P.; Perrulli, F. R.; Santeusanio, S. A novel and convenient protocol for synthesis of pyridazines. *Org. Lett.* **2009**, *11*, 309−312.

79. Maes, B. U. W.; Lemière, G. L. F.; Dommisse, R.; Augustyns, K.; Haemers, A. A new approach towards the synthesis of 3-amino-6-(hetero)arylpyridazines based on palladium catalyzed cross-coupling reactions. *Tetrahedron* **2000**, *56*, 1777−1781.

80. Gavande, N.; Johnston, G. A. R.; Hanrahan, J. R.; Chebib, M. Microwave-enhanced synthesis of 2,3,6-trisubstituted pyridazines: application to four-step synthesis of gabazine (SR-95531). *Org. Biomol. Chem.* **2010**, *8*, 4131−4136.

81. Iqbal, F.; Ellwood, R.; Mortensen, M.; Smart, T. G.; Baker, J. R. Synthesis and evaluation of highly potent $GABA_A$ receptor antagonists based on gabazine (SR-95531). *Bioorg. Med. Chem. Lett.* **2011**, *21*, 4252−4254.

82. Duittoz, A. H.; Martin, R. J. Antagonist properties of arylaminopyridazine GABA derivatives at the *Ascaris* muscle GABA receptor. *J. Exp. Biol.* **1991**, *159*, 149−164.

83. Martin, R. J.; Sitamze, J.-M.; Duittoz, A. H.; Wermuth, C. G. Novel arylaminopyridazine-GABA receptor antagonists examined electrophysiologically in *Ascaris suum*. *Eur. J. Pharmacol.* **1995**, *276*, 9−19.

CHAPTER 2

Competitive antagonism of insect GABARs by IP derivatives of GABA

2.1. Introduction

GABA is the major inhibitory neurotransmitter in the nervous system of animals. GABA released into the synapse functions by binding to two types of membrane proteins: ionotropic and metabotropic receptors.[1,2] The ionotropic GABAR belongs to the Cys-loop receptor family and mediates fast synaptic inhibition.[1,3] The receptors of this family are ligand-gated ion channels that are formed by five subunits. There are two types of ionotropic receptors in mammals: hetero-pentameric $GABA_AR$s, which are composed of α1-6, β1-3, γ1-3, δ, ε, θ, and π subunits, and homo-pentameric $GABA_CR$s, which comprise ρ1-3 subunits.[4] $GABA_AR$s with an α1-β2-γ2 combination are the most abundant subtype in the brain.[4] When GABA or an agonist binds to the orthosteric site in the α-β subunit interface of the extracellular domain of $GABA_AR$s, the integral channel rapidly opens to increase the membrane conductance of chloride ions, thereby suppressing the generation of action potentials. $GABA_AR$s are also targets for drugs such as benzodiazepines, barbiturates, and anesthetics.[5] In addition to agonists and drugs, two known types of antagonists exist for the Cys-loop receptor: competitive antagonists, which bind to the same site as agonists do, and noncompetitive antagonists, which bind to an allosteric binding site in the channel domain.[5,6] Both types of antagonists stabilize the closed conformation of the channels and block membrane conductance.

GABARs are widely distributed in both insect and mammalian nerve tissues. Insect GABARs exist not only in the central nervous system but also in the peripheral nervous system.[7] Inhibitory GABAR genes have been cloned from several insect species to date. In *Drosophila*, molecular cloning and functional expression of excitatory and metabotropic types of receptors have also been reported.[8-10] Insect inhibitory GABARs can be expressed as homo-pentamers, the subunits of which are encoded by the single gene *Rdl*, but four subunit variants are generated by alternative splicing of the exons 3 and 6 of *Rdl*.[11] Homo-oligomeric Rdl receptors share distinctive characteristics with native GABARs. Although insect GABARs are structurally similar to mammalian GABARs, these two receptors have different pharmacological characteristics, allowing GABARs to serve as important targets for insecticides and parasiticides.[11,12] For example, the noncompetitive antagonist fipronil is used as an insecticide.[13] In contrast, no competitive antagonist has been exploited in this respect. Although bicuculline and gabazine (SR 95531) (Fig. 1.6) are well known as competitive antagonists for mammalian $GABA_A$Rs,[14,15] no potent competitive antagonist for insect GABARs is known. While bicuculline is inactive for insect GABARs, gabazine was found to have moderate antagonist activity against insect GABARs.[16-18]

In this chapter, I examined whether the antagonist activity of gabazine against insect GABARs is increased by changing the 3-substituent on the pyridazine ring. Here, I used GABARs cloned from two agricultural pest insect species, SBPs and CCs, which cause serious damage to crops, and native GABARs expressed in the abdominal ganglion neurons of ACs, a noxious insect species. With GABARs from three insect species, I seek to find species differences in the receptors to utilize the information for future discovery and the development of chemicals for insect pest control.

2.2. Materials and Methods

2.2.1. Chemicals

Reagents were purchased from Wako Pure Chemical Industries, Ltd. (Osaka, Japan) and Tokyo Chemical Industry Co., Ltd. (Tokyo, Japan), unless otherwise noted.

2.2.2. Instruments

The melting points of synthesized compounds were determined using a Yanagimoto MP-500D apparatus and are uncorrected. ^{1}H NMR spectra were recorded on a JEOL JNM-A 400 spectrometer. The chemical shifts (δ values) are given in ppm relative to tetramethylsilane, and the *J* values are given in Hertz. The spin multiplicities are expressed as follows: s (singlet), d (doublet), t (triplet), q (quartet), qn (quintet), and m (multiplet). High resolution mass spectra were obtained with a Waters Synapt G2 spectrometer using the positive electrospray ionization mode.

2.2.3. General procedure for the synthesis of 3-amino-6-aryl/heteroarylpyridazines (1b-1l)

In the case of **1b-1i** and **1l**, a mixture of 3-amino-6-chloropyridazine (388 mg, 3.0 mmol), aryl/heteroarylboronic acid (4.5 mmol), tetrakis(triphenylphosphine)palladium(0) (105 mg), and a 2 M Na_2CO_3 solution (3.3 mL) in toluene (20 mL) was stirred under an argon atmosphere for 30 min at room temperature. In the case of **1j** and **1k**, a mixture of 3-amino-6-chloropyridazine (388 mg, 3.0 mmol), tributyl(heteroaryl)tin (4.1 mmol), and bis(triphenylphosphine)palladium(II) dichloride (198 mg) in THF (10 mL) was stirred under an argon atmosphere for 30 min at room temperature. In both cases, the reaction mixture was then heated under reflux with stirring under an argon atmosphere until completion of the reaction. After cooling, the reaction mixture was evaporated under reduced pressure to dryness. EtOAc

(80 mL) was added to the residue, and the flask containing the suspension was placed in an ultrasonic bath for 5 min. The mixture was filtered, and the filter paper was washed thoroughly with EtOAc (200 mL). The filtrate was evaporated under reduced pressure to dryness. The residue was purified by silica gel column chromatography to yield 3-amino-6-aryl/heteroarylpyridazine (**1b-1l**).

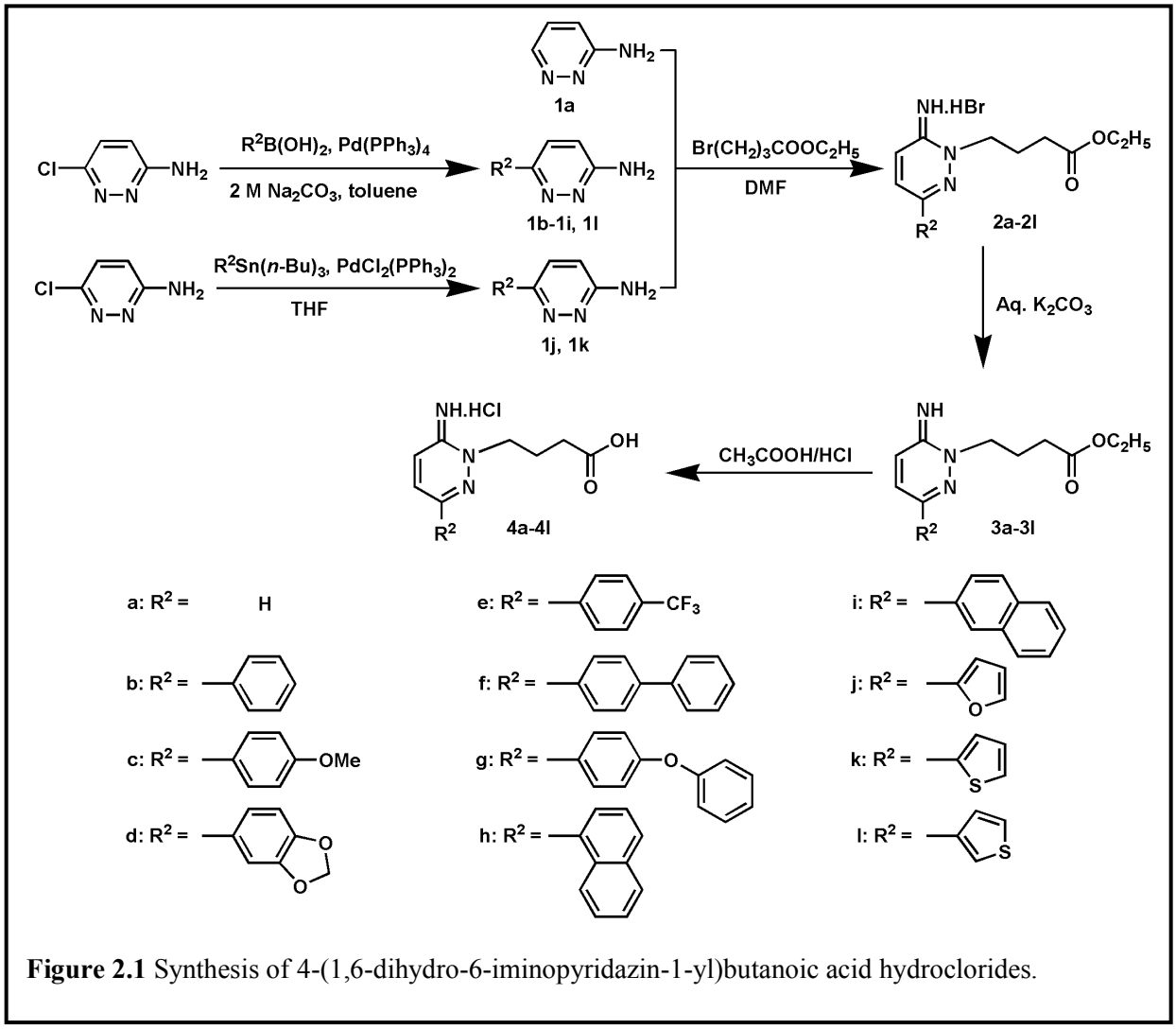

Figure 2.1 Synthesis of 4-(1,6-dihydro-6-iminopyridazin-1-yl)butanoic acid hydroclorides.

2.2.3.1. 3-Amino-6-phenylpyridazine (1b)

Yield 38%, mp 134-136 ºC. ^{1}H NMR (DMSO-d_6) δ 6.47 (s, 2H), 6.86 (d, 1H, J = 9.3 Hz), 7.36 (t, 1H, J = 7.3 Hz), 7.44 (t, 2H, J = 7.3 Hz), 7.78 (d, 1H, J = 9.3 Hz), 7.93 (d, 2H, J = 7.3 Hz).

2.2.3.2. 3-Amino-6-(4-methoxyphenyl)pyridazine (1c)

Yield 42%, mp 162-164 ºC. ^{1}H NMR ($CDCl_3$) δ 3.86 (s, 3H), 4.81 (s, 2H), 6.81 (d, 1H, J = 9.2 Hz), 6.99 (d, 2H, J = 8.5 Hz), 7.57 (d, 1H, J = 9.2 Hz), 7.89 (d, 2H, J = 8.5 Hz).

2.2.3.3. 3-Amino-6-(3,4-methylenedioxyphenyl)pyridazine (1d)

Yield 51%, mp 176-178 ºC. ^{1}H NMR (CD_3OD) δ 5.99 (s, 2H), 6.89 (d, 1H, J = 8.2 Hz), 6.97 (d, 1H, J = 9.3 Hz), 7.34 (dd, 1H, J = 8.2, 1.8 Hz), 7.41 (d, 1H, J = 1.8 Hz), 7.70 (d, 1H, J = 9.3 Hz).

2.2.3.4. 3-Amino-6-(4-trifluoromethylphenyl)pyridazine (1e)

Yield 41%, mp 116-118 ºC. ^{1}H NMR (DMSO-d_6) δ 6.65 (s, 2H), 6.88 (d, 1H, J = 9.3 Hz), 7.78 (d, 2H, J = 8.2 Hz), 7.88 (d, 1H, J = 9.3 Hz), 8.16 (d, 2H, J = 8.2 Hz).

2.2.3.5. 3-Amino-6-(4-biphenylyl)pyridazine (1f)

Yield 36%, mp 221-223 ºC. ^{1}H NMR (DMSO-d_6) δ 6.56 (s, 2H), 6.89 (d, 1H, J = 9.3 Hz), 7.38 (t, 1H, J = 7.3 Hz), 7.49 (t, 2H, J = 7.3 Hz), 7.72-7.78 (m, 4H), 7.88 (d, 1H, J = 9.3 Hz), 8.07 (d, 2H, J = 7.3 Hz).

2.2.3.6. 3-Amino-6-(4-phenoxyphenyl)pyridazine (1g)

Yield 77%, mp 152-154 ºC. ^{1}H NMR (DMSO-d_6) δ 6.46 (s, 2H), 6.86 (d, 1H, J = 9.3 Hz), 7.08 (d, 4H, J = 7.8 Hz), 7.17 (t, 1H, J = 7.5 Hz), 7.42 (t, 2H, J = 7.5 Hz), 7.79 (d, 1H, J = 9.3 Hz), 7.98 (d, 2H, J = 7.8 Hz).

2.2.3.7. 3-Amino-6-(1-naphthyl)pyridazine (1h)

Yield 78%, mp 153-155 ºC. ^{1}H NMR (DMSO-d_6) δ 6.56 (s, 2H), 6.95 (dd, 1H, J = 9.3, 1.5 Hz), 7.52-7.63 (m, 5H), 8.00 (t, 3H, J = 6.3 Hz).

2.2.3.8. 3-Amino-6-(2-naphthyl)pyridazine (1i)

Yield 19%, mp 212-214 ºC. ^{1}H NMR (DMSO-d_6) δ 6.54 (s, 2H), 6.91 (d, 1H, J = 9.6 Hz), 7.51-7.56 (m, 2H), 7.93-8.01 (m, 4H), 8.21 (d, 1H, J = 9.6 Hz), 8.47 (s, 1H).

2.2.3.9. 3-Amino-6-(2-furyl)pyridazine (1j)

Yield 75%, mp 118-120 ºC. ^{1}H NMR (DMSO-d_6) δ 6.52 (s, 2H), 6.59 (dd, 1H J = 3.4, 1.7 Hz), 6.83 (d, 1H, J = 9.3 Hz), 6.94 (d, 1H, J = 3.4 Hz), 7.60 (d, 1H, J = 9.3 Hz), 7.75 (d, 1H, J = 1.7 Hz).

2.2.3.10. 3-Amino-6-(2-thienyl)pyridazine (1k)

Yield 73%, mp 123-125 ºC. ^{1}H NMR (DMSO-d_6) δ 6.51 (s, 2H), 6.82 (d, 1H, J = 9.3 Hz), 7.09 (dd, 1H, J = 5.1, 3.7 Hz), 7.48 (dd, 1H, J = 5.1, 1.0 Hz), 7.54 (dd, 1H, J = 3.7, 1.2 Hz), 7.78 (d, 1H, J = 9.3 Hz).

2.2.3.11. 3-Amino-6-(3-thienyl)pyridazine (1l)

Yield 49%, mp 155-157 ºC. ^{1}H NMR (DMSO-d_6) δ 6.39 (s, 2H), 6.82 (d, 1H, J = 9.3 Hz), 7.61-7.63 (m, 1H), 7.70-7.71 (m, 1H), 7.74 (d, 1H, J = 9.3 Hz), 7.97-7.98 (m, 1H).

2.2.4. General procedure for the synthesis of ethyl 4-(1,6-dihydro-6-iminopyridazin-1-yl)butanoate hydrobromides (2a-2l)

A mixture of 3-amino-6-aryl/heteroarylpyridazine (**1b-1l**) (1 mmol), ethyl 4-bromobutanoate (292 mg, 1.5 mmol), and *N*,*N*-dimethylformamide (0.5 mL) was heated at 80 °C for 5 h. After cooling, the precipitate was collected and recrystallized from methanol and diethyl ether to give ethyl 4-(1,6-dihydro-6-imino-3-aryl/heteroarylpyridazin-1-yl)butanoate hydrobromides (**2b-2l**). Ethyl 4-(1,6-dihydro-6-iminopyridazin-1-yl)butanoate (**2a)** was similarly prepared from 3-aminopyridazine (**1a**).

2.2.4.1. Ethyl 4-(1,6-dihydro-6-iminopyridazin-1-yl)butanoate hydrobromide (2a)

Yield 11%, mp 212-214 ºC. ^{1}H NMR (CD_3OD) δ 1.24 (t, 3H, J = 7.2 Hz), 2.17 (qn, 2H, J = 7.1 Hz), 2.51 (t, 2H, J = 7.1 Hz), 4.11 (q, 2H, J = 7.2 Hz), 4.36 (t, 2H, J = 7.1 Hz), 7.55 (dt, 1H, J = 9.3, 1.8 Hz), 7.74 (ddd, 1H, J = 4.4, 3.4, 0.8 Hz), 8.39 (dd, 1H, J = 4.4, 1.8 Hz).

2.2.4.2. Ethyl 4-(1,6-dihydro-6-imino-3-phenylpyridazin-1-yl)butanoate hydrobromide (2b)

Yield 17% (for two steps), mp 215-217 ºC. ^{1}H NMR (DMSO-d_6) δ 1.10 (t, 3H, J = 7.0 Hz), 2.13 (qn, 2H, J = 7.0 Hz), 2.48-2.52 (m, 2H), 3.98 (q, 2H, J = 7.0 Hz), 4.38 (t, 2H, J = 7.0 Hz), 7.55-7.58 (m, 3H), 7.66 (d, 1H, J = 9.5 Hz), 7.95-7.98 (m, 2H), 8.39 (d, 1H, J = 9.5 Hz), 9.05 (broad s, 2H).

2.2.4.3. Ethyl 4-[1,6-dihydro-6-imino-3-(4-methoxyphenyl)pyridazin-1-yl]butanoate hydrobromide (2c)

Yield 30% (for two steps), mp 226-228 ºC. ^{1}H NMR (CD_3OD) δ 1.12 (t, 3H, J = 7.1 Hz), 2.24 (qn, 2H, J = 6.9 Hz), 2.58 (t, 2H, J = 6.9 Hz), 3.87 (s, 3H), 4.01 (q, 2H, J = 7.1 Hz), 4.43 (t,

2H, *J* = 6.9 Hz), 7.07 (d, 2H, *J* = 9.0 Hz), 7.60 (d, 1H, *J* = 9.5 Hz), 7.95 (d, 2H, *J* = 9.0 Hz), 8.29 (d, 1H, *J* = 9.5 Hz).

2.2.4.4. Ethyl 4-[1,6-dihydro-6-imino-3-(3,4-methylenedioxyphenyl)pyridazin-1-yl]butanoate hydrobromide (2d)

Yield 30% (for two steps), mp 238-240 ºC. ^{1}H NMR (CD_3OD) δ 1.16 (t, 3H, *J* = 7.2 Hz), 2.23 (qn, 2H, *J* = 6.8 Hz), 2.57 (t, 2H, *J* = 6.8 Hz), 4.02 (q, 2H, *J* = 7.2 Hz), 4.42 (t, 2H, *J* = 6.8 Hz), 6.06 (s, 2H), 6.98 (d, 1H, *J* = 8.3 Hz), 7.49-7.53 (m, 2H), 7.58 (d, 1H, *J* = 9.5 Hz), 8.26 (d, 1H, *J* = 9.5 Hz).

2.2.4.5. Ethyl 4-[1,6-dihydro-6-imino-3-(4-trifluoromethyphenyl)pyridazin-1-yl]butanoate hydrobromide (2e)

Yield 26% (for two steps), mp 217-219 ºC. ^{1}H NMR (CD_3OD) δ 1.14 (t, 3H, *J* = 7.2 Hz), 2.26 (qn, 2H, *J* = 6.9 Hz), 2.58 (t, 2H, *J* = 6.9 Hz), 4.02 (q, 2H, *J* = 7.2 Hz), 4.48 (t, 2H, *J* = 6.9 Hz), 7.67 (d, 1H, *J* = 9.5 Hz), 7.87 (d, 2H, *J* = 8.6 Hz), 8.19 (d, 2H, *J* = 8.6 Hz), 8.38 (d, 1H, *J* = 9.5 Hz).

2.2.4.6. Ethyl 4-[3-(4-biphenylyl)-1,6-dihydro-6-iminopyridazin-1-yl]butanoate hydrobromide (2f)

Yield 27% (for two steps), mp 205-207 ºC. ^{1}H NMR (CD_3OD) δ 1.14 (t, 3H, *J* = 8.2 Hz), 2.26 (qn, 2H, *J* = 6.8 Hz), 2.59 (t, 2H, *J* = 6.8 Hz), 4.02 (q, 2H, *J* = 8.2 Hz), 4.47 (t, 2H, *J* = 6.8 Hz), 7.37-7.41 (m, 1H), 7.47 (dd, 2H, *J* = 6.8, 1.5 Hz), 7.65 (d, 1H, *J* = 9.8 Hz), 7.68-7.71 (m, 2H), 7.82 (dd, 2H, *J* = 6.8, 2.0 Hz), 8.08 (dd, 2H, *J* = 6.8, 2.0 Hz), 8.38 (d, 1H, *J* = 9.8 Hz).

2.2.4.7. Ethyl 4-[1,6-dihydro-6-imino-3-(4-phenoxyphenyl)pyridazin-1-yl]butanoate hydrobromide (2g)

Yield 55% (for two steps), mp 195-197 ºC. ^{1}H NMR (CD_3OD) δ 1.14 (t, 3H, *J* = 7.2 Hz), 2.24 (qn, 2H, *J* = 6.6 Hz), 2.57 (t, 2H, *J* = 6.6 Hz), 4.01 (q, 2H, *J* = 7.2 Hz), 4.44 (t, 2H, *J* = 6.6 Hz), 7.06-7.12 (m, 4H), 7.20 (t, 1H, *J* = 7.3 Hz), 7.40-7.44 (m, 2H), 7.61 (d, 1H, *J* = 9.6 Hz), 7.98-8.00 (m, 2H), 8.30 (d, 1H, *J* = 9.6 Hz).

2.2.4.8. Ethyl 4-[1,6-dihydro-6-imino-3-(1-naphthyl)pyridazin-1-yl]butanoate hydrobromide (2h)

Yield 36% (for two steps), mp 178-180 ºC. ^{1}H NMR (CD_3OD) δ 1.11 (t, 3H, *J* = 7.2 Hz), 2.27 (qn, 2H, *J* = 6.9 Hz), 2.57 (t, 2H, *J* = 6.9 Hz), 4.02 (q, 2H, *J* = 7.2 Hz), 4.48 (t, 2H, *J* = 6.9 Hz), 7.57-7.65 (m, 3H), 7.68 (dd, 2H, *J* = 8.3, 1.0 Hz), 8.00-8.09 (m, 4H).

2.2.4.9. Ethyl 4-[1,6-dihydro-6-imino-3-(2-naphthyl)pyridazin-1-yl]butanoate hydrobromide (2i)

Yield 7% (for two steps), mp 232-234 ºC. ^{1}H NMR (CD_3OD) δ 1.11 (t, 3H, *J* = 7.1 Hz), 2.28 (qn, 2H, *J* = 6.8 Hz), 2.62 (t, 2H, *J* = 6.8 Hz), 4.02 (q, 2H, *J* = 7.1 Hz), 4.50 (t, 2H, *J* = 6.8 Hz), 7.57-7.63 (m, 2H), 7.66 (d, 1H, *J* = 9.3 Hz), 7.95 (d, 1H, *J* = 9.3 Hz), 8.03 (d, 2H, *J* = 8.8 Hz), 8.12 (dd, 1H, *J* = 8.8, 1.5 Hz), 8.51-8.53 (m, 2H).

2.2.4.10. Ethyl 4-[1,6-dihydro-3-(2-furyl)-6-iminopyridazin-1-yl]butanoate hydrobromide (2j)

Yield 47% (for two steps), mp 224-226 ºC. ^{1}H NMR (CD_3OD) δ 1.17 (t, 3H, *J* = 7.1 Hz), 2.22 (qn, 2H, *J* = 6.9 Hz), 2.56 (t, 2H, *J* = 6.9 Hz), 4.03 (q, 2H, *J* = 7.1 Hz), 4.39 (t, 2H, *J* = 6.9

Hz), 6.69 (dd, 1H, *J* = 3.5, 1.7 Hz), 7.24 (dd, 1H, *J* = 3.5, 0.7 Hz), 7.60 (d, 1H, *J* = 9.5 Hz), 7.80 (dd, 1H, *J* = 1.7, 0.7 Hz), 8.16 (d, 1H, *J* = 9.5 Hz).

2.2.4.11. Ethyl 4-[1,6-dihydro-6-imino-3-(2-thienyl)pyridazin-1-yl]butanoate hydrobromide (2k)

Yield 45% (for two steps), mp 237-239 ºC. ^{1}H NMR (CD_3OD) δ 1.15 (t, 3H, *J* = 7.1 Hz), 2.22 (qn, 2H, *J* = 6.9 Hz), 2.57 (t, 2H, *J* = 6.9 Hz), 4.02 (q, 2H, *J* = 7.1 Hz), 4.38 (t, 2H, *J* = 6.9 Hz), 7.20 (dd, 1H, *J* = 5.1, 3.9 Hz), 7.58 (d, 1H, *J* = 9.5 Hz), 7.69 (dd, 1H, *J* = 5.1, 1.2 Hz), 7.82 (dd, 1H, *J* = 3.9, 1.2 Hz), 8.28 (d, 1H, *J* = 9.5 Hz).

2.2.4.12. Ethyl 4-[1,6-dihydro-6-imino-3-(3-thienyl)pyridazin-1-yl]butanoate hydrobromide (2l)

Yield 33% (for two steps), mp 235-237 ºC. ^{1}H NMR (CD_3OD) δ 1.14 (t, 3H, *J* = 7.2 Hz), 2.25 (qn, 2H, *J* = 6.8 Hz), 2.57 (t, 2H, *J* = 6.8 Hz), 4.01 (q, 2H, *J* = 7.2 Hz), 4.42 (t, 2H, *J* = 6.8 Hz), 7.58 (d, 1H, *J* = 9.5 Hz), 7.61 (dd, 1H, *J* = 5.1, 2.9 Hz), 7.69 (dd, 1H, *J* = 5.1, 1.2 Hz), 8.20 (dd, 1H, *J* = 2.9, 1.2 Hz), 8.27 (d, 1H, *J* = 9.5 Hz).

2.2.5. General procedure for the synthesis of 4-(1,6-dihydro-6-iminopyridazin-1-yl)butanoic acid hydrochlorides (4a-4l)

Compounds **2b-2l** (200 mg) was dissolved in a minimal amount of water. A K_2CO_3 solution was used to make the solution alkaline, and then the solution was extracted with a 1:1 mixture of EtOAc and Et_2O. The organic layer was dried with anhydrous Na_2SO_4 and was concentrated under reduced pressure to give free base esters ethyl 4-(1,6-dihydro-6-imino-3-aryl/heteroarylpyridazin-1-yl)butanoates (**3b-3l**). Ethyl 4-(1,6-dihydro-6-iminopyridazin-1-

yl)butanoate (**3a**) was similarly prepared from **2a**. Concentrated hydrochloric acid (3 mL) in glacial acetic acid (10 mL) was added to the free base ester and heated at 100 °C for approximately 12 h. After cooling, the reaction mixture was evaporated to dryness under reduced pressure. The residue was recrystallized with AcOH and EtOAc to afford 4-(1,6-dihydro-6-imino-3-aryl/heteroarylpyridazin-1-yl)butanoic acid hydrochlorides (**4b-4l**). 4-(1,6-Dihydro-6-iminopyridazin-1-yl)butanoic acid hydrochloride (**4a**) was similarly obtained from ethyl 4-(1,6-dihydro-6-iminopyridazin-1-yl)butanoate (**3a**).

2.2.5.1. 4-(1,6-Dihydro-6-iminopyridazin-1-yl]butanoic acid hydrochloride (4a)

Yield 8% (from **1a**), mp 144-145 ºC. ^{1}H NMR (CD_3OD) δ 2.15 (qn, 2H, *J* = 7.1 Hz), 2.50 (t, 2H, *J* = 7.1 Hz), 4.37 (t, 2H, *J* = 7.1 Hz), 7.55 (dd, 1H, *J* = 9.3, 1.5 Hz), 7.73 (dd, 1H, *J* = 9.3, 4.1 Hz), 8.39 (dd, 1H, *J* = 4.1, 1.5 Hz). HRMS (ESI) *m*/*z* calcd for $C_8H_{12}N_3O_2$ $[M - Cl]^+$ 182.0930, found 182.0919.

2.2.5.2. 4-(1,6-Dihydro-6-imino-3-phenylpyridazin-1-yl)butanoic acid hydrochloride (4b)

Yield 11% (for three steps), mp 265-267 ºC (dec). ^{1}H NMR (CD_3OD) δ 2.23 (qn, 2H, *J* = 6.9 Hz), 2.56 (t, 2H, *J* = 6.9 Hz), 4.46 (t, 2H, *J* = 6.9 Hz), 7.53-7.56 (m, 3H), 7.64 (d, 1H, *J* = 9.5 Hz), 7.98-8.00 (m, 2H), 8.32 (d, 1H, *J* = 9.5 Hz). HRMS (ESI) *m*/*z* calcd for $C_{14}H_{16}N_3O_2$ $[M - Cl]^+$ 258.1243, found 258.1235.

2.2.5.3. 4-[1,6-Dihydro-6-imino-3-(4-methoxyphenyl)pyridazin-1-yl)butanoic acid hydrochloride (4c) (Gabazine)

Yield 18% (for three steps), mp 199-201 ºC. ^{1}H NMR (CD_3OD) δ 2.22 (qn, 2H, *J* = 7.0 Hz), 2.55 (t, 2H, *J* = 7.0 Hz), 3.87 (s, 3H), 4.43 (t, 2H, *J* = 7.0 Hz), 7.07 (dd, 2H, *J* = 6.9, 2.0 Hz),

7.59 (d, 1H, *J* = 9.6 Hz), 7.95 (dd, 2H, *J* = 6.9, 2.0 Hz), 8.28 (d, 1H, *J* = 9.6 Hz). HRMS (ESI) *m*/*z* calcd for $C_{15}H_{18}N_3O_3$ $[M - Cl]^+$ 288.1348, found 288.1329.

2.2.5.4. 4-[1,6-Dihydro-6-imino-3-(3,4-methylenedioxyphenyl)pyridazin-1-yl)butanoic acid hydrochloride (4d)

Yield 19% (for three steps), mp 214-215 ºC. ^{1}H NMR (CD_3OD) δ 2.21 (qn, 2H, *J* = 6.9 Hz), 2.55 (t, 2H, *J* = 6.9 Hz), 4.42 (t, 2H, *J* = 6.9 Hz), 6.06 (s, 2H), 6.97 (dd, 1H, *J* = 7.6, 1.3 Hz), 7.52 (dd, 2H, *J* = 7.6, 1.3 Hz), 7.57 (d, 1H, *J* = 9.8 Hz), 8.25 (d, 1H, *J* = 9.8 Hz). HRMS (ESI) *m*/*z* calcd for $C_{15}H_{16}N_3O_4$ $[M - Cl]^+$ 302.1141, found 302.1142.

2.2.5.5. 4-[1,6-Dihydro-6-imino-3-(4-trifluoromethylphenyl)pyridazin-1-yl)butanoic acid hydrochloride (4e)

Yield 17% (for three steps), mp 257-260 ºC (dec). ^{1}H NMR (CD_3OD) δ 2.25 (qn, 2H, *J* = 6.9 Hz), 2.57 (t, 2H, *J* = 6.9 Hz), 4.49 (t, 2H, *J* = 6.9 Hz), 7.68 (d, 1H, *J* = 9.7 Hz), 7.86 (d, 2H, *J* = 8.8 Hz), 8.19 (d, 2H, *J* = 8.8 Hz), 8.38 (d, 1H, *J* = 9.7 Hz). HRMS (ESI) *m*/*z* calcd for $C_{15}H_{15}F_3N_3O_2$ $[M - Cl]^+$ 326.1116, found 326.1102.

2.2.5.6. 4-[1,6-Dihydro-3-(4-biphenylyl)-6-iminopyridazin-1-yl)butanoic acid hydrochloride (4f)

Yield 21% (for three steps), mp 234-236 ºC. ^{1}H NMR (CD_3OD) δ 2.24 (qn, 2H, *J* = 6.9 Hz), 2.57 (t, 2H, *J* = 6.9 Hz), 4.47 (t, 2H, *J* = 6.9 Hz), 7.39 (t, 1H, *J* = 6.8 Hz), 7.47-7.50 (m, 2H), 7.64 (d, 1H, *J* = 9.6 Hz), 7.68-7.71 (m, 2H), 7.81 (dd, 2H, *J* = 6.8, 2.0 Hz), 8.08 (dd, 2H, *J* = 6.8, 2.0 Hz), 8.37 (d, 1H, *J* = 9.6 Hz). HRMS (ESI) *m*/*z* calcd for $C_{20}H_{20}N_3O_2$ $[M - Cl]^+$ 334.1556, found 334.1537.

2.2.5.7. 4-[1,6-Dihydro-6-imino-3-(4-phenoxyphenyl)pyridazin-1-yl)butanoic acid hydrochloride (4g)

Yield 50% (for three steps), mp 208-210 ºC. ^{1}H NMR (CD_3OD) δ 2.22 (qn, 2H, *J* = 6.9 Hz), 2.55 (t, 2H, *J* = 6.9 Hz), 4.44 (t, 2H, *J* = 6.9 Hz), 7.06-7.10 (m, 4H), 7.18-7.22 (m, 1H), 7.39-7.44 (m, 2H), 7.61 (d, 1H, *J* = 9.6 Hz), 7.98-8.00 (m, 2H), 8.30 (d, 1H, *J* = 9.6 Hz). HRMS (ESI) *m*/*z* calcd for $C_{20}H_{20}N_3O_3$ $[M - Cl]^+$ 350.1505, found 350.1479.

2.2.5.8. 4-[1,6-Dihydro-6-imino-3-(1-naphthyl)pyridazin-1-yl)butanoic acid hydrochloride (4h)

Yield 23% (for three steps), mp 219-221 ºC. ^{1}H NMR (CD_3OD) δ 2.25 (qn, 2H, *J* = 6.9 Hz), 2.57 (t, 2H, *J* = 6.9 Hz), 4.47 (t, 2H, *J* = 6.9 Hz), 7.56-7.64 (m, 3H), 7.67-7.70 (m, 2H), 8.00-8.08 (m, 4H). HRMS (ESI) *m*/*z* calcd for $C_{18}H_{18}N_3O_2$ $[M - Cl]^+$ 308.1399, found 308.1405.

2.2.5.9. 4-[1,6-Dihydro-6-imino-3-(2-naphthyl)pyridazin-1-yl)butanoic acid hydrochloride (4i)

Yield 5% (for three steps), mp 199-201 ºC. ^{1}H NMR (CD_3OD) δ 2.26 (qn, 2H, *J* = 6.9 Hz), 2.59 (t, 2H, *J* = 6.9 Hz), 4.49 (t, 2H, *J* = 6.9 Hz), 7.57-7.62 (m, 2H), 7.66 (d, 1H, *J* = 9.8 Hz), 7.93-7.95 (m, 1H), 8.02 (d, 2H, *J* = 8.8 Hz), 8.12 (dd, 1H, *J* = 8.8, 2.0 Hz), 8.50 (d, 2H, *J* = 9.8 Hz). HRMS (ESI) *m*/*z* calcd for $C_{18}H_{18}N_3O_2$ $[M - Cl]^+$ 308.1399, found 308.1405.

2.2.5.10. 4-[1,6-Dihydro-3-(2-furyl)-6-iminopyridazin-1-yl)butanoic acid hydrochloride (4j)

Yield 34% (for three steps), mp 230-232 ºC (dec). ^{1}H NMR (CD_3OD) δ 2.19 (qn, 2H, *J* = 6.9 Hz), 2.54 (t, 2H, *J* = 6.9 Hz), 4.39 (t, 2H, *J* = 6.9 Hz), 6.68 (dd, 1H, *J* = 3.6, 1.8 Hz), 7.24

(dd, 1H, *J* = 3.6, 0.7 Hz), 7.59 (d, 1H, *J* = 9.5 Hz), 7.79 (dd, 1H, *J* = 1.8, 0.7 Hz), 8.15 (d, 1H, *J* = 9.5 Hz). HRMS (ESI) *m*/*z* calcd for $C_{12}H_{14}N_3O_3$ $[M - Cl]^+$ 248.1035, found 248.1041.

2.2.5.11. 4-[1,6-Dihydro-6-imino-3-(2-thienyl)pyridazin-1-yl)butanoic acid hydrochloride (4k)

Yield 23% (for three steps), mp 225-227 ºC. ^{1}H NMR (CD_3OD) δ 2.20 (qn, 2H, *J* = 6.9 Hz), 2.55 (t, 2H, *J* = 6.9 Hz), 4.37 (t, 2H, *J* = 6.9 Hz), 7.20 (dd, 1H, *J* = 5.1, 3.7 Hz), 7.57 (d, 1H, *J* = 9.5 Hz), 7.68 (dd, 1H, *J* = 5.1, 1.2 Hz), 7.81 (dd, 1H, *J* = 3.7, 1.2 Hz), 8.27 (d, 1H, *J* = 9.5 Hz). HRMS (ESI) *m*/*z* calcd for $C_{12}H_{14}N_3O_2S$ $[M - Cl]^+$ 264.0807, found 264.0802.

2.2.5.12. 4-[1,6-Dihydro-6-imino-3-(3-thienyl)pyridazin-1-yl)butanoic acid hydrochloride (4l)

Yield 21% (for three steps), mp 215-217 ºC. ^{1}H NMR (CD_3OD) δ 2.21 (qn, 2H, *J* = 6.9 Hz), 2.54 (t, 2H, *J* = 6.9 Hz), 4.41 (t, 2H, *J* = 6.9 Hz), 7.57-7.61 (m, 2H), 7.70 (dd, 1H, *J* = 5.1, 1.5 Hz), 8.19-8.20 (m, 1H), 8.27 (d, 1H, *J* = 9.3 Hz). HRMS (ESI) *m*/*z* calcd for $C_{12}H_{14}N_3O_2S$ $[M - Cl]^+$ 264.0807, found 264.0802.

2.2.6. FMP assays

A *Drosophila* S2 cell line expressing GABARs from SBPs (GenBank accession AB253526.1) or CCs (GenBank DD171257.1) was used in this assay. These stable cell lines were generated as previously reported.[18] The cells were washed and dispersed in a saline buffer (120 mM of NaCl, 5 mM of KCl, 2 mM of $CaCl_2$, 8 mM of $MgCl_2$, 10 mM of HEPES, and 32 mM of sucrose, adjusted to pH 7.2 with an NaOH solution), and aliquots (100 μL each) of this cell suspension (5 x 10^5 cells) were added to 96-well microplates for the fluorescent assay. After

10 min, the cells were spun down at 1400 rpm for 5 min and loaded with the FMP blue dye (Molecular Devices; 100 μL) at room temperature for 20 min. Gabazine and gabazine analogs were first dissolved in DMSO and diluted with a saline buffer. Gabazine or a gabazine analog in a saline buffer (25 μL) containing 1% DMSO was added to the cells in each well and incubated with for 74 s. Subsequently, GABA in a saline buffer (25 μL) was added to each well. GABA concentrations corresponding to the EC_{50}s for SBP and CC receptors (1.0 μM and 2.5 μM, respectively) were used for receptor activation. The fluorescent intensity at 560 nm, upon excitation at 530 nm, was monitored using a FlexStation II plate reader (Molecular Devices). The inhibition percentage was determined based on changes in fluorescence before (the average value for 20 s) and after (the maximal value after 10-60 s) the addition of GABA. Each assay was repeated twice, unless otherwise noted.

2.2.7. Electrophysiology

2.2.7.1. Isolation of neurons from ACs

The sixth abdominal ganglia were dissected from adult male ACs and were placed in Ca^{2+}-free saline containing 200 mM of NaCl, 3.1 mM of KCl, 4 mM of $MgCl_2$, 20 mM of D-glucose, and 10 mM of HEPES, adjusted to pH 7.4 with an NaOH solution. The ganglia were incubated for 20 min at 25 °C in Ca^{2+}-free saline containing collagenase (0.5 mg mL^{-1}) and trypsin (0.2 mg mL^{-1}) and were rinsed with Ca^{2+}-free saline twice. The ganglia were then placed in Ca^{2+}-containing saline (200 mM of NaCl, 3.1 mM of KCl, 4 mM of $MgCl_2$, 5 mM of $CaCl_2$, 20 mM of D-glucose, and 10 mM of HEPES-acid, adjusted to pH 7.4 with NaOH) supplemented with 10% fetal bovine serum (Invitrogen). The neurons were dissociated using a pipette tip. The dissociated neurons were kept on coverslips coated with poly-D-lysine solution (1 mg mL^{-1},

Sigma-Aldrich) for 45 min. The neurons were incubated at 25 °C for 16 h before whole-cell current recordings.

2.2.7.2. Whole-cell patch clamp analysis

Membrane currents were recorded with the whole-cell recording arrangement using a patch clamp amplifier (EPC-8; HEKA) at 20 °C. The AC neurons were perfused continuously with an external solution containing 200 mM of NaCl, 3.1 mM of KCl, 4 mM of $MgCl_2$, 5 mM of $CaCl_2$, 25 mM of D-glucose, and 10 mM of HEPES-acid, adjusted to pH 7.4 by an NaOH solution (405 mOsm L^{-1}). The recording electrodes had a resistance of 3-5 MΩ when filled with the pipette solution containing 15 mM of NaCl, 170 mM of KCl, 1 mM of $MgCl_2$, 0.5 mM of $CaCl_2$, 10 mM of EGTA, 10 mM of HEPES, and 5 mM of ATP, adjusted to pH 7.4 by an NaOH solution (405 mOsm L^{-1}). GABA, gabazine, and its analogs were dissolved in the external solution. The external solution surrounding the cells was completely changed with a solution containing GABA or antagonists within 2 s. Sixth abdominal ganglion neurons were incubated 2 min in a cockroach saline solution followed by the 2-3-s application of 30 μM GABA (a concentration corresponding to the EC_{50} for AC receptors). GABA-induced currents were measured at a holding potential of -60 mV. This process was repeated 2 or 3 times to confirm the constant amplitude of GABA-induced currents. After this process, the neurons were perfused with a bath solution containing gabazine or a gabazine analog, and during the perfusion, GABA was repeatedly applied 5 times to obtain the highest and constant inhibition. Finally, GABA was applied to confirm the integrity of the cell. Each assay was repeated three or four times.

2.2.8. Molecular modeling and ligand docking studies

The homology model of the HF GABAR was generated using the X-ray crystal structure of the *C. elegans* glutamate-gated chloride channel (GluCl, PDB: 3RIF) as a template.[19] MOE 2010.10 software (Chemical Computing Group) was used to create the model. The sequence of the HF GABAR Rdl_{bd} subunit (accession No. AB177547) was retrieved from GenBank. The alignment of the two protein sequences was carried out using ClustalW software. Geometry optimization was performed using the AMBER99 force field. The structures of the zwitter ion forms of GABA and **4f** used in the docking studies were created using the Molecule Builder of MOE. Compound **4f** was docked as a protonated imino form, although it exists as resonance forms.[20] The created ligands were docked into the potential binding site of the generated model using ASEDock 2011.01.27 software (Chemical Computing Group). The energy of the receptor and ligands was minimized using the MMFF94x force field. The potential docking site was searched using the Site Finder of MOE. The stable conformations of ligands were obtained by the conformational search. Tether weight was added to all receptor backbone atoms within 4.5 Å from a ligand, while others were free. The binding mode with the highest score was chosen for the final representation.

2.3. Results and discussion

2.3.1. Chemistry

In this study, I synthesized a series of IP derivatives of GABA, which consisted of 4-(1,6-dihydro-6-iminopyridazin-1-yl)butanoic acids, by modifying the 3-position of the pyridazine ring of gabazine (Fig. 2.1). Wermuth and coworkers first described a seven-step synthetic approach including pyridazinone intermediates for **4b**, **4c** (gabazine, SR95531), **4k**, and **4l**.[21] The synthesis

of **4d** was reported by Melikian and coworkers,[22] which also required seven synthetic steps. Recently, Gavande and coworkers described a four-step synthesis procedure for **4c** under microwave irradiation conditions starting with 3,6-dichloropyridazine.[23] Here, I have demonstrated an efficient three-step synthesis of eleven 3-aryl/heteroaryl analogs starting with 3-amino-6-chloropyridazine, and a two-step synthesis of a 3-unsubstituted analog from 3-aminopyridazine (Fig. 2.1). The first intermediates of nine analogs (**1b-1i, 1l**) were synthesized in 19-78% yields using the Suzuki-Miyaura cross-coupling reaction where aryl/heteroarylboronic acid was coupled with 3-amino-6-chloropyridazine in presence of a palladium catalyst and a base such as sodium carbonate. The first intermediates of two analogs (**1j**, **1k**) were synthesized in a 73% and a 75% yield, respectively, using the Stille cross-coupling reaction between tributyl(heteroaryl)tin and 3-amino-6-chloropyridazine in the presence of a palladium catalyst. The *N*(2)-alkylated compounds **2a-2l** in the second step were synthesized in 11-74% yields by the reactions between **1a-1l** and ethyl 4-bromobutanoate. Free base esters of the alkylated compounds **3a-3l** were prepared in 77-93% yields from **2a-2l** using K_2CO_3. Hydrolysis of the free base esters was carried out in acetic acid and hydrochloric acid at 100 °C in 63-97% yields to give the target compounds **4a-4l**.

2.3.2. Antagonism of SBP and CC GABARs

The application of GABA to membrane potential probe-loaded cells expressing GABARs increases fluorescence, which is detected by FMP assays.[24,25] Antagonist activity can be assessed from a fluorescence reduction induced by a co-applied compound. When tested at 100 μM, an analog with no substituent at the 3-position of the pyridazine ring (**4a**) showed no or little antagonism against SBP and CC GABARs (Figs. 2.2 and 2.3). The introduction of a phenyl

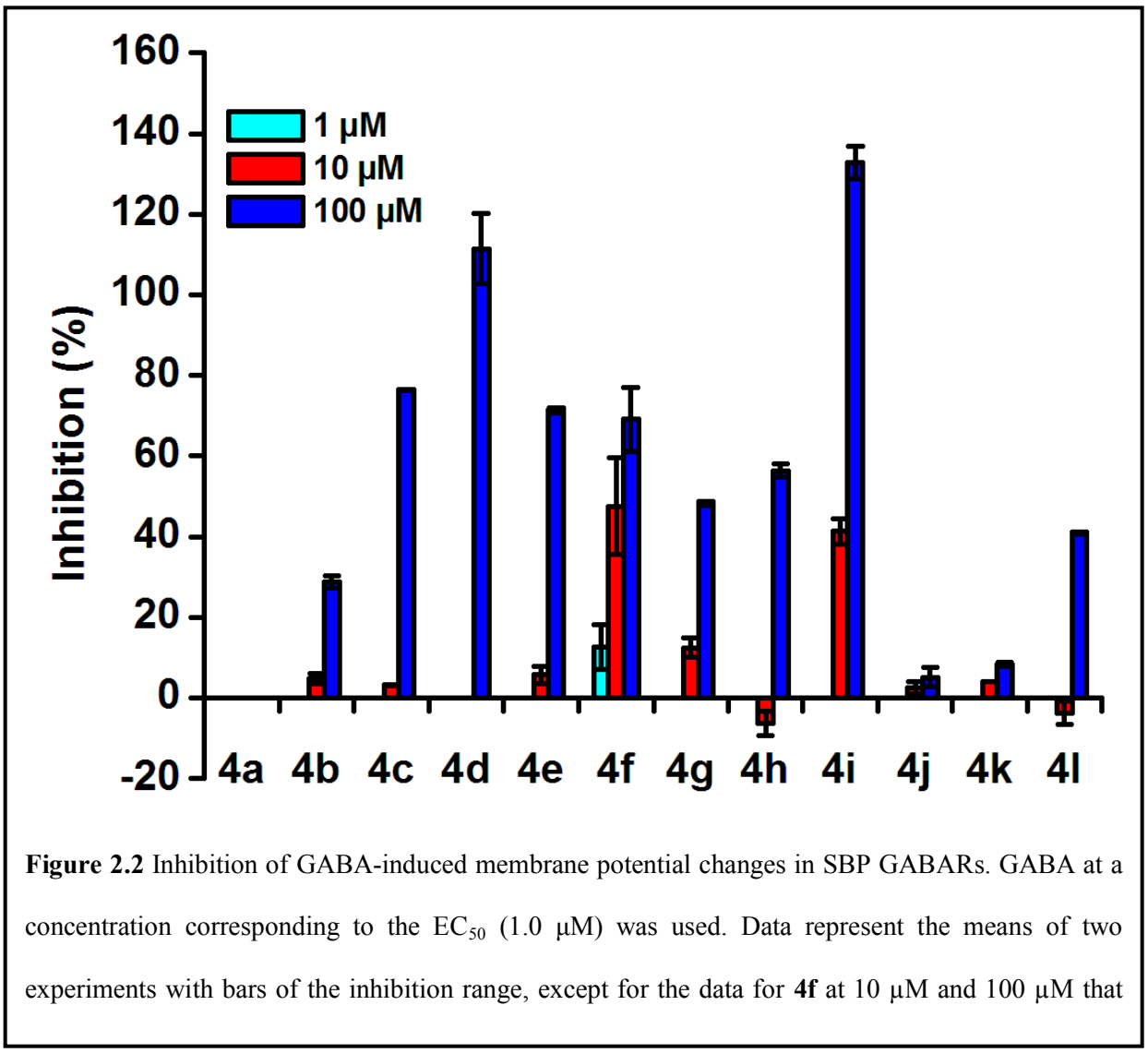

Figure 2.2 Inhibition of GABA-induced membrane potential changes in SBP GABARs. GABA at a concentration corresponding to the EC_{50} (1.0 μM) was used. Data represent the means of two experiments with bars of the inhibition range, except for the data for **4f** at 10 μM and 100 μM that

group into the 3-position of **4a** led to **4b** with weak activity. The inclusion of a methoxy group at the 4-position of the phenyl group of **4b** to give gabazine (**4c**) resulted in a 2.7- and 3.3-fold increase in the inhibition of GABA-induced fluorescence increases in SBP and CC receptors, respectively. The replacement of the 4-methoxy group of **4c** with a 3,4-methylenedioxy group, yielding **4d**, led to complete inhibition and 85.8% inhibition in SBP and CC GABARs, respectively. The antagonist activity of the 4-trifluoromethylphenyl analog (**4e**) was comparable to that of the 4-methoxyphenyl analog (**4c**) in SBP receptors but **4e** showed lower activity than

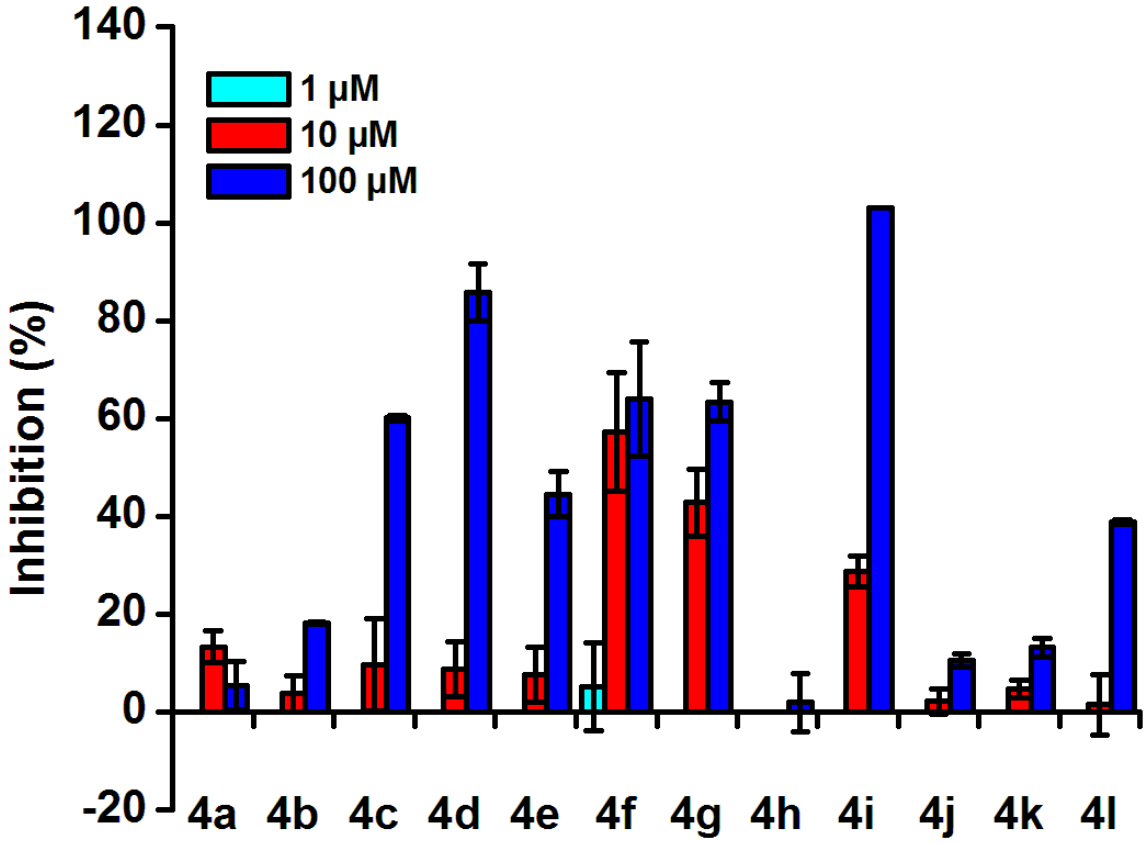

Figure 2.3 Inhibition of GABA-induced membrane potential changes in CC GABARs. GABA at a concentration corresponding to the EC_{50} (2.5 μM) was used. Data represent the means of two experiments with bars of the inhibition range, except for the data for **4f** at 10 μM and 100 μM that

4c in CC receptors. The 4-biphenylyl analog (**4f**) did not exceed **4c** in terms of antagonist activity at 100 μM in SBP receptors and showed inhibition comparable to that of **4c** in CC receptors, but it is notable that **4f** showed a moderate activity even at 10 μM in both receptors. The 4-phenoxyphenyl analog (**4g**) was inferior to the 4-biphenylyl analog (**4f**) in SBP receptors whereas they are comparable in CC receptors. While the 1-naphthyl analog (**4h**) was only moderately active or inactive at 100 μM in SBP and CC receptors, the 2-naphthyl analog (**4i**) completely inhibited GABA-induced responses at 100 μM in both receptors and showed

approximately 41% and 29% inhibition at 10 μM in SBP and CC receptors, respectively. Thus, the 2-naphthyl substitution is preferable to the 1-naphthyl substitution; the naphthyl ring of **4h** may provide a significant amount of steric hindrance for binding to the site. The 2-naphthyl analog (**4i)** per se showed agonist-like activity (i.e., caused an increase in fluorescence) at 100 μM, and co-application of GABA failed to induce an increase in fluorescence (data not shown). The substitution of the 3-substituent with 2-furyl and 2-thienyl groups to yield **4j** and **4k** nearly eliminated the antagonist activity. Substitution with a 3-thienyl group produced an analog (**4l**) with moderate activity in both receptors.

Finally, I examined whether competitive GABAR antagonism leads to insecticidal activity against SBP and CC larvae. While showing significant antagonism against the GABARs of these insects, the 4-biphenylyl analog (**4f**) did not exert insecticidal effects (data not shown), indicating that higher *in vitro* potency is necessary for insecticidal activity.

2.3.3. Antagonism of AC GABARs

The antagonism of native AC GABARs by the synthesized analogs was measured using the whole-cell patch-clamp technique. Figure 2.4A shows that GABA-induced currents are inhibited by the 4-biphenylyl analog (**4f**). After the confirmation of the constant amplitude of GABA-induced currents in neurons, the neurons were perfused with an external solution containing 500 μM **4f**. During the perfusion, GABA was repeatedly applied five times. This analog attenuated the currents progressively, and a maximum inhibition of 92.0% was attained after the third application. The other analogs were also tested in this fashion.

The phenyl (**4b**) and 4-methoxyphenyl (**4c**; gabazine) analogs were not effective against the AC GABAR when tested at 500 μM (Fig. 2.4B). This finding is in agreement with a previous

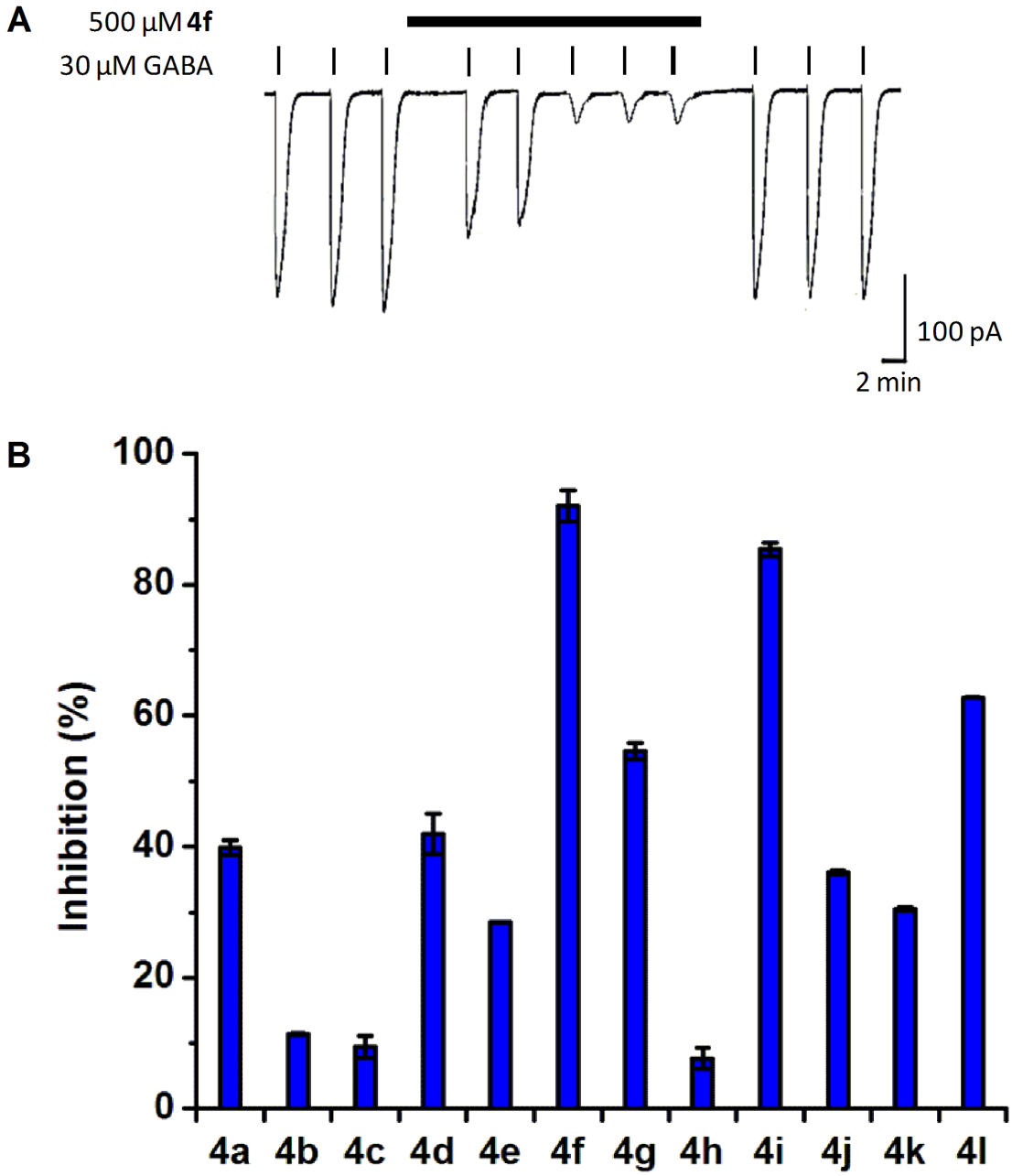

Figure 2.4 Inhibition of GABA-induced currents in AC GABARs. (A) Application protocol represented by current traces of inhibition by 500 μM of **4f**. (B) Inhibition by 500 μM of gabazine and its analogs. GABA at a concentration corresponding to the EC_{50} (30 μM) was used. Data are the means ± standard deviations of three or four experiments.

finding with **4c** tested at 10 μM by a patch clamp technique using AC brain neurons.[26] The analog lacking a 3-substituent (**4a**) demonstrated greater inhibition rather than **4c**. The low activity of **4c** is unexpected when compared with the 3,4-methylenedioxyphenyl (**4d**) and 4-trifluoromethylphenyl (**4e**) analogs, which showed moderate activity. The replacement of the 3-substituent with a 3,4-methylenedioxyphenyl group to give **4d** resulted in a 4-fold increase in inhibition when compared with **4c**. An analog with a 4-trifluoromethylphenyl group (**4e**) showed 3-fold greater inhibition than **4c**. Among the synthesized compounds, the 4-biphenylyl analog (**4f**) showed the greatest activity, with a 92.0% inhibition, an approximately 10-fold increase compared to **4c**. The 4-phenoxyphenyl analog (**4g**) showed approximately 6-fold enhanced inhibition when compared with **4c**, but decreased inhibition compared with **4f**. The introduction of a 1-naphthyl group to yield **4h** resulted in a drop in inhibition. In contrast, the 2-naphthyl analog (**4i**) displayed 9-fold greater inhibition than **4c**. The high activity of **4f** and **4i** suggests that long aromatic substituents at the 3-position of the pyridazine ring are tolerated. The replacement of the 4-methoxyphenyl group of **4c** with 5-membered heteroaromatic substituents to give **4j**, **4k**, and **4l** increased the inhibition percentage by 3- to 6-fold. The 3-thienyl analog (**4l**) showed a relatively high activity among analogs with a heteroaromatic 3-substituent, indicating that the lone-pair electrons on the heteroatom of the analog at this position may provide some favorable electronegative effects toward receptor interaction. Overall, the inhibition pattern of AC GABARs by the analogs differs from that of SBP and CC receptors, suggesting the existence of structural differences in the binding sites between insect species.

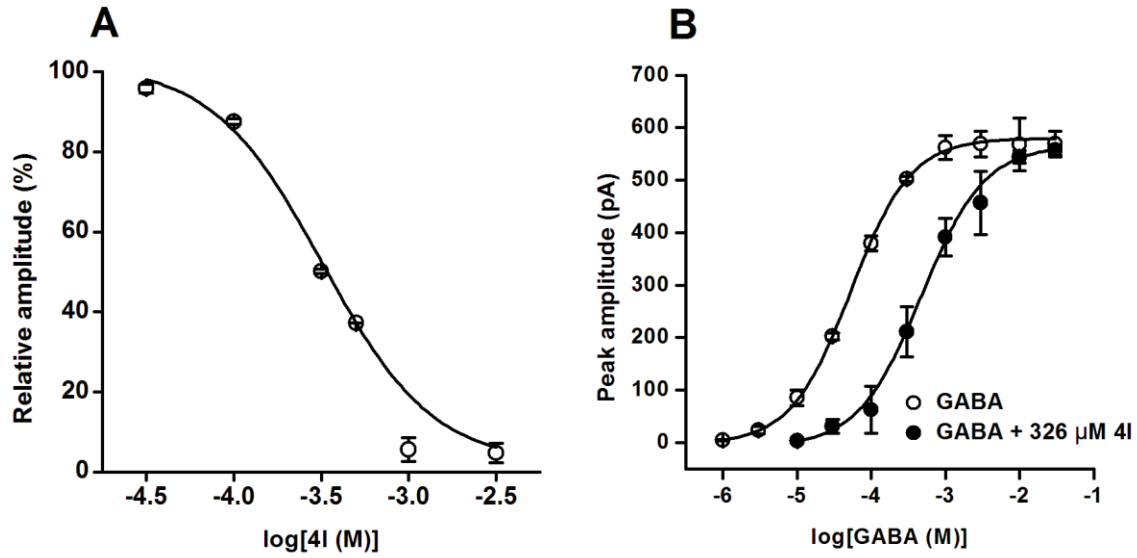

Figure 2.5 Action of **4l** on AC GABA receptors. The receptors were activated by 30 µM GABA. (A) Concentration-dependent inhibition of GABA-induced currents by **4l**. (B) GABA concentration-response curves in the presence (filled circles) and absence (open circles) of 326 µM of **4l**. Data represent the mean ± standard deviation of three experiments.

2.3.4. Mode of antagonism

To determine whether the synthesized compounds act as competitive antagonists, I examined the GABA concentration-response relationships in the presence and absence of a selected analog, **4l**, in AC neurons. The IC_{50} value of **4l** was determined to be 346 ± 18 (SD) µM (n =3) from its concentration-response relationships (Fig. 2.5A). The GABA concentration-response curve in the presence of **4l** showed a parallel rightward shift relative to that in the absence of **4l** (Fig. 2.5B), indicating that **4l** is a competitive antagonist.

2.3.5. Homology modeling and ligand docking

The orthosteric binding site in Cys-loop receptors is located at the extracellular interface between the principal and complementary faces of adjacent subunits.[27] Loops A–C from the principal face and loops D–F from the complementary face jointly form the GABA binding site. To examine the mechanisms of the interaction of gabazine analogs with insect GABARs, I performed ligand docking studies using a homology model. The zwitter ion forms of GABA and the 4-biphenylyl analog (**4f**) were docked into a homology model of the HF GABAR constructed using the X-ray crystal structure of the *C. elegans* GluCl as a template.[19] I used the HF GABAR for homology modeling in the present study, because the full-length gene encoding the AC GABAR subunit has not been cloned and the amino acid sequence of the HF GABAR Rdl_{bd} subunit (GenBank accession AB177547) has a high shared identity (71.1%) with a partial sequence of the AC GABAR Rdl (GenBank accession FJ612451).

In the docking of GABA into the orthosteric site, which is formed by six loops designated A–F,[28] the side chain of Glu202 and the backbone carbonyl oxygen atom of Ser203 in loop B were predicted to function as hydrogen acceptors for the protonated amino group of GABA (Fig. 2.6A). Arg109 in loop D and Ser174 in loop E serve as hydrogen donors for the carboxylate anion of GABA. Phe204 in loop B and Tyr252 in loop C likely exist near the protonated amino group of GABA (Fig. 2.6A). These aromatic amino acids may have cation/π interactions with it, as was recently suggested for the *Drosophila* GABAR.[29] Amino acids at the equivalent positions are implicated in GABA binding in the $GABA_AR$.[30]

In the docking of the 4-biphenylyl analog (**4f**) into the orthosteric site, amino acid residues similar to those presumed to be involved in GABA binding were predicted to interact with the

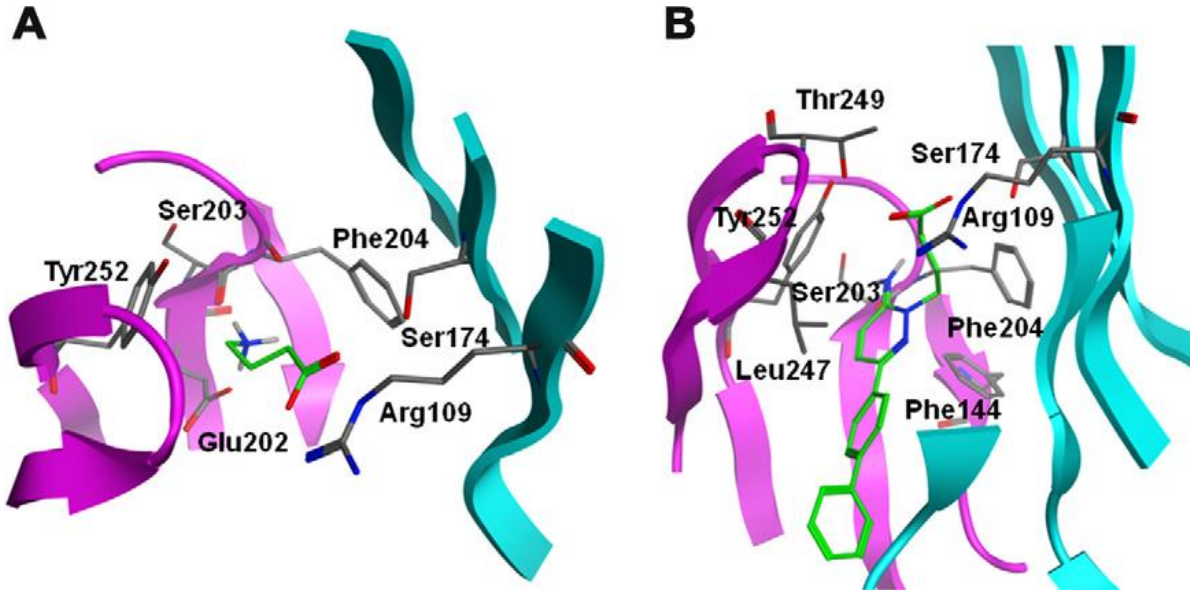

Figure 2.6 Homology modeling and docking simulation. (A) Docking of GABA into the orthosteric site of a HF GABAR homology model. (B) Docking of **4f**.

carboxyl group and the imino group (Fig. 2.6B). Hydrogen bonding of the dissociated carboxyl and protonated imino groups of gabazine analogs with neighboring amino acid residues (Arg109, Ser174, Ser203, and Phe204) appeared to play a major role in the binding of gabazine analogs (Fig. 2.6B). The backbone carbonyl group of Phe204 in loop B was predicted to function as an acceptor for the imino hydrogen atom in place of Glu202, which interacts with GABA. The amino acid of the rat $GABA_AR$ α1 subunit that is equivalent to Arg109 has been implicated in interacting with gabazine.[31] However, the location of bound gabazine seems to differ from that in our predicted binding pocket.

The docking studies of **4f** predict that its large 3-substituent is tolerable in the potential orthosteric binding site. The model shows that hydrophobic interactions predominate in the area that accommodates the 3-substituents of the analogs. The phenyl group at one end of the **4f**

molecule is likely exposed outside the receptor. Tyr88, Leu90, Tyr107, Val146, Val224, Arg254, Ile245, and Leu247 are predicted to contribute to encompassing the 3-substituent of gabazine analogs. The aromatic 3-substituents may form CH/π interactions with Val146 in loop A and Leu247 in loop C. In the rat $GABA_ARs$ and $GABA_CRs$, amino acid residues equivalent to Tyr107 and Phe111 in loop D and Phe144 in loop A were reported to contribute to gabazine binding.[32,33] Tyr107 and Phe144 are found near the **4f** molecule in the docking model, but Phe111 is away from the binding pocket. It is of interest to note that in the rat GABARs, gabazine sensitivity depended on whether amino acids at the 107- and 144-positions are phenylalanine or tyrosine and that the three insect GABARs used in the present study contain the same amino acids at the 107- and 144-positions as the $GABA_CR$, which has low affinity for gabazine. In addition to Phe144, Val146, a nearby amino acid in loop A, faces the **4f** molecule, which is consistent with the finding that a homologous amino acid lines the GABA binding pocket of the rat receptor.[34] In the model, Val180 in loop F exists at the position where the apex phenyl group of **4f** interacts. This finding is consistent with the finding that this region of loop F in the rat $GABA_AR$ was identified as a region lining the GABA binding site.[35]

2.4. Conclusion

In this study, I synthesized gabazine analogs that are more potent than gabazine against insect GABARs, but their potency levels are still low compared with the levels reported with $GABA_ARs$.[31] Analogs with nanomolar affinity for $GABA_ARs$ and an analog with low micromolar affinity for $GABA_CRs$ have recently been reported.[36,37] Information from ligand docking studies with a homology model using the *C. elegans* GluCl X-ray structure as a template proved to be useful for studying the receptor-ligand interaction. Analogs with higher potencies for insect GABARs may be obtained by further modification of gabazine.

References

1. Hevers, W.; Lüddens, H. The diversity of GABAA receptors. Pharmacological and electrophysiological properties of $GABA_A$ channel subtypes. *Mol. Neurobiol.* **1998**, *18*, 35−86.
2. Bettler, B.; Kaupmann, K.; Mosbacher, J.; Gassmann, M. Molecular structure and physiological functions of $GABA_B$ receptors. *Physiol. Rev.* **2004**, *84*, 835−867.
3. Sine, S. M.; Engel, A. G. Recent advances in Cys-loop receptor structure and function. *Nature* **2006**, *440*, 448−455.
4. Whiting, P. J.; Bonnert, T. P.; McKernan, R. M.; Farrar, S.; Le Bourdellés, B.; Heavens, R. P.; Smith, D. W.; Hewson, L.; Rigby, M. R.; Sirinathsinghji, D. J. S.; Thompson, S. A.; Wafford, K. A. Molecular and functional diversity of the expanding GABA-A receptor gene family. *Ann. N. Y. Acad. Sci.* **1999**, *868*, 645−653.
5. Johnston, G. A. R. $GABA_A$ receptor pharmacology. *Pharmacol. Ther.* **1996**, *69*, 173−198.
6. Krishek, B. J.; Moss, S. J.; Smart, T. G. A functional comparison of the antagonists bicuculline and picrotoxin at recombinant $GABA_A$ receptors. *Neuropharmacology* **1996**, *35*, 1289−1298.
7. Buckingham, S. D.; Sattelle, D. B. In *Comprehensive Molecular Insect Science*; Gilbert, L. I.; Iatrou, K.; Gill, S. S., Eds.; Elsevier Pergamon: Amsterdam, 2004; Vol. 5, pp. 107−142.
8. ffrench-Constant, R. H.; Rocheleau, T. A.; Steichen, J. C.; Chalmers, A. E. A point mutation in a *Drosophila* GABA receptor confers insecticide resistance. *Nature* **1993**, *363*, 449−451.
9. Mezler, M.; Müller, T.; Raming, K. Cloning and functional expression of $GABA_B$ receptors from *Drosophila*. *Eur. J. Neurosci.* **2001**, *13*, 477−486.

10. Gisselmann, G.; Plonka, J.; Pusch, H.; Hatt, H. *Drosophila melanogaster* GRD and LCCH3 subunits form heteromeric GABA-gated cation channels. *Br. J. Pharmacol.* **2004**, *142*, 409−413.
11. Buckingham, S. D.; Biggin, P. C.; Sattelle, B. M.; Brown, L. A.; Sattelle, D. B. Insect GABA receptors: splicing, editing, and targeting by antiparasitics and insecticides. *Mol. Pharmacol.* **2005**, *68*, 942−951.
12. Ozoe, Y.; Takeda, M.; Matsuda, K. In *Biorational Control of Arthropod Pests*; Ishaaya, I.; Horowitz, A. R., Eds.; Springer: Heidelberg, 2009; pp. 131−162.
13. Raymond-Delpech, V.; Matsuda, K.; Sattelle, B. M.; Rauh, J. J.; Sattelle, D. B. Ion channels: molecular targets of neuroactive insecticides. *Invert. Neurosci.* **2005**, *5*, 119−133.
14. Ueno, S.; Bracamontes, J.; Zorumski, C.; Weiss, D. S.; Steinbach, J. H. Bicuculline and gabazine are allosteric inhibitors of channel opening of the $GABA_A$ receptor. *J. Neurosci.* **1997**, *17*, 625−634.
15. Chambon, J.-P.; Feltz, P.; Heaulme, M.; Restle, S.; Schlichter, R.; Biziere, K.; Wermuth, C. G. An arylaminopyridazine derivative of γ-aminobutyric acid (GABA) is a selective and competitive antagonist at the $GABA_A$ receptor site. *Proc. Natl. Acad. Sci. USA* **1985**, *82*, 1832−1836.
16. Hosie, A. M.; Sattelle, D. B. Agonist pharmacology of two *Drosophila* GABA receptor splice variants. *Br. J. Pharmacol.* **1996**, *119*, 1577−1585.
17. Satoh, H.; Daido, H.; Nakamura, T. Preliminary analysis of the GABA-induced current in cultured CNS neurons of the cutworm moth, *Spodoptera litura*. *Neurosci. Lett.* **2005**, *381*, 125−130.

18. Narusuye, K.; Nakao, T.; Abe, R.; Nagatomi, Y.; Hirase, K.; Ozoe, Y. Molecular cloning of a GABA receptor subunit from *Laodelphax striatella* (Fallén) and patch clamp analysis of the homo-oligomeric receptors expressed in a *Drosophila* cell line. *Insect Mol. Biol.* **2007**, *16*, 723−733.
19. Hibbs, R. E.; Gouaux, E. Principles of activation and permeation in an anion-selective Cys-loop receptor. *Nature* **2011**, *474*, 54−60.
20. Van der Brempt, C.; Evrard, G.; Durant, F. Structure of an aminopyridazine derivative. *Acta Cryst*. **1986**, *C42*, 1206−1208.
21. Wermuth, C.-G.; Bourguignon, J.-J.; Schlewer, G.; Gies, J.-P.; Schoenfelder, A.; Melikian, A.; Bouchet, M.-J.; Chantreux, D.; Molimard, J.-C.; Heaulme, M.; Chambon, J.-P.; Biziere, K. Synthesis and structure-activity relationships of a series of aminopyridazine derivatives of γ-aminobutyric acid acting as selective GABA-A antagonists. *J. Med. Chem.* **1987**, *30*, 239−249.
22. Melikian, A.; Schlewer, G.; Chambon, J.-P.; Wermuth, C. G. Condensation of muscimol or thiomuscimol with aminopyridazines yields GABA-A antagonists. *J. Med. Chem.* **1992**, *35*, 4092−4097.
23. Gavande, N.; Johnston, G. A. R.; Hanrahan, J. R.; Chebib, M. Microwave-enhanced synthesis of 2,3,6-trisubstituted pyridazines: application to four-step synthesis of gabazine (SR-95531). *Org. Biomol. Chem.* **2010**, *8*, 4131−4136.
24. Schroeder, K. S.; Neagle, B. D. FLIPR: a new instrument for accurate, high throughput optical screening. *J. Biomol. Screen.* **1996**, *1*, 75−80.
25. Joesch, C.; Guevarra, E.; Parel, S. P.; Bergner, A.; Zbinden, P.; Konrad, D.; Albrecht, H. Use of FLIPR membrane potential dyes for validation of high-throughput screening with the

FLIPR and μARCS technologies: identification of ion channel modulators acting on the $GABA_A$ receptor. *J. Biomol. Screen.* **2008**, *13*, 218−228.

26. Aydar, E.; Beadle, D. J. The pharmacological profile of GABA receptors on cultured insect neurons. *J. Insect Physiol.* **1999**, *45*, 213−219.
27. Miller, P. S.; Smart, T. G. Binding, activation and modulation of Cys-loop receptors. *Trends Pharmacol. Sci.* **2010**, *31*, 161−174.
28. Sander, T.; Frølund, B.; Bruun, A. T.; Ivanov, I.; McCammon, J. A.; Balle, T. New insights into the $GABA_A$ receptor structure and orthosteric ligand binding: receptor modeling guided by experimental data. *Proteins* **2011**, *79*, 1458−1477.
29. Lummis, S. C. R.; McGonigle, I.; Ashby, J. A.; Dougherty, D. A. Two amino acid residues contribute to a cation-π binding interaction in the binding site of an insect GABA receptor. *J. Neurosci.* **2011**, *31*, 12371−12376.
30. Amin, J.; Weiss, D. S. $GABA_A$ receptor needs two homologous domains of the β-subunit for activation by GABA but not by pentobarbital. *Nature* **1993**, *366*, 565−569.
31. Holden, J. H.; Czajkowski, C. Different residues in the $GABA_A$ receptor α_1T60-α_1K70 region mediate GABA and SR-95531 actions. *J. Biol. Chem.* **2002**, *277*, 18785−18792.
32. Sigel, E.; Baur, R.; Kellenberger, S.; Malherbe, P. Point mutations affecting antagonist affinity and agonist dependent gating of $GABA_A$ receptor channels. *EMBO J.* **1992**, *11*, 2017−2023.
33. Zhang, J.; Xue, F.; Chang, Y. Structural determinants for antagonist pharmacology that distinguish the ρ1 $GABA_C$ receptor from $GABA_A$ receptors. *Mol. Pharmacol.* **2008**, *74*, 941−951.

34. Boileau, A. J.; Newell, J. G.; Czajkowski, C. $GABA_A$ receptor β_2 Tyr^{97} and Leu^{99} line the GABA-binding site. *J. Biol. Chem.* **2002**, 277, 2931−2937.

35. Newell, J. G.; Czajkowski, C. The $GABA_A$ receptor α_1 subunit Pro^{174}-Asp^{191} segment is involved in GABA binding and channel gating. *J. Biol. Chem.* **2003**, *278*, 13166−13172.

36. Iqbal, F.; Ellwood, R.; Mortensen, M.; Smart T. G.; Baker, J. R. Synthesis and evaluation of highly potent $GABA_A$ receptor antagonists based on gabazine (SR-95531). *Bioorg. Med. Chem. Lett.* **2011**, *21*, 4252−4254.

37. Yamamoto, I.; Carland, J. E.; Locock, K.; Gavande, N.; Absalom, N.; Hanrahan, J. R.; Allan, R. D.; Johnston, G. A. R.; Chebib, M. Structurally diverse GABA antagonists interact differently with open and closed conformational states of the ρ_1 receptor. *ACS Chem. Neurosci.* **2012**, *3*, 293−301.

CHAPTER 3

Synthesis of 1,3-di- and 1,3,4-trisubstituted IPs as competitive antagonists of insect GABARs

3.1. Introduction

GABA, the primary inhibitory neurotransmitter in the central nervous system of mammals, mediates inhibitory neurotransmission through two types of receptors: ionotropic and metabotropic.[1-4] The ionotropic GABAR belongs to the Cys-loop receptor family of ligand-gated ion channels, including nicotinic acetylcholine, glycine, and serotonin type 3 receptors.[5,6] Ionotropic GABARs are categorized into two types: hetero-pentameric $GABA_A$Rs, which consist of α1-6, β1-3, γ1-3, δ, ε, θ, and π subunits, and homo-pentameric $GABA_C$Rs, which include ρ1-3 subunits.[7,8] Each subunit consists of a large extracellular GABA-binding domain, a transmembrane domain containing four α-helical segments, and a large intracellular loop. The second transmembrane segments of five subunits form a central chloride channel pore.[9] The $GABA_A$Rs that contain two α subunits, two β subunits, and one γ subunit are the most abundant subtype in the adult brain.[7,10] GABA or an agonist binds to the orthosteric binding site in the extracellular interface between the α and β subunits of $GABA_A$Rs, which triggers the opening of the channel, thus enhancing chloride permeability through the neuronal membrane and inhibiting the generation of action potentials. The orthosteric agonist binding site is composed of six discontinuous loops, A–F, located in adjacent subunits; loops A–C are in the principal subunit and loops D–F are in the complementary subunit.[9] Competitive antagonists, which share a common binding site with the agonist GABA, stabilize the closed conformation of the channel.

$GABA_A$Rs represent targets for clinically important drugs such as benzodiazepines, barbiturates, neurosteroids, and anesthetics.[11]

In insects, GABARs play important physiological roles not only in the nervous system but also in the peripheral tissues.[12,13] The insect ionotropic GABAR consists of five Rdl subunits.[12-14] The Rdl transcript is alternatively spliced at exons 3 and 6 to produce four variant subunits (Rdl_{ac}, Rdl_{ad}, Rdl_{bc}, and Rdl_{bd}). Insect GABARs represent important targets for insecticides and parasiticides.[12,13,15] Phenylpyrazole insecticides, such as fipronil, exert insecticidal effects by acting as noncompetitive antagonists.[16] However, the development of resistance to fipronil due to its extensive use has been reported in several insect species.[17-19] Although two novel classes of insecticidal GABAR antagonists, isoxazolines and 3-benzamido-*N*-phenylbenzamides, have recently been reported,[20-23] there are continuing efforts to develop novel insecticides that inhibit GABAR functions. High-affinity competitive antagonists for insect GABARs could also be potential insecticides. Bicuculline and gabazine (SR 95531) (Fig. 1.6) represent competitive antagonists of mammalian $GABA_A$Rs.[24,25] However, a potent competitive antagonist for insect GABARs is not available. Whereas bicuculline is inactive against most insect GABARs, gabazine shows weak or moderate antagonistic activity against insect GABARs.[26-28] It has been previously reported that the introduction of substituents at the 5-position of pyridazine ring of gabazine produces competitive antagonists with micromolar-affinity against the parasitic nematode *Ascaris suum*, whereas the 5-substitutent is detrimental to rat GABARs.[29,30] This selectivity is informative in terms of the design of insecticides. In the previous study described in Chapter 2, I synthesized 1,6-dihydro-6-iminopyridazines (IPs) in which the 3-position of the pyridazine ring of gabazine was modified (Fig. 1.6), and enhanced antagonism of insect GABARs were observed.[31] These findings prompted the synthesis of other analogs. Here, I

describe the synthesis of 1,3-di- and 1,3,4-trisubstituted IPs and their antagonism of GABARs cloned from two agricultural insect pest species and a sanitary insect species. In this new synthesis, I examined the effects of the carboxylate bioisosteres at the 1-position on the antagonist potency of IP derivatives in insect GABARs.

3.2. Materials and Methods

3.2.1. Chemicals

Reagents were obtained from Wako Pure Chemical Industries, Ltd. (Osaka, Japan) and Tokyo Chemical Industry Co., Ltd. (Tokyo, Japan), unless otherwise noted. Intermediates **6a**, **6d**, **6f**, and **6g** were available from the Chapter 2. Namgel NAM-200H (Nagara Science) was used for the purification of **8** and **9**.

3.2.2. Instruments

The melting points of synthesized compounds were determined on a cover glass with a Yanagimoto MP-500D apparatus and are uncorrected. ^{1}H NMR spectra were recorded on a JEOL JNM-A 400 spectrometer. Chemical shifts (δ values) are given in ppm relative to tetramethylsilane (TMS) and the *J* values are given in Hertz. Spin multiplicities are expressed as follows: s (singlet), d (doublet), t (triplet), q (quartet), qn (quintet), and m (multiplet). High-resolution mass spectrometry (HRMS) analyses were performed on a Waters SYNAPT G2 spectrometer using the positive electrospray ionization mode.

3.2.3. Synthesis of 3-amino-6-chloro-5-cyclobutylpyridazine (1)

Water (20 mL) and H_2SO_4 (0.40 mL, 1.5 mol eqv., sp. gr. = 1.84) were added to 3-amino-6-chloropyridazine (648 mg, 5.0 mmol). The mixture was heated to 70 °C for 10 min.

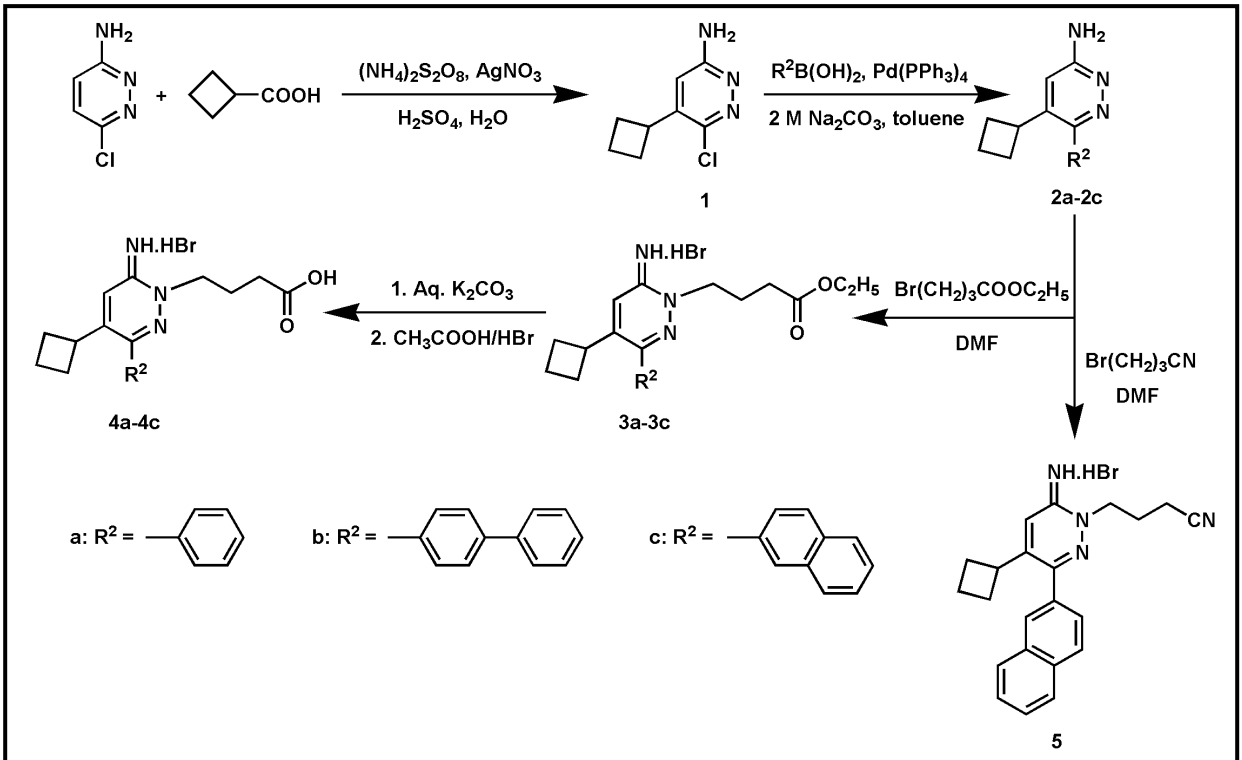

Figure 3.1 Synthesis of 4-(3-aryl-4-cyclobutyl-1,6-dihydro-6-iminopyridazin-1-yl)butanoic acid hydrobromide salts (**4a-4c**) and 4-[4-cyclobutyl-1,6-dihydro-6-imino-3-(2-naphthyl)pyridazin-1-yl]butyronitrile hydrobromide (**5**).

Cyclobutanecarboxylic acid (1.15 g, 2.3 mol eqv.) and $AgNO_3$ (85 mg, 0.1 mol eqv.) were then added to the mixture. The reaction mixture was stirred under an argon atmosphere for 15 min, and a solution of ammonium persulfate (1.71 g, 1.5 mol eqv.) in H_2O (10 mL) was added *via* a syringe over 5 min. The reaction mixture was heated at 70 °C for 15 h. The reaction mixture was then transferred into a flask containing ice and was basified to pH 8-9 with aqueous ammonia. The product was extracted with CH_2Cl_2 (3 x 100 mL). The combined organic layer was dried over anhydrous Na_2SO_4 and filtered. The solvent was evaporated under reduced pressure to dryness. The residue was purified by column chromatography on silica gel to give 3-amino-6-

chloro-5-cychlobutylpyridazine (**1**). Yield 18%, mp 155-157 °C. ^{1}H NMR (DMSO-d_6) δ 1.77-1.79 (m, 1H), 1.92-2.07 (m, 3H), 2.32-2.38 (m, 2H), 3.43-3.45 (m, 1H), 6.27 (s, 2H), 7.22 (s, 1H).

3.2.4. General procedure for the synthesis of 3-amino-6-aryl-5-cyclobutylpyridazine (2a-2c)

A mixture of **1** (183.5 mg, 1.0 mmol), arylboronic acid (1.5 mmol), tetrakis(triphenylphosphine)palladium(0) (35 mg), and a 2 M Na_2CO_3 solution (1.1 mL) in toluene (10 mL) was stirred under an argon atmosphere for 30 min at room temperature. The reaction mixture was then heated under reflux with stirring in an argon atmosphere until the starting material disappeared (~48 h). After cooling, the reaction mixture was concentrated to dryness under reduced pressure. EtOAc (30 mL) was added to the flask containing the residue, and the flask was placed in an ultrasonic bath for 5 min. The mixture was filtered and the filter paper was washed thoroughly with EtOAc (100 mL). The combined filtrate was concentrated to dryness under reduced pressure. The residue was purified by silica gel column chromatography to yield 3-amino-6-aryl-5-cyclobutylpyridazine (**2a-2c**).

3.2.4.1. 3-Amino-5-cyclobutyl-6-phenylpyridazine (2a)

Yield 13% (for two steps), mp 166-168 °C. ^{1}H NMR (CD_3OD) δ 1.88-1.98 (m, 1H), 2.09-2.26 (m, 3H), 2.45-2.52 (m, 2H), 3.48-3.56 (m, 1H), 7.39-7.49 (m, 3H), 7.60 (d, 1H, J = 1.5 Hz), 7.87-7.90 (m, 2H).

3.2.4.2. 3-Amino-6-(4-biphenylyl)-5-cyclobutylpyridazine (2b)

Yield 13% (for two steps), mp 175-177 °C. ^{1}H NMR (CD_3OD) δ 1.92-1.96 (m, 1H), 2.13-2.27 (m, 3H), 2.46-2.53 (m, 2H), 3.49-3.55 (m, 1H), 7.32-7.37 (m, 1H), 7.43-7.47 (m, 2H), 7.65-7.68 (m, 3H), 7.73-7.75 (m, 2H), 7.98-8.00 (m, 2H).

3.2.4.3. 3-Amino-5-cyclobutyl-6-(2-naphthyl)pyridazine (2c)

Yield 16% (for two steps), mp 172-174 °C. ^{1}H NMR (DMSO-d_6) δ 1.84-1.88 (m, 1H), 1.98-2.18 (m, 1H), 2.21-2.23 (m, 2H), 2.41-2.46 (m, 2H), 3.48-3.54 (m, 1H), 6.19 (s, 2H), 7.50-7.56 (m, 2H), 7.79 (s, 1H), 7.93 (d, 1H, J = 7.6 Hz), 7.99 (d, 1H, J = 8.8 Hz), 8.03 (d, 1H, J = 7.6 Hz), 8.27 (d, 1H, J = 8.8 Hz), 8.55 (s, 1H).

3.2.5. General procedure for the synthesis of ethyl 4-(3-aryl-4-cyclobutyl-1,6-dihydro-6-iminopyridazin-1-yl)butanoate hydrobromide (3a-3c)

A mixture of **2a**, **2b**, or **2c** (1 mmol), ethyl 4-bromobutanoate (292 mg, 1.5 mmol), and DMF (0.5 mL) was heated at 80 °C until the starting material disappeared (~40 h). After cooling, the precipitate was collected and washed with EtOAc (5 mL). The residue was recrystallized from MeOH and EtOAc to give ethyl 4-(3-aryl-4-cyclobutyl-1,6-dihydro-6-iminopyridazin-1-yl)butanoate hydrobromide (**3a-3c**).

3.2.5.1. Ethyl 4-(4-cyclobutyl-1,6-dihydro-6-imino-3-phenylpyridazin-1-yl)butanoate hydrobromide (3a)

Yield 8% (for three steps), mp 208-210 °C. ^{1}H NMR (CD_3OD) δ 1.12 (t, 3H, J = 7.1 Hz), 1.95-2.01 (m, 1H), 2.19-2.38 (m, 5H), 2.52-2.60 (m, 4H), 3.66-3.71 (m, 1H), 3.99 (q, 2H, J = 7.1 Hz), 4.51 (t, 2H, J = 7.1 Hz), 7.55-7.56 (m, 3H), 8.01-8.04 (m, 2H), 8.08 (d, 1H, J = 1.5 Hz).

3.2.5.2. Ethyl 4-[3-(4-biphenylyl)-4-cyclobutyl-1,6-dihydro-6-iminopyridazin-1-yl]butanoate hydrobromide (3b)

Yield 9% (for three steps), mp 204-206 °C. ^{1}H NMR (CD_3OD) δ 1.13 (t, 3H, *J* = 7.1 Hz), 1.97-2.02 (m, 1H), 2.17-2.37 (m, 5H), 2.54-2.62 (m, 4H), 3.68-3.72 (m, 1H), 4.01 (q, 2H, *J* = 7.1 Hz), 4.52 (t, 2H, *J* = 6.8 Hz), 7.37-7.41 (m, 1H), 7.46-7.50 (m, 2H), 7.69-7.71 (m, 2H), 7.81-7.83 (m, 2H), 8.11-8.13 (m, 3H).

3.2.5.3. Ethyl 4-[4-cyclobutyl-1,6-dihydro-6-imino-3-(2-naphthyl)pyridazin-1-yl]butanoate hydrobromide (3c)

Yield 5% (for three steps), mp 212-214 °C. ^{1}H NMR (CD_3OD) δ 1.09 (t, 3H, *J* = 7.1 Hz), 1.98-2.03 (m, 1H), 2.18-2.36 (m, 3H), 2.38-2.43 (m, 2H), 2.55-2.63 (m, 4H), 3.71 (t, 1H, *J* = 8.3 Hz), 3.99 (q, 2H, *J* = 7.1 Hz), 4.54 (t, 2H, *J* = 6.8 Hz), 7.57-7.60 (m, 2H), 7.93-7.95 (m, 1H), 8.01-8.05 (m, 2H), 8.13 (dd, 1H, *J* = 6.8, 2.0 Hz), 8.26 (d, 1H, *J* = 1.0 Hz), 8.58 (s, 1H).

3.2.6. General procedure for the synthesis of 4-(3-aryl-4-cyclobutyl-1,6-dihydro-6-iminopyridazin-1-yl)butanoic acid hydrobromide (4a-4c)

Compound **3a**, **3b**, or **3c** (200 mg) was dissolved in a minimal amount of aqueous K_2CO_3 solution to yield an alkaline solution. The solution was then extracted with a 1:1 mixture of EtOAc and Et_2O. The organic layer was dried over anhydrous Na_2SO_4 and filtered. The filtrate was concentrated under reduced pressure to give free base ester. Hydrobromic acid in AcOH (10 mL, 30%) was added to the free base ester and heated at 100 °C for ~12 h. After cooling, the reaction mixture was concentrated to dryness under reduced pressure. The residue was recrystallized with MeOH and EtOAc to afford 4-(3-aryl-4-cyclobutyl-1,6-dihydro-6-iminopyridazin-1-yl)butanoic acid hydrobromide (**4a-4c**).

3.2.6.1. 4-(4-Cyclobutyl-1,6-dihydro-6-imino-3-phenylpyridazin-1-yl)butanoic acid hydrobromide (4a)

Yield 7% (for four steps), mp 181-183 °C. ^{1}H NMR (CD_3OD) δ 1.95-2.10 (m, 1H), 2.09-2.23 (m, 3H), 2.27-2.37 (m, 4H), 2.53-2.60 (m, 2H), 3.63-3.71 (m, 1H), 4.48 (t, 2H, J = 7.8 Hz), 7.53-7.55 (m, 3H), 8.00-8.03 (m, 3H). HRMS (ESI) m/z calcd for $C_{18}H_{22}N_3O_2$ ([M - Br])$^+$, 312.1712; found, 312.1727.

3.2.6.2. 4-[3-(4-Biphenylyl)-4-cyclobutyl-1,6-dihydro-6-iminopyridazin-1-yl]butanoic acid hydrobromide (4b)

Yield 6% (for four steps), mp 217-219 °C. ^{1}H NMR (CD_3OD) δ 1.98-2.02 (m, 1H), 2.15-2.40 (m, 5H), 2.54-2.60 (m, 4H), 3.66-3.75 (m, 1H), 4.52 (t, 2H, J = 7.3 Hz), 7.37-7.41 (m, 1H), 7.46-7.49 (m, 2H), 7.69 (d, 2H, J = 8.8 Hz), 7.80-7.83 (m, 2H), 8.11-8.13 (m, 3H). HRMS (ESI) m/z calcd for $C_{24}H_{26}N_3O_2$ (M - Br)$^+$, 388.2025; found, 388.2024.

3.2.6.3. 4-[4-Cyclobutyl-1,6-dihydro-6-imino-3-(2-naphthyl)pyridazin-1-yl]butanoic acid hydrobromide (4c)

Yield 4% (for four steps), mp 218-220 °C. ^{1}H NMR (CD_3OD) δ 1.95-2.02 (m, 1H), 2.18-2.33 (m, 3H), 2.35-2.42 (m, 2H), 2.57-2.61 (m, 4H), 3.66-3.75 (m, 1H), 4.53 (t, 2H, J = 7.1 Hz), 7.56-7.61 (m, 2H), 7.92-7.94 (m, 1H), 8.00-8.05 (m, 2H), 8.12-8.15 (m, 1H), 8.24 (d, 1H, J = 1.0 Hz), 8.58 (s, 1H). HRMS (ESI) m/z calcd for $C_{22}H_{24}N_3O_2$ ([M - Br])$^+$, 362.1869; found, 362.1893.

3.2.7. Synthesis of 4-[4-cyclobutyl-1,6-dihydro-6-imino-3-(2-naphthyl)pyridazin-1-yl]butyronitrile hydrobromide (5)

A mixture of **2c** (275 mg, 1.0 mmol), 4-bromobutyronitrile (178 mg, 1.2 mmol), and DMF (0.5 mL) was heated at 80 °C until the starting material disappeared (~20 h). After cooling, the precipitate was collected and washed with EtOAc (5 mL). The residue was recrystallized from MeOH and EtOAc to give 4-[4-cyclobutyl-1,6-dihydro-6-imino-3-(2-naphthyl)pyridazin-1-yl]butyronitrile hydrobromide (**5**). Yield 10% (for three steps), mp 228-230 °C. ^{1}H NMR (DMSO-d_6) δ 1.87-1.90 (m, 1H), 2.03-2.10 (m, 1H), 2.17-2.23 (qn, 2H, J = 6.3 Hz), 2.28-2.35 (m, 2H), 2.49-2.50 (m, 2H), 2.67-2.70 (m, 2H), 3.63-3.67 (m, 1H), 4.43 (t, 2H, J = 6.3 Hz), 7.59-7.62 (m, 2H), 7.98-8.00 (m, 1H), 8.05-8.07 (m, 3H), 8.11-8.17 (m, 1H), 8.69 (s, 1H). HRMS (ESI) m/z calcd for $C_{22}H_{23}N_4$ $(M - Br)^+$, 343.1923; found, 343.1944.

3.2.8. General procedure for the synthesis of 3-amino-6-(aryl/heteroaryl)pyridazine (6a-6g)

A mixture of 3-amino-6-chloropyridazine (388 mg, 3.0 mmol), aryl/heteroarylboronic acid (4.5 mmol), tetrakis(triphenylphosphine)palladium(0) (105 mg), and a 2 M Na_2CO_3 solution (3.3 mL) in toluene (30 mL) was stirred in an argon atmosphere at room temperature for 30 min. The reaction mixture was then heated under reflux with stirring in an argon atmosphere until the starting material disappeared (~70 h). After cooling, the reaction mixture was concentrated to dryness under reduced pressure. EtOAc (80 mL) was added to the residue, and the flask containing the suspension was placed in an ultrasonic bath for 5 min. The mixture was filtered, and the filter paper was washed thoroughly with EtOAc (200 mL). The combined filtrate was concentrated to dryness under reduced pressure. The residue was purified by silica gel column

chromatography to yield 3-amino-6-aryl/heteroarylpyridazine (**6a-6g**). It is noted that the intermediates that appeared in Chapter 2 are renumbered in this Chapter.

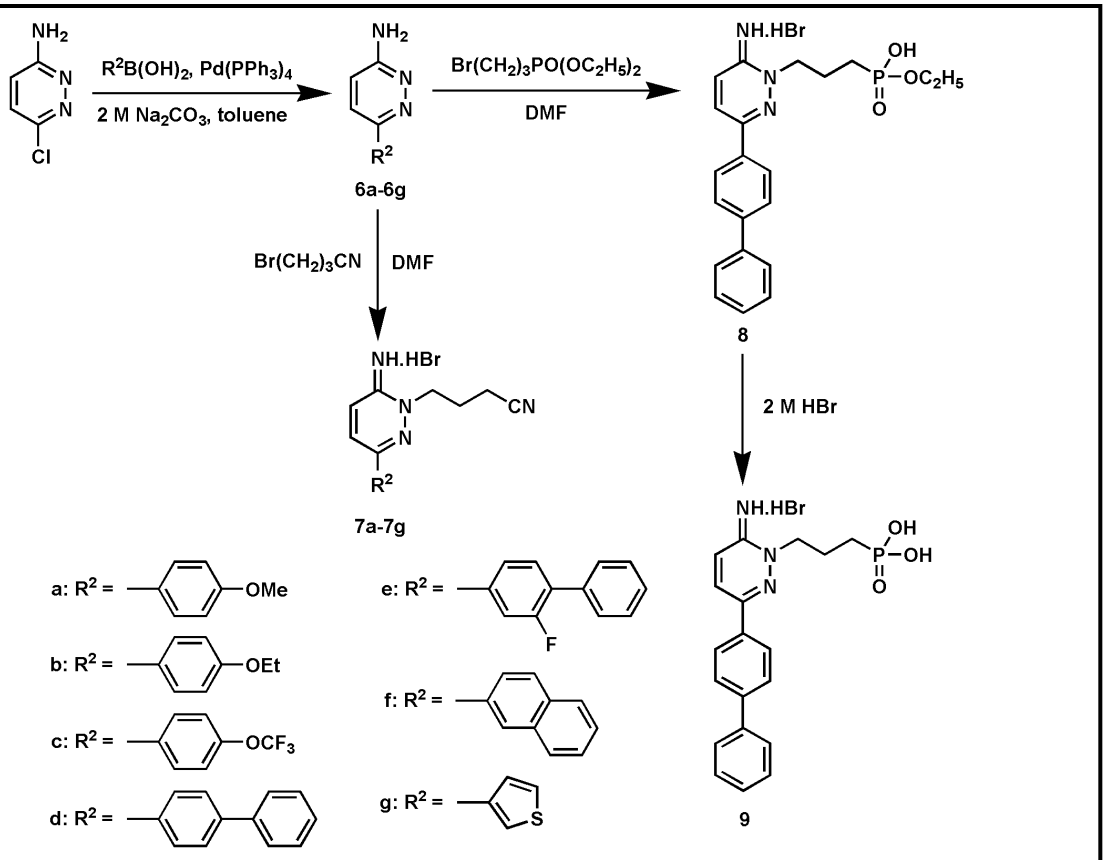

Figure 3.2 Synthesis of 4-(3-aryl/heteroaryl-1,6-dihydro-6-iminopyridazin-1-yl)butyronitrile hydrobromide salts (**7a-7g**), ethyl 3-[3-(4-biphenylyl)-1,6-dihydro-6-iminopyridazin-1-yl]propylphosphonate hydrobromide (**8**), and 3-[3-(4-biphenylyl)-1,6-dihydro-6-iminopyridazin-1-yl]propylphosphonic acid hydrobromide (**9**).

3.2.8.1. 3-Amino-6-(4-methoxyphenyl)pyridazine (6a)

This intermediate appeared in Chapter 2, section 2.2.3.2.

3.2.8.2. 3-Amino-6-(4-ethoxyphenyl)pyridazine (6b)

Yield 59%, mp 151-153 °C. ^{1}H NMR (DMSO-d_6) δ 1.34 (t, 3H, J = 7.1 Hz), 4.07 (q, 2H, J = 7.1 Hz), 6.33 (s, 2H), 6.82 (d, 1H, J = 9.3 Hz), 6.99 (dd, 2H, J = 6.8, 2.0 Hz), 7.73 (d, 1H, J = 9.3 Hz), 7.87 (dd, 2H, J = 6.8, 2.0 Hz).

3.2.8.3. 3-Amino-6-(4-trifluoromethoxyphenyl)pyridazine (6c)

Yield 42%, mp 107-109 °C. ^{1}H NMR (DMSO-d_6) δ 6.55 (s, 2H), 6.87 (d, 1H, J = 9.3 Hz), 7.45 (d, 2H, J = 8.8 Hz), 7.84 (d, 1H, J = 9.3 Hz), 8.08 (d, 2H, J = 8.8 Hz).

3.2.8.4. 3-Amino-6-(4-biphenylyl)pyridazine (6d)

This intermediate appeared in Chapter 2, section 2.2.3.5.

3.2.8.5. 3-Amino-6-(2-fluoro-4-biphenylyl)pyridazine (6e)

Yield 64%, mp 154-156 °C. ^{1}H NMR (DMSO-d_6) δ 6.57 (s, 2H), 6.88 (d, 1H, J = 9.3 Hz), 7.42 (t, 1H, J = 6.8 Hz), 7.48-7.56 (m, 2H), 7.60-7.64 (m, 4H), 7.88-7.92 (m, 2H).

3.2.8.6. 3-Amino-6-(2-naphthyl)pyridazine (6f)

This intermediate appeared in Chapter 2, section 2.2.3.8.

3.2.8.7. 3-Amino-6-(3-thienyl)pyridazine (6g)

This intermediate appeared in Chapter 2, section 2.2.3.11.

3.2.9. General procedure for the synthesis of 4-[3-(aryl/heteroaryl)-1,6-dihydro-6-iminopyridazin-1-yl]butyronitrile hydrobromide (7a-7g)

A mixture of **6a**, **6b**, **6c**, **6d**, **6e**, **6f**, or **6g** (1 mmol), 4-bromobutyronitrile (178 mg, 1.2 mmol), and DMF (0.5 mL) was heated at 80 °C until the starting material disappeared (~15 h). After cooling, the precipitate was collected and washed with EtOAc (5 mL). The residue was recrystallized from MeOH and EtOAc to give 4-[3-(aryl/heteroaryl)-1,6-dihydro-6-iminopyridazin-1-yl]butyronitrile hydrobromide (**7a-7g**).

3.2.9.1. 4-[1,6-Dihydro-6-imino-3-(4-methoxyphenyl)pyridazin-1-yl]butyronitrile hydrobromide (7a)

Yield 33% (for two steps), mp 247-249 °C. ^{1}H NMR (DMSO-d_6) δ 2.19 (qn, 2H, J = 7.0 Hz), 2.67 (t, 2H, J = 7.0 Hz), 3.84 (s, 3H), 4.38 (t, 2H, J = 7.0 Hz), 7.11 (d, 2H, J = 8.8 Hz), 7.62 (d, 1H, J = 9.5 Hz), 7.95 (d, 2H, J = 8.8 Hz), 8.38 (d, 1H, J = 9.5 Hz), 9.02 (broad s, 2H). HRMS (ESI) m/z calcd for $C_{15}H_{17}N_4O$ $(M - Br)^+$, 269.1402; found, 269.1431.

3.2.9.2. 4-[1,6-Dihydro-3-(4-ethoxyphenyl)-6-iminopyridazin-1-yl]butyronitrile hydrobromide (7b)

Yield 48% (for two steps), mp 257-259 °C. ^{1}H NMR (DMSO-d_6) δ 1.36 (t, 3H, J = 7.0 Hz), 2.18 (qn, 2H, J = 7.0 Hz), 2.69 (t, 2H, J = 7.0 Hz), 4.12 (q, 2H, J = 7.0 Hz), 4.39 (t, 2H, J = 7.0 Hz), 7.10 (d, 2H, J = 8.8 Hz), 7.65 (d, 1H, J = 9.8 Hz), 7.95 (d, 2H, J = 8.8 Hz), 8.40 (d, 1H, J = 9.8 Hz), 9.09 (broad s, 2H). HRMS (ESI) m/z calcd for $C_{16}H_{19}N_4O$ $(M - Br)^+$, 283.1559; found, 283.1577.

3.2.9.3. 4-[1,6-Dihydro-6-imino-3-(4-trifluoromethoxyphenyl)pyridazin-1-yl]butyronitrile hydrobromide (7c)

Yield 29% (for two steps), mp 223-225 °C. ^{1}H NMR (DMSO-d_6) δ 2.20 (qn, 2H, J = 6.9 Hz), 2.69 (t, 2H, J = 6.9 Hz), 4.42 (t, 2H, J = 6.9 Hz), 7.58 (d, 2H, J = 7.8 Hz), 7.71 (d, 1H, J = 9.5 Hz), 8.13 (d, 2H, J = 7.8 Hz), 8.44 (d, 1H, J = 9.5 Hz), 9.22 (broad s, 2H). HRMS (ESI) m/z calcd for $C_{15}H_{14}F_3N_4O$ $(M - Br)^+$, 323.1120; found, 323.1116.

3.2.9.4. 4-[3-(4-Biphenylyl)-1,6-dihydro-6-iminopyridazin-1-yl]butyronitrile hydrobromide (7d)

Yield 28% (for two steps), mp 267-269 °C. ^{1}H NMR (DMSO-d_6) δ 2.21 (qn, 2H, J = 6.9 Hz), 2.72 (t, 2H, J = 6.9 Hz), 4.44 (t, 2H, J = 6.9 Hz), 7.43 (t, 1H, J = 7.4 Hz), 7.51 (t, 2H, J = 7.4 Hz), 7.72-7.78 (m, 3H), 7.89 (d, 2H, J = 8.3 Hz), 8.10 (d, 2H, J = 8.3 Hz), 8.50 (d, 1H, J = 9.3 Hz), 9.18 (broad s, 2H). HRMS (ESI) m/z calcd for $C_{20}H_{19}N_4$ $(M - Br)^+$, 315.1610; found, 315.1617.

3.2.9.5. 4-[1,6-Dihydro-3-(2-fluoro-4-biphenylyl)-6-iminopyridazin-1-yl]butyronitrile hydrobromide (7e)

Yield 37% (for two steps), mp 223-225 °C. ^{1}H NMR (DMSO-d_6) δ 2.21 (qn, 2H, J = 6.9 Hz), 2.71 (t, 2H, J = 6.9 Hz), 4.44 (t, 2H, J = 6.9 Hz), 7.46 (t, 1H, J = 7.2 Hz), 7.53 (t, 2H, J = 7.2 Hz), 7.63 (d, 2H, J = 7.2 Hz), 7.71-7.78 (m, 2H), 7.95-8.01 (m, 2H), 8.52 (d, 1H, J = 9.8 Hz), 9.27 (broad s, 2H). HRMS (ESI) m/z calcd for $C_{20}H_{18}FN_4$ $(M - Br)^+$, 333.1515; found, 333.1552.

3.2.9.6. 4-[1,6-Dihydro-6-imino-3-(2-naphthyl)pyridazin-1-yl]butyronitrile hydrobromide (7f)

Yield 12% (for two steps), mp 261-263 °C. ^{1}H NMR (DMSO-d_6) δ 2.24 (qn, 2H, J = 7.0 Hz), 2.72 (t, 2H, J = 7.0 Hz), 4.45 (t, 2H, J = 7.0 Hz), 7.63-7.66 (m, 2H), 7.71 (d, 1H, J = 9.3 Hz), 8.00-8.15 (m, 4H), 8.60 (d, 1H, J = 9.3 Hz), 8.63 (s, 1H), 9.17 (broad s, 2H). HRMS (ESI) m/z calcd for $C_{18}H_{17}N_4$ (M - Br)$^+$, 289.1453; found, 289.1489.

3.2.9.7. 4-[1,6-Dihydro-6-imino-3-(3-thienyl)pyridazin-1-yl]butyronitrile hydrobromide (7g)

Yield 35% (for two steps), mp 246-248 °C. ^{1}H NMR (DMSO-d_6) δ 2.17 (qn, 2H, J = 6.9 Hz), 2.68 (t, 2H, J = 6.9 Hz), 4.37 (t, 2H, J = 6.9 Hz), 7.66-7.69 (m, 2H), 7.76-7.78 (m, 1H), 8.37-8.40 (m, 2H), 9.14 (broad s, 2H). HRMS (ESI) m/z calcd for $C_{12}H_{13}N_4S$ (M - Br)$^+$, 245.0861; found, 245.0886.

3.2.10. Synthesis of ethyl 3-[3-(4-biphenylyl)-1,6-dihydro-6-iminopyridazin-1-yl]propylphosphonate hydrobromide (8)

A mixture of **6d** (247 mg, 1 mmol), diethyl (3-bromopropyl)phosphonate (328 mg (95%), 1.2 mmol), and DMF (0.5 mL) was heated at 80 °C until the starting material disappeared (72 h). After cooling, the precipitate was collected and washed with EtOAc (5 mL). The residue was purified by silica gel column chromatography (MeOH:EtOAc = 1:1) to yield ethyl 3-[3-(4-biphenylyl)-1,6-dihydro-6-iminopyridazin-1-yl]propylphosphonate hydrobromide (**8**). Yield 19% (for two steps), mp 161-163 °C. ^{1}H NMR (CD_3OD) δ 1.26 (t, 3H, J = 7.1 Hz), 1.66-1.74 (m, 2H), 2.16-2.28 (m, 2H), 3.94 (q, 2H, J = 7.1 Hz), 4.50 (t, 2H, J = 7.3 Hz), 7.38 (t, 1H, J = 7.4 Hz), 7.46 (t, 2H, J = 7.4 Hz), 7.59 (d, 1H, J = 9.6 Hz), 7.66 (d, 2H, J = 8.3 Hz), 7.77 (d, 2H, J = 8.3

Hz), 8.03 (d, 2H, J = 8.3 Hz), 8.28 (d, 1H, J = 9.6 Hz). HRMS (ESI) m/z calcd for $C_{21}H_{25}N_3O_3P$ $(M - Br)^+$, 398.1634; found, 398.1637.

3.2.11. Synthesis of 3-[3-(4-biphenylyl)-1,6-dihydro-6-iminopyridazin-1-yl]propylphosphonic acid hydrobromide (9)

A mixture of **8** (239 mg, 0.5 mmol) and 2 M hydrobromic acid (10 mL) was refluxed for 40 h. After cooling, the reaction mixture was concentrated to dryness under reduced pressure and washed with EtOAc (5 mL). The residue was purified by silica gel column chromatography (MeOH:EtOAc = 1:1) to yield 3-[3-(4-biphenylyl)-1,6-dihydro-6-iminopyridazin-1-yl]propylphosphonic acid hydrobromide (**9**). Yield 18% (for three steps), mp 290-293 °C. ^{1}H NMR (DMSO-d_6) δ 1.64-1.73 (m, 2H), 2.06-2.11 (m, 2H), 4.41 (t, 2H, J = 7.1 Hz), 7.43 (d, 1H, J = 7.4 Hz), 7.51 (t, 2H, J = 7.4 Hz), 7.67 (d, 1H, J = 9.3 Hz), 7.76 (d, 2H, J = 7.4 Hz), 7.89 (d, 2H, J = 8.3 Hz), 8.09 (d, 2H, J = 8.3 Hz), 8.47 (d, 1H, J = 9.3 Hz), 9.24 (broad s, 2H). HRMS (ESI) m/z calcd for $C_{19}H_{21}N_3O_3P$ $(M - Br)^+$, 370.1321; found, 370.1352.

3.2.12. FMP assays

Drosophila S2 cell lines stably expressing small brown planthopper (SBP, *Laodelphax striatellus*) and common cutworm (CC, *Spodoptera litura*) GABARs were created by transfecting respective Rdl_{bd} subunit cDNAs (DDBJ accession Nos. AB253526 and DD171257) as previously described.[28,32] FMP assays were performed using these cell lines as described in the previous Chapter.

3.2.13. Expression of HF GABARs in *Xenopus* oocytes and TEVC recordings

TEVC experiments were performed as previously reported.[33] After a mature female African clawed frog (*Xenopus laevis*) was anesthetized with 0.1% (w/v) ethyl *m*-aminobenzoate methanesulfonate, the ovarian lobes were surgically removed. The ovarian lobes were treated with collagenase (2 mg/mL; Sigma-Aldrich) in Ca^{2+}-free standard oocyte solution (SOS) (100 mM of NaCl, 2 mM of KCl, 1 mM of $MgCl_2$, 5 mM of HEPES, pH 7.6) for 90-120 min at room temperature. The oocytes were then gently washed with a sterile SOS (100 mM of NaCl, 2 mM of KCl, 1.8 mM of $CaCl_2$, 1 mM of $MgCl_2$, 5 mM of HEPES, pH 7.6) supplemented with 2.5 mM of sodium pyruvate, 50 μg of gentamycin/mL (Gibco), 100 U of penicillin/mL (Invitrogen) and 100 μg of streptomycin/mL (Invitrogen) and were incubated at 16 °C overnight in the buffer. The oocytes were injected with 5 ng of cRNA encoding the HF Rdl_{ac} subunit and were incubated under the same conditions for 2 days. The capped cRNA was synthesized using T7 polymerase (Ambion mMESSAGE mMACHINE T7 Ultra Kit), the primer pcDNA3-cRNAF (5'-CTC-TCT-GGC-TAA-CTA-GAG-AAC-C-3'), and cDNA encoding the ac variant of the HF GABAR subunit [DDBJ accession Nos. AB177547 (RDL_{bd}, complete cds), AB824728 (exon 3 a version, partial cds), and AB824729 (exon 6 c version, partial cds)].

GABA-induced currents were recorded using an OC-725C Oocyte Clamp amplifier (Warner Instruments) at a holding potential of -80 mV. The recorded currents were analyzed by Data-Trax2™ software (World Precision Instruments). The glass capillary electrodes were filled with 2 M of KCl and had a resistance of 0.5-1.5 MΩ at 18-22 °C. GABA was dissolved in SOS, and the IPs were dissolved in DMSO and then diluted by SOS to the final concentration (0.1% DMSO, v/v). After 10 μM (EC_{50}) of GABA was added to the oocytes a few times for 3 s to detect a control response, the IP solution was applied over 1 min before the following

applications of GABA and during the remainder of the experiments. The EC_{50} of GABA was applied repeatedly in the presence of an IP solution for 3 s at 1-min intervals until a maximum inhibition of GABA response was reached. The inhibition percentage was calculated from the ratio of the average of two minimum responses during the application of IP to the average of a few responses induced by 10 μM of GABA. EC_{50}s, Hill coefficients (n_Hs), and half maximal inhibitory concentrations (IC_{50}s) were obtained from concentration-response relationships by nonlinear regression analysis using OriginPro 8J software (Origin-Lab).

3.2.14. Homology modeling and docking simulation

A homology model of a homomeric HF GABAR containing Rdl_{ac} subunits was built using the X-ray crystal structure of the *C. elegans* GluCl (PDB: 3RIF) as a template.[34] The model was created using MOE 2011.10 software (Chemical Computing Group) according to the method described in Chapter 2. The structures of GABA and **7e** were created in the zwitterionic and protonated imino forms, respectively, using the MOE Builder.

3.3. Results and Discussion

3.3.1. Chemistry

In the present study, I synthesized thirteen IPs with various R^1, R^2, and R^3 substituents on the pyridazine ring, starting from 3-amino-6-chloropyridazine (Figs. 1.6, 3.1, and 3.2). The synthesized IPs are categorized into three types. The first type consists of the 3-substituted 1-(3-carboxypropyl)-4-cyclobutyl-IPs (**4a**-**4c**). The second type consists of a 3-substituted 1-cyanopropyl-4-cyclobutyl-IP (**5**) and the 3-substituted 1-cyanopropyl-IPs (**7a**-**7g**). The third type consists of a 3-substituted 1-(ethyl phosphonopropyl)-IP (**8**) and a 3-substituted 1-phosphonopropyl-IP (**9**).

Introduction of a cyclobutyl group onto the 5-position of 3-amino-6-chloropyridazine to afford **1** was achieved by the Minisci reaction with cyclobutanecarboxylic acid, albeit in a low (18%) yield (Fig. 3.1). The Suzuki-Miyaura cross-coupling reaction between **1** and arylboronic acid in the presence of a palladium catalyst afforded **2a**-**2c** in 70-88% yields. *N*(2)-Alkylation of **2a**-**2c** with ethyl 4-bromobutanoate provided **3a**-**3c** in 33-66% yields. Compounds **3a**-**3c** were then converted to free base esters by treatment with K_2CO_3, followed by hydrolysis in acetic acid and hydrobromic acid at 100 °C to give IPs **4a**-**4c** in 71-85% yields. The Suzuki-Miyaura cross-coupling reaction between 3-amino-6-chloropyridazine and aryl/heteroarylboronic acid gave **6a**-**6g** in 19-64% yields (Fig. 3.2). *N*(2)-Alkylation of **6a**-**6g** with 4-bromobutyronitrile afforded IPs **7a**-**7g** in 58-82% yields. *N*(2)-Alkylation of **2c** with 4-bromobutyronitrile produced IP **5** in a 65% yield (Fig. 3.1). *N*(2)-Alkylation of **6d** with diethyl (3-bromopropyl)phosphonate generated IP **8** in a 52% yield. The hydrolysis of **8** in a 2 M hydrobromic acid under reflux gave IP **9** in a 95% yield (Fig. 3.2).

3.3.2. Antagonism of SBP and CC GABARs

I first examined the IP antagonism of GABARs constituted from Rdl_{bd} subunits cloned from two agricultural insect pests, the SBP and the CC, that cause serious damage to crops. In these tests, I used FMP technology.[35,36] Application of GABA to *Drosophila* cell lines stably expressing SBP and CC GABARs induces chloride ion efflux and membrane depolarization, which is then recorded with a fluorescent dye loaded in the cells. The maximum increase in fluorescence was measured after the application of the EC_{50} of GABA to cells expressing GABARs. The levels of antagonism by IPs were evaluated as a decrease in fluorescence when IPs were applied simultaneously with GABA. When tested at 100 μM, IPs **4a**, **4b**, and **4c**, in which R^2 = phenyl, 4-biphenylyl, and 2-naphthyl, respectively, R^1 = COOH, and R^3 =

cyclobutyl, showed less than 50% inhibition of the GABA response in SBP and CC GABARs (Figs. 3.3 and 3.4). Previous study described in Chapter 2 showed that gabazine (R^1 = COOH, R^2 = 4-methoxyphenyl, and R^3 = H) exhibited 76.4% and 60.2% inhibition of the GABA response in SBP and CC GABARs, respectively, at 100 μM.[31] Therefore, the cyclobutyl group is detrimental in this case.

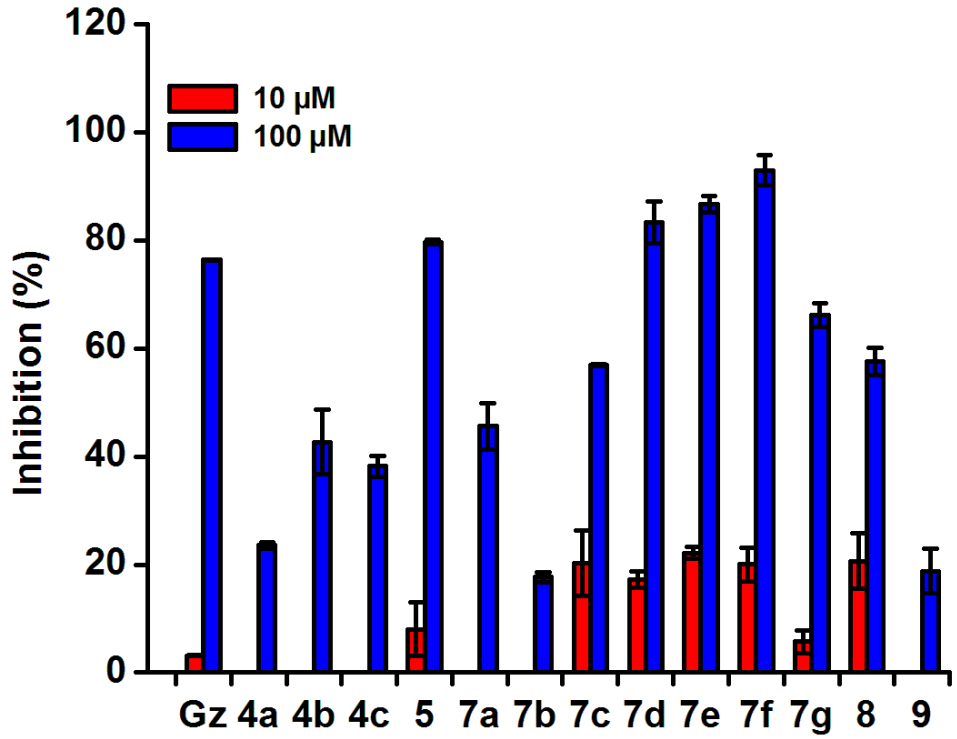

Figure 3.3 Inhibition of GABA-induced responses by IPs in SBP GABARs. Receptors were activated by 1.0 μM (EC_{50}) of GABA. Data represent the means of two experiments with bars indicating the range of duplicates. Inhibition percentages at 10 μM are shown for IPs with >50% inhibition at 100 μM. Inhibition data of gabazine (Gz) are taken from a previous report.[31]

Replacement of the carboxyl group of gabazine with a cyano group, affording **7a**, resulted in a 45.6% and a 73.1% inhibition of the GABA response in SBP and CC GABARs, respectively, at the same concentration, indicating that the carboxyl and cyano groups are bioisosteric in this case. While a dramatic change in activity was not observed with the carboxyl/cyano group substitution in insect GABARs, the conversion of gabazine to **7a** led to an ~8-fold increase in potency in human ρ1 GABARs.[37] IPs **7b** and **7c**, in which R^2 = 4-ethoxyphenyl and 4-trifluoromethoxyphenyl, respectively, R^1 = CN, and R^3 = H, displayed less than a 60% inhibition

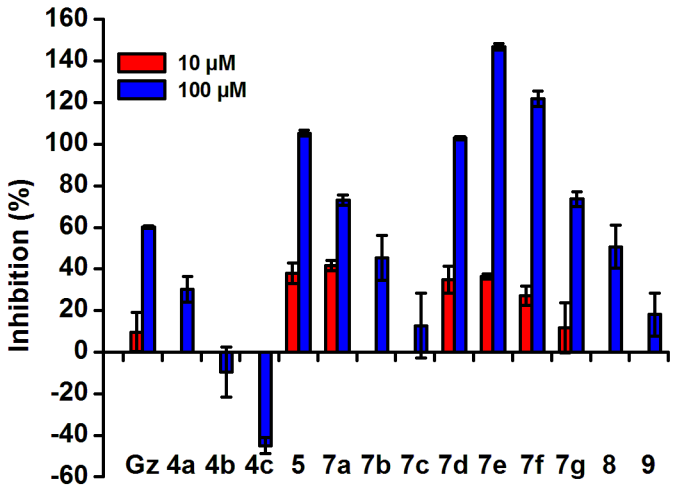

Figure 3.4 Inhibition of GABA-induced responses by IPs in CC GABARs. Receptors were activated by 2.5 µM (EC_{50}) of GABA. Greater than 100% inhibition was observed for **5**, **7d**, **7e**, and **7f** due to their hyperpolarizing effects on cells. The negative value for **4b** and **4c** is due to their agonistic or potentiating effects on cells. Data represent the means of two experiments with bars indicating the range of duplicates. Inhibition percentages at 10 µM are shown for IPs with >50% inhibition at 100 µM. Inhibition data of gabazine (Gz) are taken from a previous report.[31]

of the GABA response in SBP and CC GABARs. IPs **7d**, **7e**, and **7f**, in which R^2 = 4-biphenylyl, 2-fluoro-4-biphenylyl, and 2-naphthyl, respectively, R^1 = CN, and R^3 = H, showed 83.4%, 86.7%, and 93.0% inhibitions, respectively, of the GABA response in SBP GABARs. The GABA-induced responses in CC GABARs were completely inhibited by **7d**, **7e**, and **7f** when tested at 100 μM. IP **7g**, in which R^1 = CN, R^2 = 3-thienyl, and R^3 = H, showed a 66.2% and a 73.6% inhibition of the GABA response in SBP and CC GABARs, respectively. Replacement of the carboxyl group of **4c,** a trisubstituted IP, with a cyano group to give **5** led to a 79.7% and a complete inhibition of the GABA response in SBP and CC GABARs, respectively. 4-Cyclobutyl substitution on **5**, a 1-(3-cyanopropyl) analog, was not detrimental as compared with **7f** This result is in contrast to that of **4c**, a 1-(3-carboxypropyl) analog, in which a reduction in the percentage of inhibition was observed by the introduction of a cyclobutyl group at the 4-position.

An IP with R^1 = P(=O)(OH)(OC_2H_5), R^2 = 4-biphenylyl, and R^3 = H (**8**) displayed a 57.6% and a 50.7% inhibition of the GABA response in SBP and CC GABARs, respectively, at 100 μM. Replacement of P(=O)(OH)(OC_2H_5) with P(=O)$(OH)_2$ on **8**, yielding **9**, showed ~3-fold lower inhibition of the GABA response in SBP and CC GABARs than did **8**.

3.3.3. Antagonism of HF GABARs

The IP antagonism of HF GABARs was subsequently examined using the *Xenopus* oocyte expression system and the TEVC technique. HF GABARs were transiently expressed in oocytes by injecting cRNA encoding the HF Rdl_{ac} subunit as previously described.[23] The inhibition percentages at 100 μM of each compound are shown in Fig. 3.5A. Compounds **4a**-**4c**, which have a cyclobutyl group at the 4-position, showed weak or no activity. However, removal of the cyclobutyl group of **4b** and **4c** increased inhibition percentages to 67.6 ± 5.1% and 47.8 ± 2.9%,

respectively. In this case, the cyclobutyl group is detrimental to IP activity. The disadvantage of the introduction of the 4-cyclobutyl group can also be seen in **5** as compared with **7f**.

In HF GABARs, gabazine had little activity in inhibiting GABA-induced currents (Fig. 3.5A). Substitution of a cyano group for the carboxyl group of gabazine to give **7a** did not result in an increase in activity. Replacement of the methoxyphenyl group of **7a** with an ethoxyphenyl or trifluoromethoxyphenyl group to give **7b** or **7c**, respectively, resulted in slight increases in activity. Replacement of the 4-methoxyphenyl group of **7a** with 4-biphenylyl, 2-fluoro-4-biphenylyl, and 2-naphthyl groups to give **7d, 7e**, and **7f**, respectively, led to ~20-, ~21-, and

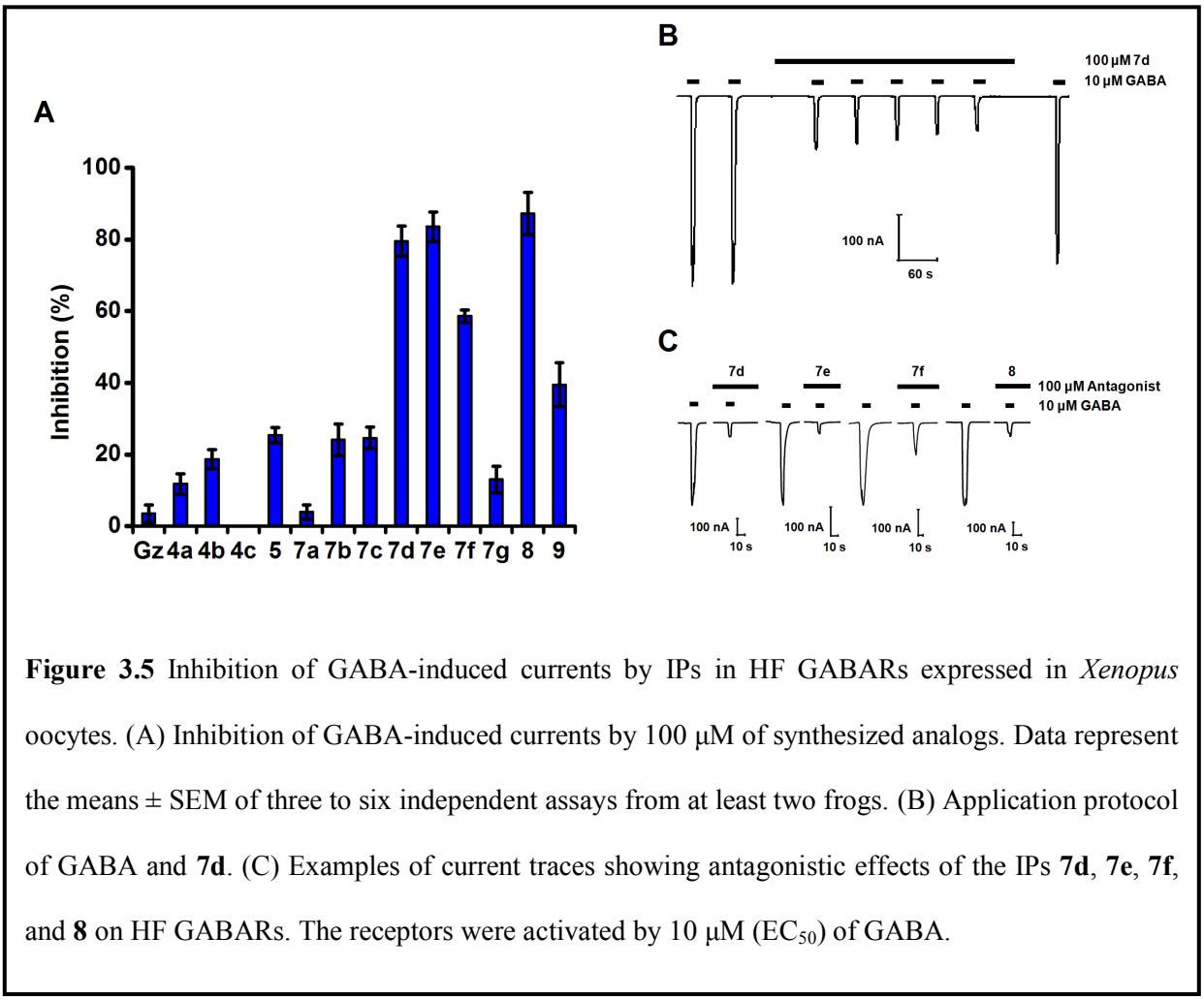

Figure 3.5 Inhibition of GABA-induced currents by IPs in HF GABARs expressed in *Xenopus* oocytes. (A) Inhibition of GABA-induced currents by 100 µM of synthesized analogs. Data represent the means ± SEM of three to six independent assays from at least two frogs. (B) Application protocol of GABA and **7d**. (C) Examples of current traces showing antagonistic effects of the IPs **7d**, **7e**, **7f**, and **8** on HF GABARs. The receptors were activated by 10 µM (EC_{50}) of GABA.

~15-fold greater inhibition percentages, respectively, as compared to **7a**, indicating that the bulky aromatic rings at this position are favorable. The IP inhibition of GABA-activated currents in the HF GABARs gradually proceeded with repeated application of GABA, and the maximum inhibition of currents at each concentration of the IPs was recorded, as shown by **7d** (Fig. 3.5B). The inhibition of currents by **7d**, **7e**, **7f**, and **8** is presented in Fig. 3.5C. The IC_{50}s of **7d**, **7e**, and **7f** were calculated to be 37.9 ± 3.0 μM, 42.3 ± 1.8 μM, and 75.5 ± 7.9 μM, respectively, from concentration-current inhibition relationships (Fig. 3.6A).

IP **8**, in which the cyano group of **7d** is replaced with an ethyl phosphonate, exhibited the greatest inhibition among the IPs tested in the present study, with an 87.3% inhibition at 100 μM and an IC_{50} of 18.8 ± 3.8 μM (Fig. 3.6A). Removal of the ethyl group of **8** to give **9** resulted in a lower inhibition (39.5%).

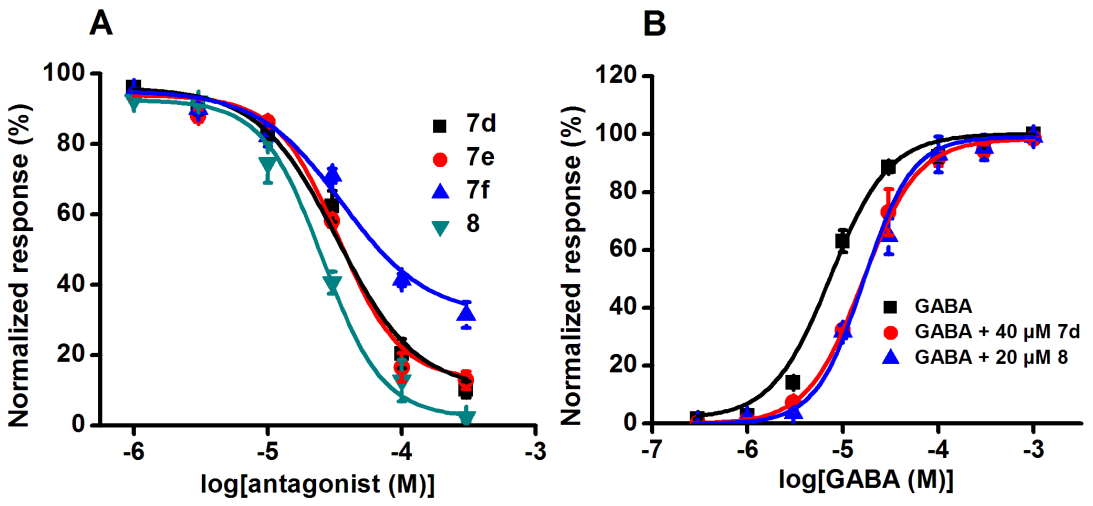

Figure 3.6 Potencies and modes of antagonism of IPs in HF GABARs expressed in *Xenopus* oocytes. (A) Concentration-current inhibition curves of **7d** (black squares), **7e** (red circles), **7f** (blue triangles), and **8** (dark cyan inverted triangles). (B) GABA concentration-response curves in the absence (black squares and presence of 40 μM of **7d** (red circles) and 20 μM of **8** (blue triangles). Data are the means ± SEM of three to four independent assays from at least two frogs.

3.3.4. Mode of antagonism

Gabazine-type IPs with a carboxypropyl side chain were previously reported to act as competitive antagonists of AC GABARs.[31] To determine the mode of antagonism of synthesized IPs, in particular, IPs with cyano and phosphonate functionalities at the end of the side chain, GABA concentration-response relationships were examined in HF GABARs expressed in *Xenopus* oocytes in the presence and absence of **7d** and **8**. A rightward shift was observed in the concentration-response curves in the presence of the cyanide **7d** (40 μM) and the ethyl phosphonate **8** (20 μM), indicating the competitive antagonism of these compounds (Fig. 3.6B). The EC_{50} and the n_H of GABA were 7.42 ± 0.56 μM and 1.80 ± 0.16 (means ± SEM, n = 3-4), respectively, in the absence of IPs. The EC_{50}s were 16.1 ± 2.1 μM and 16.6 ± 1.2 μM in the presence of **7d** and **8**, respectively, and n_Hs were 1.49 ± 0.29 and 1.72 ± 0.26 in the presence of **7d** and **8**, respectively. The maximum current amplitudes did not change in the presence of both compounds. These findings indicate that IPs with the cyano and ethyl phosphonate functionalities at the end of the side chain bind to the orthosteric site.

3.3.5. Homology modeling and ligand docking

To understand the interaction between synthesized IPs and the amino acid residues in the orthosteric site of insect GABARs, ligand-docking studies were performed using an HF GABAR homology model. The model was built using the X-ray crystal structure of the *Caenorhabditis elegans* GluCl as a template.[34] The zwitterion form of GABA and the protonated form of IP **7e** were docked into the constructed model. The binding poses of GABA and **7e** with the highest docking score were selected for presentation (Fig. 3.7).

The docking studies of GABA showed that the side chain of Glu202 and the backbone carbonyl oxygen atom of Ser203 in loop B function as hydrogen acceptors for the protonated amino group of GABA and that Arg109 in loop D and Ser174 in loop E serve as hydrogen donors for the carboxylate anion of GABA (Fig. 3.7A). Both experimental evidence and molecular dynamics simulation indicated that the amino acid residue corresponding to Arg109

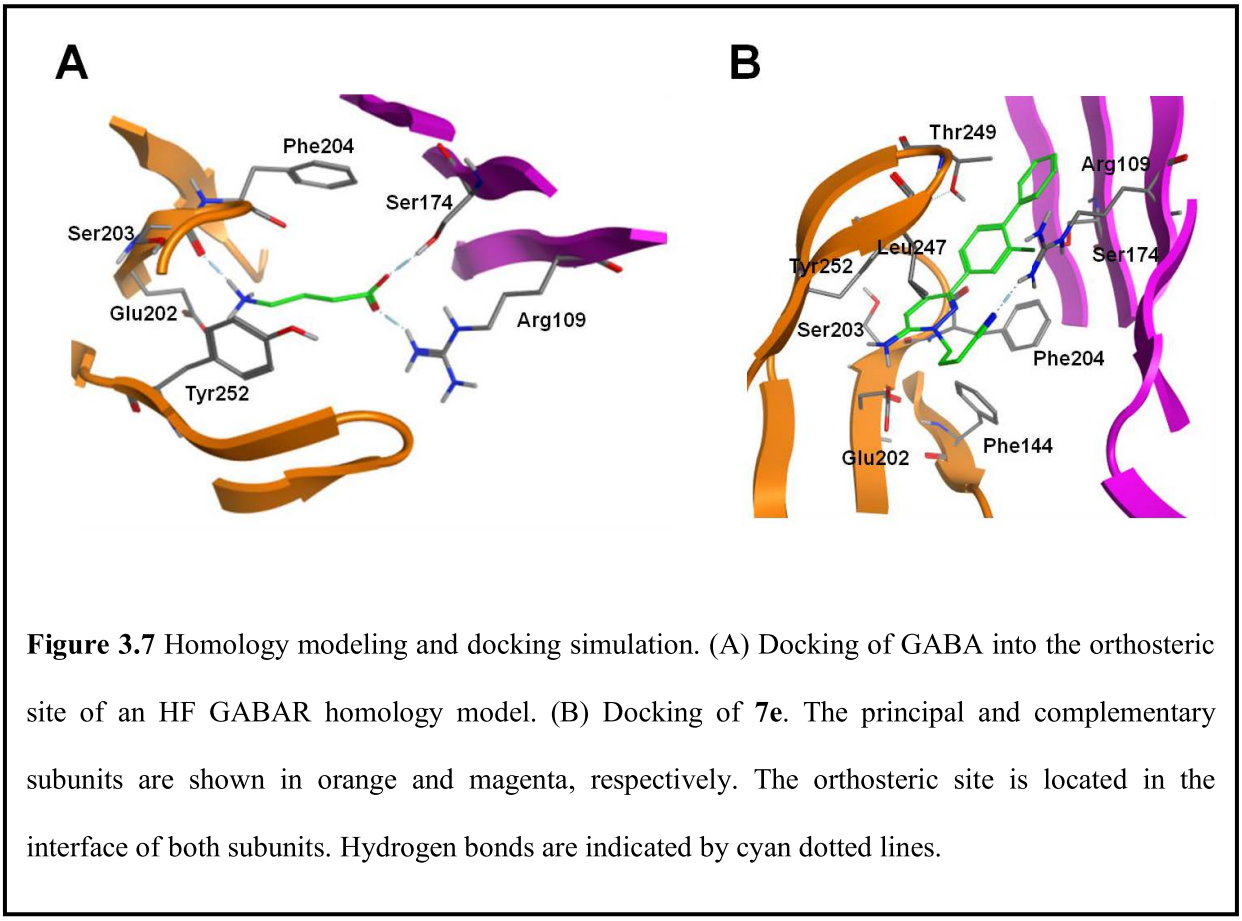

Figure 3.7 Homology modeling and docking simulation. (A) Docking of GABA into the orthosteric site of an HF GABAR homology model. (B) Docking of **7e**. The principal and complementary subunits are shown in orange and magenta, respectively. The orthosteric site is located in the interface of both subunits. Hydrogen bonds are indicated by cyan dotted lines.

plays a critical role in the interaction with GABA in *Drosophila* Rdl GABAR.[38] The two aromatic amino acids, Phe204 in loop B and Tyr252 in loop C, surround the protonated amino group of GABA and may produce cation-π interactions, as proposed for *Drosophila* Rdl

GABARs.[38-40] The bound GABA is in an extended conformation that is similar to that of the *Drosophila* Rdl GABAR and $GABA_CR$ but not to that of the $GABA_AR$.[38,40]

Several amino acids located in loops D, E, and F of the α1 and ρ1 subunits and those in loop A and C of the β2 and ρ1 subunits in $GABA_ARs$ and $GABA_CRs$ have been identified as gabazine-interacting residues by site-directed mutagenesis and functional analysis of the mutants.[41-47] The docking studies of **7e** using an HF GABAR homology model showed that the side chain carboxylate of Glu202 in loop B functions as an acceptor of the protonated imino hydrogen and that the guanidino group of Arg109 in loop D serves as a hydrogen donor for the lone pair of electrons of the nitrile nitrogen (Fig. 3.7B). The amino acid equivalent to Arg109 in the α1 subunit of $GABA_ARs$ was reported to be involved in the interaction with gabazine.[43] Tyr252 in loop C could form an aromatic π-π interaction with the pyridazine ring of **7e**. Because **7e** does not possess a carboxyl group, interaction with Ser174 was not observed in the binding of this ligand. The present docking studies of **7e** predict that its bulky aromatic substituent at the 3-position is tolerable in the orthosteric binding site. However, when an IP analog with R^1 = COOH, R^2 = 4-biphenylyl, and R^3 = H was docked into an HF Rdl_{bd} GABAR model in a previous study, the biphenylyl group was oriented in a direction opposite to that observed in the present study.[31] It is necessary to determine the orientation of the 3-substituent, as this is prerequisite for the development of IP derivatives with high potency against insect GABARs.

3.4. Conclusion

I synthesized IP competitive antagonists with low-micromolar IC_{50} through the bioisosteric replacement of the carboxyl group of gabazine. Ligand docking studies using an HF GABAR homology model predicted that an aromatic substituent at the 3-position of the pyridazine ring is

tolerable in the orthosteric site of insect GABARs. The IP analogs could be a lead for the development of insecticides.

References

1. Chebib, M.; Johnston, G. A. R. GABA-activated ligand gated ion channels: medicinal chemistry and molecular biology. *J. Med. Chem.* **2000**, *43*, 1427−1447.
2. Bowery, N. G.; Enna, S. J. γ-Aminobutyric $acid_B$ receptors: first of the functional metabotropic heterodimers. *J. Pharmacol. Exp. Ther.* **2000**, *292*, 2−7.
3. Bettler, B.; Kaupmann, K.; Mosbacher, J.; Gassmann, M. Molecular structure and physiological functions of $GABA_B$ receptors. *Physiol. Rev.* **2004**, *84*, 835−867.
4. Olsen, R. W.; Sieghart, W. $GABA_A$ receptors: subtypes provide diversity of function and pharmacology. *Neuropharmacology* **2009**, *56*, 141−148.
5. Sine, S. M.; Engel, A. G. Recent advances in Cys-loop structure and function. *Nature* **2006**, *440*, 448−455.
6. Thompson, A. J.; Lester, H. A.; Lummis, S. C. R. The structural basis of function in Cys-loop receptors. *Quar. Rev. Biophys.* **2010**, *43*, 449−499.
7. Whiting, P. J.; Bonnert, T. P.; McKernan, R. M.; Farrar, S.; Le Bourdellès, B.; Heavens, R. P.; Smith, D. W.; Hewson, L.; Rigby, M. R.; Sirinathsinghji, D. J.; Thompson, S. A.; Wafford, K. A. Molecular and functional diversity of the expanding GABA-A receptor gene family. *Ann. N. Y. Acad. Sci.* **1999**, *868*, 645−653.
8. Zhang, D.; Pan, Z.-H.; Awobuluyi, M.; Lipton, S. A. Structure and function of $GABA_C$ receptors: a comparison of native versus recombinant receptors. *Trends Pharmacol. Sci.* **2001**, *22*, 121−132.

9. Miller, P. S.; Smart, T. G. Binding, activation and modulation of Cys-loop receptors. *Trends Pharmacol. Sci.* **2010**, *31*, 161−174.
10. Mckernan, R. M.; Whiting, P. J. Which $GABA_A$-receptor subtypes really occur in the brain? *Trends Neurosci.* **1996**, *19*, 139−143.
11. Johnston, G. A. R. $GABA_A$ receptor pharmacology. *Pharmacol. Ther.* **1996**, *69*, 173−198.
12. Buckingham, S. D.; Sattelle, D. B. GABA receptors of insect. In Gilbert, L. I., Gill, S. S., Eds.; Insect Pharmacology: Channels, Receptors, Toxins and Enzymes; Elsevier: Amsterdam, 2010; pp. 29−64.
13. Ozoe, Y. γ-Aminobutyrate- and glutamate-gated chloride channels as targets of insecticides. *Adv. Insect Physiol.* **2013**, *44*, 211−286.
14. ffrench-Constant, R. H.; Rocheleau, T. A.; Steichen, J. C.; Chalmers, A. E. A point mutation in a *Drosophila* GABA receptor confers insecticide resistance. *Nature* **1993**, *363*, 449−451.
15. Buckingham, S. D.; Biggin, P. C.; Sattelle, B. M.; Brown, L. A.; Sattelle, D. B. Insect GABA receptors: splicing, editing, and targeting by antiparasitics and insecticides. *Mol. Pharmacol.* **2005**, *68*, 942−951.
16. Perret, P.; Sarda, X.; Wolff, M.; Wu, T.-T.; Bushey, D.; Goeldner, M. Interaction of non-competitive blockers within the γ-aminobutyric acid type A chloride channel using chemically reactive probes as chemical sensors for cysteine mutants. *J. Biol. Chem.* **1999**, *274*, 25350−25354.
17. Nakao, T.; Naoi, A.; Kawahara, N.; Hirase, K. Mutation of the GABA receptor associated with fipronil resistance in the whitebacked planthopper, *Sogatella furcifera*. *Pestic. Biochem. Physiol.* **2010**, *97*, 262−266.

18. Nakao, T.; Kawase, A.; Kinoshita, A.; Abe, R.; Hama, M.; Kawahara, N.; Hirase, K. The A2'N mutation of the RDL gamma-aminobutyric acid receptor conferring fipronil resistance in *Laodelphax striatellus* (Hemiptera: Delphacidae). *J. Econ. Entomol.* **2011**, *104*, 646−652.
19. Nakao, T.; Hama, M.; Kawahara, N.; Hirase, K. Fipronil resistance in *Sogatella furcifera*: Molecular cloning and functional expression of wild-type and mutant RDL GABA receptor subunits. *J. Pestic. Sci.* **2012**, *37*, 37−44.
20. Ozoe, Y.; Asahi, M.; Ozoe, F.; Nakahira, K.; Mita, T. The antiparasitic isoxazoline A1443 is a potent blocker of insect ligand-gated chloride channels. *Biochem. Biophys. Res. Commun.* **2010**, *391*, 744−749.
21. Lahm, G. P.; Cordova, D.; Barry, J. D.; Pahutski, T. F.; Smith, B. K.; Long, J. K.; Benner, E. A.; Holyoke, C. W.; Joraski, K.; Xu, M.; Schroeder, M. E.; Wagerle, T.; Mahaffey, M. J.; Smith, R. M.; Tong, M.-H. 4-Azolylphenyl isoxazoline insecticides acting at the GABA gated chloride channel. *Bioorg. Med. Chem. Lett.* **2013**, *23*, 3001−3006.
22. Nakao, T.; Banba, S.; Nomura, M.; Hirase, K. Meta-diamide insecticides acting on distinct sites of RDL GABA receptor from those for conventional noncompetitive antagonists. *Insect Biochem. Mol. Biol.* **2013**, *43*, 366−375.
23. Ozoe, Y.; Kita, T.; Ozoe, F.; Nakao, T.; Sato, K.; Hirase, K. Insecticidal 3-benzamido-*N*-phenylbenzamides specifically bind with high affinity to a novel allosteric site in housefly GABA receptors. *Pestic. Biochem. Physiol.* **2013**, *107*, 285−292.
24. Wermuth, C.-G.; Bourguignon, J.-J.; Schlewer, G.; Gies, J.-P.; Schoenfelder, A.; Melikian, A.; Bouchet, M.-J.; Chantreux, D.; Molimard, J.-C.; Heaulme, M.; Chambon, J.-P.; Biziere, K. Synthesis and structure-activity relationships of a series of aminopyridazine derivatives

of γ-aminobutyric acid acting as selective GABA-A antagonists. *J. Med. Chem.* **1987**, *30*, 239−249.

25. Ueno, S.; Bracamontes, J.; Zorumski, C.; Weiss, D. S.; Steinbach, J. H. Bicuculline and gabazine are allosteric inhibitors of channel opening of the $GABA_A$ receptor. *J. Neurosci.* **1997**, *17*, 625−634
26. Hosie, A. M.; Sattelle, D. B. Agonist pharmacology of two *Drosophila* GABA receptor splice variants. *Br. J. Pharmacol.* **1996**, *119*, 1577−1585.
27. Satoh, H.; Daido, H.; Nakamura, T. Preliminary analysis of the GABA-induced current in cultured CNS neurons of the cutworm moth, *Spodoptera litura*. *Neurosci. Lett.* **2005**, *381*, 125−130.
28. Narusuye, K.; Nakao, T.; Abe, R.; Nagatomi, Y.; Hirase, K.; Ozoe, Y. Molecular cloning of a GABA receptor subunit from *Laodelphax striatella* (Fallén) and patch clamp analysis of the homo-oligomeric receptors expressed in a Drosophila cell line. *Insect Mol. Biol.* **2007**, *16*, 723−733.
29. Duittoz, A. H.; Martin, R. J. Antagonist properties of arylaminopyridazine GABA derivatives at the *Ascaris* muscle GABA receptor. *J. Exp. Biol.* **1991**, *159*, 149−164.
30. Martin, R. J.; Sitamze, J.-M.; Duittoz, A. H.; Wermuth, C. G. Novel arylaminopyridazine-GABA receptor antagonists examined electrophysiologically in *Ascaris suum*. *Eur. J. Pharmacol.* **1995**, *276*, 9−19.
31. Rahman, M. M.; Akiyoshi, Y.; Furutani, S.; Matsuda, K.; Furuta, K.; Ikeda, I.; Ozoe, Y. Competitive antagonism of insect GABA receptors by iminopyridazine derivatives of GABA. *Bioorg. Med. Chem.* **2012**, *20*, 5957−5964.

32. Nakao, T.; Hirase, K. A comparison of the modes of action of novel meta-diamide insecticides and conventional noncompetitive antagonists on the *Spodopter litura* RDL GABA receptor. *J. Pestic. Sci.* **2013**, *38*, 123−128.

33. Eguchi, Y.; Ihara, M.; Ochi, E.; Shibata, Y.; Matsuda, K.; Fushiki, S.; Sugama, H.; Hamasaki, Y.; Niwa, H.; Wada, M.; Ozoe, F.; Ozoe, Y. Functional characterization of *Musca* glutamate- and GABA-gated chloride channels expressed independently and coexpressed in *Xenopus* oocytes. *Insect Mol. Biol.* **2006**, *15*, 773−783.

34. Hibbs, R. E.; Gouaux, E. Principles of activation and permeation in an anion-selective Cys-loop receptor. *Nature* **2011**, *474*, 54−60.

35. Schroeder, K. S.; Neagle, B. D. FLIPR: a new instrument for accurate, high throughput optical screening. *J. Biomol. Screen.* **1996**, *1*, 75−80.

36. Joesch, C.; Guevarra, E.; Parel, S. P.; Bergner, A.; Zbinden, P.; Konrad, D.; Albrecht, H. Use of FLIPR membrane potential dyes for validation of high-throughput screening with the FLIPR and μARCS technologies: identification of ion channel modulators acting on the $GABA_A$ receptor. *J. Biomol. Screen.* **2008**, *13*, 218−228.

37. Yamamoto, I.; Carland, J. E.; Locock, K.; Gavande, N.; Absalom, N.; Hanrahan, J. R.; Allan, R. D.; Johnston, G. A. R.; Chebib, M. Structurally diverse GABA antagonists interact differently with open and closed conformational states of the ρ_1 receptor. *ACS Chem. Neurosci.* **2012**, *3*, 293−301.

38. Ashby, J. A.; McGonigle, I. V.; Price, K. L.; Cohen, N.; Comitani, F.; Dougherty, D. A.; Molteni, C.; Lummis, S. C. R. GABA binding to an insect GABA receptor: A molecular dynamics and mutagenesis study. *Biophys. J.* **2012**, *103*, 2071−2081.

39. McGonigle, I.; Lummis, S. C. R. Molecular characterization of agonists that bind to an insect GABA receptor. *Biochemistry* **2010**, *49*, 2897−2902.

40. Comitani, F.; Cohen, N.; Ashby, J.; Botten, D.; Lummis, S. C. R.; Molteni, C. Insights into the binding of GABA to the insect RDL receptor from atomistic simulations: a comparison of models. *J. Comput. Aided Mol. Des.* **2014**, *28*, 35−48.

41. Sigel, E.; Baur, R.; Kellenberger, S.; Malherbe, P. Point mutations affecting antagonist affinity and agonist dependent gating of $GABA_A$ receptor channels. *EMBO J.* **1992**, *11*, 2017−2023.

42. Wagner, D. A.; Czajkowski, C. Structure and dynamics of the GABA binding pocket: A narrowing cleft that constricts during activation. *J. Neurosci.* **2001**, *21*, 67−74.

43. Holden, J. H.; Czajkowski, C. Different residues in the $GABA_A$ receptor α_1T60-α_1K70 region mediate GABA and SR-95531 actions. *J. Biol. Chem.* **2002**, *277*, 18785−18792.

44. Newell, J. G.; Czajkowski, C. The $GABA_A$ receptor α_1 subunit Pro^{174}-Asp^{191} segment is involved in GABA binding and channel gating. *J. Biol. Chem.* **2003**, *278*, 13166−13172.

45. Wagner, D. A.; Czajkowski, C.; Jones, M. W. An arginine involved in GABA binding and unbinding but not gating of the $GABA_A$ receptor. *J. Neurosci.* **2004**, *24*, 2733−2741.

46. Kloda, J. H.; Czajkowski, C. Agonist-, antagonist-, and benzodiazepine-induced structural changes in the α_1Met^{113}-Leu^{132} region of the $GABA_A$ receptor. *Mol. Pharmacol.* **2007**, *71*, 483−493.

47. Zhang, J.; Xue, F.; Chang, Y. Structural determinants for antagonist pharmacology that distinguish the ρ1 $GABA_C$ receptor from $GABA_A$ receptors. *Mol. Pharmacol.* **2008**, *74*, 941−951.

CHAPTER 4

Conclusion

GABA is the widely distributed inhibitory neurotransmitter in the central nervous system of animals. GABA mediates inhibitory neuronal activity by binding to two classes of membrane proteins: ionotropic and metabotropic. The ionotropic GABARs belong to the Cys-loop receptor family of ligand-gated ion channel comprising of five subunits. The ionotropic GABARs are subdivided into two categories: hetero-pentameric $GABA_A$Rs and homo-pentameric $GABA_C$Rs. The binding of GABA to the orthosteric agonist binding site converts the chemical signal to an electrical signal by rapidly opening a channel to allow the flux of negatively-charged chloride ions into the cell to suppress the nerve excitation. The insect GABARs are targets for commercially available insecticides; fipronil is the extensively used phenylpyrazole insecticide that exerts its insecticidal effects by acting as noncompetitive antagonists. However, fipronil resistance in several insect species has been reported. Efforts continue to develop novel GABAR insecticides. Competitive antagonists with high-affinity could also be developed as potential GABAR-targeting insecticides because they cause the same effect on GABARs as do nocompetitive antagonists, i.e., blockade of channel. However, no potent competitive antagonist is available for insect GABARs. Bucuculline and gabazine are competitive antagonists of mammalian GABARs. Whereas bicuculline is inactive against most insect GABARs, gabazine shows weak or moderate antagonism of insect GABARs. Therefore, in the present study, I synthesized gabazine-related IP analogs in which substituents on the pyridazine ring of gabazine are modified and examined their antagonism of insect GABARs.

In the first part of my studies described in Chapter 2, I synthesized a series of 4-(1,6-dihydro-6-imino-3-aryl/heteroarylpyridazin-1-yl)butanoic acids and examined their antagonism of GABARs cloned from SBPs and CCs using FMP assays. Antagonism of native GABARs isolated from the abdominal ganglion neurons of ACs was also examined using a whole-cell patch clamp technique. When tested at 100 μM, 4-[1,6-dihydro-6-imino-3-(4-methoxyphenyl)pyridazin-1-yl]butanoic acid (gabazine) showed moderate activity with 71.5% and 60.2% inhibition of the GABA responses in SBP and CC GABARs, respectively. However, it was not an effective antagonist in AC GABARs when tested at 500 μM. When the methoxyphenyl group of gabazine is replaced with a 3,4-methylenedioxyphenyl and a 2-naphthyl groups, the resulting analogs exhibited complete inhibition of GABA-induced responses in SBP GABARs at 100 μM. These two analogs inhibited GABA responses by 85.8% and completely in CC GABARs, respectively, at the same concentration. In AC GABARs, these two analogs displayed 42.0% and 85.4% inhibition of GABA-induced currents, respectively at 500 μM. Whereas the 2-naphthyl analog showed relatively high activity, the 1-naphthyl analog showed weak activity in all three receptors. The 1-naphthyl ring may provide significant amount of steric hindrance for the binding site. At 100 μM, the 4-biphenylyl congener did not exceed the activity of gabazine in SBP GABARs and showed inhibition comparable to that of gabazine in CC GABARs, but it showed moderate activity even at 10 μM in both receptors. This analog showed the greatest activity, with 92.0% inhibition in AC GABARs at 500 μM. The high activity of the 4-biphenylyl and 2-naphthyl analogs suggests that long aromatic substituents at the 3-position of the pyridazine ring are tolerated. The 3-thienyl analog showed a relatively high activity than the 2-furyl and 2-thienyl analogs in all three receptors, indicating that the lone-pair electrons on the heteroatom of the analog at the 3-position of five membered ring may provide some favorable

electronegative effects on receptor interaction. The inhibition pattern of AC GABARs differs from that of SBP and CC GABARs, suggesting the existence of structural differences in the orthosteric binding sites between insect species. The 3-thienyl analog demonstrated a competitive mode of inhibition in AC GABARs. The docking simulation of the 4-biphenylyl analog into the orthosteric site of a HF Rdl_{bd} GABAR homology model indicated that the amino acid predicted to interact with the carboxyl and imino groups were similar to those to be involved in GABA binding and that hydrophobic interactions predominate in the area that accommodates the 3-substituents.

In the second part of my studies described in Chapter 3, I synthesized thirteen 1,3-di- and 1,3,4-trisubstituted IPs with various substituents on the pyridazine ring and examined their antagonism of SBP and CC GABARs using FMP assays. Antagonism of HF Rdl_{ac} GABARs expressed in *Xenopus* oocytes was also examined using two-electrode voltage clamp technique. Of the synthesized analogs, 4-[4-cyclobutyl-1,6-dihydro-6-imino-3-(2-naphthyl)pyridazin-1-yl]butyronitrile exhibited 79.7% and complete inhibition of GABA-activated responses in SBP and CC GABARs, respectively, when tested at 100 μM. This analog showed approximately 25.4% inhibition of GABA-induced currents in HF GABARs at the same concentration. Removal of the cyclobuty group showed 93.0% and complete inhibition of GABA responses in SBP and CC GABARs, respectively, and the level of inhibition was increased to 58.6% in HF GABARs with an IC_{50} value of 75.5 μM. The 3-(4-biphenylyl) and 3-(2-fluoro-4-biphenylyl) congeners showed 83.4% and 86.7% inhibition of GABA responses in SBP GABARs and complete inhibition in CC GABARs, respectively. These two analogs showed 79.6% and 83.6% inhibition in HF GABARs, with IC_{50}s of 37.9 μM and 42.3 μM, respectively. Ethyl 3-[3-(4-biphenylyl)-1,6-dihydro-6-iminopyridazin-1-yl]propylphosphonate showed 57.6% and 50.7%

inhibition of GABA responses in SBP and CC GABARs, respectively. This analog exhibited the greatest inhibition of GABA-induced currents (87.3%), with an IC_{50} of 18.8 μM in HF GABARs. Removal of the ethyl group from this analog resulted in lower inhibition in all three receptors. GABA concentration-response analyses in the presence of IP analogs with butyronitrile and phosphonate side chains indicated that these analogs antagonize GABA responses in a manner that is competitive with GABA. Docking simulation of an IP analog with a butyronitrile side chain into a HF Rdl_{ac} GABAR homology model predicted that the orthosteric GABA-binding site accommodates an IP with a nitrile functionality and an aromatic substituent at the 3-position of the pyridazine ring.

I synthesized IPs that show competitive antagonism of insect GABARs, with low-micromolar IC_{50} through the biosteric replacement of the carboxylic group of gabazine. This synthetic information with homology modeling and docking studies should prove helpful for designing new competitive antagonist type of insecticides.

Summary

γ-Aminobutyric acid (GABA) is a major inhibitory neurotransmitter widely distributed in the central nervous system of animals. Insect ionotropic GABARs are important targets for insecticides and parasiticides. Commercially available insecticides such as fipronil act as noncompetitive antagonist. However, a potent competitive antagonist for insect GABARs is not available. The present study aimed to synthesize IP antagonists for insect GABARs by modifying substituents on the pyridazine ring of gabazine.

Twelve 4-(1,6-dihydro-6-imino-3-aryl/heteroarylpyridazin-1-yl)butanoic acids were first synthesized and examined for their antagonism of small brown planthopper (SBP) and common cutworm (CC) GABARs using fluorometric imaging plate reader (FLIPR) membrane potential (FMP) assays. Antagonism of GABARs was also examined in native American cockroach (AC) using a whole-cell patch clamp technique. Gabazine (aryl/heteroaryl = 4-methoxyphenyl) was moderately active in SBP and CC GABARs at 100 μM. However, it was not active in AC GABARs at 500 μM. IPs with ary/heteroaryl = 3,4-methylenedioxyphenyl and 2-naphthyl exhibited complete inhibition of GABA responses in SBP GABARs and inhibited GABA responses by 85.8% and completely in CC GABARs, respectively. The 2-naphthyl analog displayed 85.4% inhibition of GABA-induced currents in AC GABARs at 500 μM. The 4-biphenylyl analog showed 47.6% and 57.3% inhibition of GABA responses in SBP and CC GABARs, respectively, at 10 μM. This analog showed the greatest activity with 92.0% inhibition of GABA-induced currents in AC GABARs at 500 μM. The high activity of 4-biphenylyl and 2-naphthyl analogs suggests that long aromatic substituents at the 3-position of the pyridazine ring are tolerated. The 3-thienyl analog demonstrated a competitive mode of inhibition in AC GABARs. Hydrophobic interactions were predicted to predominate in the area of the orthosteric

site that accommodates the 3-substituents when docked into the homology model of HF GABAR containing Rdl_{bd} subunits.

Thirteen 1,3-di- and 1,3,4-trisubstituted IPs with various substituents on the pyridazine ring of gabazine were next synthesized and examined for their antagonism of SBP and CC GABARs using FMP assays. Antagonism of HF GABARs expressed in *Xenopus* oocytes was also examined using a two-electrode voltage clamp technique. 4-[4-Cyclobutyl-1,6-dihydro-6-imino-3-(2-naphthyl)pyridazin-1-yl]butyronitrile showed 79.7% and complete inhibition of GABA-activated responses in SBP and CC GABARs, respectively at 100 μM. However, this analog showed <30% inhibition in HF GABARs at the same concentration. Removal of the cyclobutyl group from this analog reduces in 93.0% and complete inhibition of GABA responses in SBP and CC GABARs, respectively, and it increased the inhibition percentage to 58.6% in HF GABARs, with an IC_{50} value of 75.5 μM. 4-[3-(4-Biphenylyl)-1,6-dihydro-6-iminopyridazin-1-yl]butyronitrile and the 2-fluoro-4-biphenylyl congener exhibited 83.4% and 86.7% inhibition of GABA responses in SBP GABARs, respectively, and complete inhibition in CC GABARs. These two analogs showed 79.6% and 83.6% inhibition in HF GABARs, with IC_{50}s of 37.9 μM and 42.3 μM, respectively. Ethyl 3-[3-(4-biphenylyl)-1,6-dihydro-6-iminopyridazin-1-yl]propylphosphonate analog showed the highest activity with 87.3% inhibition, with an IC_{50} value of 18.8 μM in HF GABARs. 4-[3-(4-Biphenylyl)-1,6-dihydro-6-iminopyridazin-1-yl]butyronitrile and ethyl 3-[3-(4-biphenylyl)-1,6-dihydro-6-iminopyridazin-1-yl]propylphosphonate exhibited a competitive mode of antagonism of GABA responses in HF GABARs. Docking simulation of an IP into a HF Rdl_{ac} GABAR homology model predicted that the orthosteric GABA-binding site accommodates an IP with a cyano functionality and an aromatic substituent at the 3-position of the pyridazine ring. The results obtained from this study might provide useful information for the designing of new type of insecticide.

要旨

γ-アミノ酪酸 (GABA) は動物の中枢神経系に広く存在している主要な抑制性神経伝達物質である。昆虫のイオンチャネル型 GABA 受容体は殺虫剤や駆虫薬の重要なターゲットとなっている。フィプロニルのような市販されている殺虫剤は非競合アンタゴニストとして働く。しかし、昆虫 GABA 受容体に対する強力な競合アンタゴニストは存在していない。本研究では、gabazine のピリダジン環を修飾することにより昆虫 GABA 受容体にアンタゴニスト作用を示す IP を合成することを目的としている。

まず初めに 12 種類の 4-(1,6-dihydro-6-imino-3-aryl/heteroarylpyridazin-1-yl)butanoic acid を合成し、ヒメトビウンカ (SBP) とハスモンヨトウ (CC) の GABA 受容体に対するそれらのアンタゴニスト活性を蛍光イメージングプレートリーダー (FLIPR) 膜電位 (FMP) 測定法を用いて試験した。また、ワモンゴキブリ (AC) GABA 受容体に対するアンタゴニスト活性はホールセルパッチクランプ法で試験した。Gabazine (aryl/heteroaryl = 4-methoxyphenyl) は SBP および CC の GABA 受容体に対して 100 μM で中程度の活性を示した。しかしながら、AC の GABA 受容体に対しては 500 μM でも活性を示さなかった。Aryl/heteroaryl を 3,4-methylenedioxyphenyl または 2-naphthyl に置換した IP では、100 μM において SBP の GABA 受容体での GABA 応答を完全に阻害し、CC では 3,4-methylenedioxyphenyl 類縁体で 85.4%、2-naphthyl 類縁体で完全な阻害を示した。2-naphthyl 類縁体は 500 μM において、AC の GABA 受容体内の GABA 応答を 85.4%阻害した。4-biphenylyl 類縁体は 10 μM で SBP および CC の GABA 応答をそれぞれ 47.6%および 57.3%阻害した。この類縁体は 500 μM で AC GABA 受容体の GABA 応答に対して 92.0%と最も高い阻害活性を示した。4-Biphenylyl および 2-naphthyl 類縁体が高い活性を示したことから、ピリダジン環の 3 位に置換を行った長い芳香族化合物は許容されると考えられる。3-Thienyl 類縁体は AC GABA 受容体で競合的アンタゴニスト様式を示した。Rdl_{bd} サブユニットを含む HF GABA 受容体のホモロジーモデルへのド

ッキングによって、3 位置換基を収容するオルトステリック結合部位では顕著な疎水的相互作用が起こると予測された。

次に、gabazine のピリダジン環を置換した 13 種類の 1,3-di-および 1,3,4-tri 置換 IP 化合物を合成し、FMP アッセイによって SBP および CC GABA 受容体でのアンタゴニスト活性を調べた。*Xenopus* 卵母細胞に発現させた HF GABA 受容体のアンタゴニスト活性は二電極膜電位固定法で調べた。4-[4-Cyclobutyl-1,6-dihydro-6-imino-3-(2-naphthyl)pyridazin-1-yl]butyronitrile は 100 μM で SBP に対して GABA 応答を 79.7%阻害し、CC に対しては完全に阻害した。しかしながらこの類縁体は、同じ濃度で HF GABA 受容体に対しては 30%未満の阻害しか見られなかった。この類縁体から cyclobutyl 基を除去すると SBP と CC における GABA 応答をそれぞれ 93.0%および完全に阻害した。HF GABA 受容体では 58.6%と阻害率が増加し、IC_{50} 値は 75.5 μM であった。4-[3-(4-Biphenylyl)-1,6-dihydro-6-iminopyridazin-1-yl]butyronitrile および 2-fluoro-4-biphenylyl 同族体は SBP GABA 受容体で GABA 応答をそれぞれ 83.4%および 86.7%阻害し、CC では完全に阻害した。これら 2 種類の類縁体は HF GABA 受容体でそれぞれ 79.6%および 83.6%の阻害を示し、IC_{50} 値は 37.9 μM および 42.3 μM であった。Ethyl 3-[3-(4-biphenylyl)-1,6-dihydro-6-iminopyridazin-1-yl]propylphosphonate analog は HF GABA 受容体で 87.3%と最も高い阻害活性を示し、IC_{50} 値は 18.8 μM であった。4-[3-(4-Biphenylyl)-1,6-dihydro-6-iminopyridazin-1-yl]butyronitrile および ethyl 3-[3-(4-biphenylyl)-1,6-dihydro-6-iminopyridazin-1-yl]propylphosphonate は HF GABA 受容体で、競合的アンタゴニスト様式を示した。IP の HF Rdl_{ac} GABA 受容体のホモロジーモデルへのドッキングシミュレーションから、オルソステリックな GABA 結合部位はシアノ基およびピリダジン環の 3 位に芳香族置換基を持つ IP を収容すると予測された。この研究で得られた成果は新規殺虫剤のデザインを行う際に有益な情報を提供すると考えられる。

List of Publications

1. Rahman, M. M.; Akiyoshi, Y.; Furutani, S.; Matsuda, K.; Furuta, K.; Ikeda, I.; Ozoe, Y. Competitive antagonism of insect GABA receptors by iminopyridazine derivatives of GABA. *Bioorg. Med. Chem.* **2012**, *20*, 5957-5964 (Chapter 2).
2. Rahman, M. M.; Liu, G.; Furuta, K.; Ozoe, F.; Ozoe, Y. Synthesis of 1,3-di- and 1,3,4-trisubstituted 1,6-dihydro-6-iminopyridazines as competitive antagonists of insect GABA receptors. *J. Pestic. Sci.* **2014**, *39(3)*, 133-143 (accepted) (Chapter 3).

Acknowledgements

All praises to almighty Allah, the most gracious and most merciful, who accepted me to complete the present work successively and write this dissertation. He made me fortunate enough to be associated with so many competent and academically stimulating individuals who guided me at every stage of my PhD research.

First, and foremost, I would like to express my deep appreciation, gratefulness, and the sincere gratitude to my respected research advisor Dr. Yoshihisa Ozoe, Professor, Department of Life Science and Biotechnology, Faculty of Life and Environmental Science, Shimane University, Japan for his excellent guidance and encouragement throughout my research work. I was extremely fortunate to work under his supervision for my PhD.

The author expresses his indebtedness to his co-supervisor Dr. Kenjiro Furuta, Assistant Professor, Shimane University for his valuable suggestions and cooperation for the progress of study.

The author expresses his thanks to Dr. Hiromitsu Nakajima, Professor, School of Agricultural, Biological, and Environmental Sciences, Faculty of Agriculture, Tottori University for his valuable advice and cooperation for the progress of study.

I would like to express my gratefulness to Dr. Izumi Ikeda, Associate professor for his valuable advice and sincere cooperation during the study.

I express my cordial gratitude to Ms. Fumiyo Ozoe, Senior researcher for her valuable suggestions during the work.

I am grateful to Ms Yuki Akiyoshi for the whole-cell patch clamp assays of my synthesized compounds and her contribution to the first paper. I also would like to thank her whole-hearted cooperation during my stay in Japan.

The author expresses his gratefulness to Dr. T. Nakao, Mitsui Chemicals Agro, Inc., Japan for his kindness to perform FMP assays that included in second paper.

I would also like to extend my gratefulness to all my lab members specially Dr. T. Kita, Mr. T. Fuse, Mr. K. Nomura, Ms. M. Takashima, and Mr. G. Liu for their kind cooperation during the whole study and my stay in Japan.

I would like to thank my family members specially my wife Ms. Mirajum Billah for their continuous support during this study.

I would like to thanks all the staffs of Shimane and Tottori University for their kind cooperation.

Finally, I would like to express my special thanks to the Ministry of Education, Culture, Sports, Science and Technology (Monbukagakusho: MEXT), Government of Japan to grant me the scholarship for this novel research.